Herpetological Monographs, 34, 2020, 131–177

Taxonomic Review of South American Butter Frogs: Phylogeny, Geographic Patterns, and Species Delimitation in the *Leptodactylus latrans* Species Group (Anura: Leptodactylidae)

Felipe de M. Magalhães[1,16], Mariana L. Lyra[2], Thiago R. de Carvalho[2], Diego Baldo[3], Francisco Brusquetti[4], Pamela Burella[5,15], Guarino R. Colli[6], Marcelo C. Gehara[7], Ariovaldo A. Giaretta[8], Célio F.B. Haddad[2], José A. Langone[9], Javier A. López[5,10], Marcelo F. Napoli[11], Diego J. Santana[12], Rafael O. de Sá[13], and Adrian A. Garda[1,14]

[1] Programa de Pós-Graduação em Ciências Biológicas, Universidade Federal da Paraíba (UFPB), Centro de Ciências Exatas e da Natureza, Cidade Universitária, CEP 58000-000, João Pessoa, Paraíba, Brazil

[2] Universidade Estadual Paulista (UNESP), Instituto de Biociências, Campus Rio Claro, Departamento de Biodiversidade e Centro de Aquicultura (CAUNESP), CEP 13506-900, Rio Claro, São Paulo, Brazil

[3] Instituto de Biología Subtropical (IBS, CONICET-UNaM), Laboratorio de Genética Evolutiva, Facultad de Ciencias Exactas, Universidad Nacional de Misiones, CP N3300LQF, Posadas, Misiones, Argentina

[4] Instituto de Investigación Biológica del Paraguay (IIBP), Del Escudo 1607, CP 1425 Asunción, Paraguay

[5] Departamento de Ciencias Naturales, Facultad de Humanidades y Ciencias, Universidad Nacional del Litoral. Ciudad Universitaria UNL, 3000, Santa Fe, Argentina

[6] Departamento de Zoologia, Universidade de Brasília (UNB), CEP 70910-900, Brasília, Distrito Federal, Brazil

[7] Department of Biological Sciences, Rutgers University, Newark, New Jersey, 07102, USA

[8] Laboratório de Taxonomia e Sistemática de Anuros Neotropicais (LTSAN), Instituto de Ciências Exatas e Naturais do Pontal (ICENP), Universidade Federal de Uberlândia (UFU), Ituiutaba, Minas Gerais, Brazil

[9] Departamento de Herpetología, Museo Nacional de Historia Natural, Casilla de Correo 399, CP 11.000, Montevideo, Uruguay

[10] Instituto Nacional de Limnología (CONICET-UNL), Ciudad Universitaria UNL, Santa Fe, Argentina

[11] Laboratório de Taxonomia e História Natural de Anfíbios (AMPHIBIA), Museu de História Natural, Instituto de Biologia, Universidade Federal da Bahia (UFBA), CEP 40170–115, Salvador, Bahia, Brazil

[12] Mapinguari – Laboratório de Biogeografia e Sistemática de Anfíbios e Répteis, Universidade Federal de Mato Grosso do Sul (UFMS), CEP 79002-970 Campo Grande, Mato Grosso, Brazil

[13] Department of Biology, University of Richmond, Richmond, Virginia, 23173, USA

[14] Laboratório de Anfíbios e Répteis (LAR), Departamento de Botânica e Zoologia da Universidade Federal do Rio Grande do Norte (UFRN), CEP 59078-900, Natal, Rio Grande do Norte, Brazil

Abstract: The *Leptodactylus latrans* species group currently comprises eight medium- to large-sized frog species with a convoluted taxonomic history, particularly related to the specific limits of the *L. latrans* complex, and the species pair *Leptodactylus chaquensis–Leptodactylus macrosternum*. Their homogeneous external morphology and continental geographic distribution in South America have posed severe limitations to a comprehensive review, such that taxonomic consensus and species limits remain uncertain. This is further worsened by the presence of chromatic polymorphism among coexisting species that can hardly be distinguished by external morphology. Based on a large-scale geographic sampling including multilocus DNA analyses, and acoustic and morphological data, we provide a comprehensive evaluation of the taxonomic status and species limits of the *L. latrans* group, focusing on the resolution of the *L. latrans* complex and the species pair *L. chaquensis–L. macrosternum*. We gathered 728 mitochondrial sequences from 429 localities, encompassing the entire geographic distribution of the group. Both generalized mixed Yule coalescent and automatic barcode gap discovery species delimitation methods recovered four major mitochondrial evolutionary lineages within the *L. latrans* complex, also supported by distribution patterns, multilocus molecular, morphological and/or bioacoustic data. One lineage is linked to nominal *L. latrans*, one revalidated as *Leptodactylus luctator*, and the other two are formally named and described. Another lineage encompasses all specimens previously assigned to the species pair *L. chaquensis–L. macrosternum*, clustered as a single evolutionary entity and is now regarded as *L. macrosternum*. We provide a revised diagnosis for these species based on acoustic data, morphological/chromatic variation, and phylogenetic relationships of all species currently included in the *L. latrans* group. Our findings reinforce the view that Neotropical diversity is highly underestimated and stress that appropriate geographic sampling in an integrative framework is crucial for the establishment of specific limits among broadly distributed and morphologically cryptic Neotropical frogs.

Key words: Bioacoustics; Cryptic species; Geographic distribution; Mitochondrial species delimitation; Molecular systematics; Morphology; Morphometrics

The Genus *Leptodactylus* Fitzinger 1826 currently comprises 78 small- to large-sized species arranged in four groups supported by morphological, behavioral, and genetic data: the *L. fuscus*, *L. pentadactylus*, *L. latrans*, and *L. melanonotus* species groups (see Heyer 1969; de Sá et al. 2014; Frost 2020 and references therein). The *L. latrans* species group, also known as butter frogs because of their slippery skin, includes eight species: *Leptodactylus bolivianus* (Boulenger 1898), *L. chaquensis* (Cei 1950), *L. guianensis* (Heyer and de Sá 2011), *L. insularum* (Barbour 1906), *L. latrans* (Steffen 1815), *L. macrosternum* (Miranda-Ribeiro 1926), *L. silvanimbus* McCranie Wilson and Porras 1980 (McCranie et al., 1980), and *L. viridis* (Jim and Spirandeli-Cruz 1979). Members of this species group are distributed from Central America and some Caribbean islands off South America coast (e.g., *L. silvanimbus* and *L. insularum*) to Argentina (e.g., *L. latrans* and *L. chaquensis*), and throughout all South American biomes east of the Andes (de Sá et al. 2014). Most species are conspicuous, abundant, and active (although not necessarily breeding) throughout most of the year in pristine or disturbed open habitats, making them some of the most common frogs in South America (Lutz 1930; Cei 1962; de Sá et al. 2014). Members of the group are mainly recognized based on thumb spines

[15] This author passed away in October 2019 and she is sorely missed by her friends and colleagues. This paper is dedicated to her memory.

[16] Correspondence: e-mail, felipemm17@gmail.com

and vocal sac morphology (despite both being absent in females and nonbreeding/juvenile males), arrangement of body dermal longitudinal folds, pigmentation patterns of body and thighs, and advertisement call (Cei 1980; Heyer and de Sá 2011; de Sá et al. 2014). However, species in the *L. latrans* group are morphologically cryptic, and three species complexes are recognized (de Sá et al. 2014): the *L. bolivianus* complex, which encompasses *L. bolivianus*, *L. guianensis*, and *L. insularum* (thoroughly reviewed by Heyer and de Sá 2011), the *L. latrans* complex and the species pair *L. chaquensis–L. macrosternum* complex (hereinafter referred to as LCM complex clade). The LCM complex likely harbors undescribed taxa and has been long known as a group of species that needs a thorough taxonomic review (De la Riva and Maldonado 1999; de Sá et al. 2014; Heyer 2014).

The taxonomic history of the *Leptodactylus latrans* complex is challenging. It dates back to the beginning of the 19th century, when many scientific expeditions took place in Brazil (Lavilla et al. 2010; Frost 2020). During that period, many representatives of the complex were deposited in European and North American collections (Boulenger 1882; Cochran 1961; Glaw and Franzen 2006) and subsequently described as new species (Raddi 1823; Spix 1824; Girard 1853). At the present moment, 15 valid names are in the synonymy of *L. latrans* (Lavilla et al. 2010; de Sá et al. 2014; Frost 2020). Unfortunately, many species descriptions are brief and uninformative, lacking illustrations and precise geographic information, and type specimens were either lost or poorly preserved (Hoogmoed and Gruber 1983; Lavilla et al. 2010), precluding the use of morphological or geographic information for species identification. Moreover, the broad geographic distribution (spanning more than 30° of latitude) and the existence of cryptic species in syntopy (Cei 1950, 1962; Gallardo 1964) hampered the advance of the taxonomy and the establishment of clear species limits within this species group.

An essential contribution towards the taxonomic resolution of the *Leptodactylus latrans* complex was provided by Lavilla et al. (2010). They elucidated the identity of *L. ocellatus* (now *L. latrans*), designated and described a neotype from the southeastern Brazilian Atlantic Forest. Specimens assigned to *L. latrans* are widely distributed across ca. 3500 km, mostly along the eastern South America coastal zone, from Argentina to northeastern Brazil (referred to as *L. ocellatus* in Miranda-Ribeiro 1927; Cei 1962; Gallardo 1964). However, considering an uncertainty related to the broad geographic distribution and that *L. latrans* might correspond to a complex of morphologically cryptic species, de Sá et al. (2014) did not consider the occurrence records outside the type locality. No further advances on this topic have been made ever since, and thus the species limits remain uncertain to date.

A second major issue in the *Leptodactylus latrans* group involves the specific limits of *L. chaquensis–L. macrosternum* and whether they correspond to a single species (De la Riva and Maldonado 1999; de Sá et al. 2014). These two species are considered morphologically cryptic and are only recognized by their allopatric distributions (but see De la Riva et al. 2000) and subtle differences in head shape (Gallardo 1964). *Leptodactylus chaquensis* is a well-known species with respect to aspects of reproduction and morphology and regarded as an abundant taxon distributed in the South American Gran Chaco (hereafter Chaco) and also in adjacent regions outside the Chaco of Bolivia and Brazil (Cei 1950, 1962; De la Riva and Maldonado 1999; de Sá et al. 2014). This species is distinguished from *L. latrans* by a few morphological characteristics (Gallardo 1964; Cei 1980; Langone 1995; Teixeira et al. 2017), but there are striking differences in their advertisement calls (Barrio 1966; Heyer and Giaretta 2009), male gametogenesis cycles (Cei 1948, 1950), and physiological (e.g., Cei and Bertini 1961; Cei and Cohen 1965) and serological data (Maxson and Heyer 1988).

On the other hand, there is not much evidence to help elucidate the identity and geographic distribution of *Leptodactylus macrosternum*, as information regarding its type locality is vague (Bahia province; Miranda-Ribeiro 1926). Bokermann (1966) stated that the type locality of *L. macrosternum* should probably correspond to the municipality of Salvador (Bahia state, in northeastern Brazil) or somewhere around the region of Salvador, where Mr. B. Bicego (a naturalist hired by the former Museu Paulista, currently Museu de Zoologia of the University of São Paulo; MZUSP) conducted field expeditions in 1896 and collected 13 representatives of the LCM complex (see Miranda-Ribeiro 1926, 1927). Interestingly, the presence of 10 dermal longitudinal folds is a feature that distinguishes *L. macrosternum* from all other morphs of *L. latrans* (exhibiting up to eight dermal longitudinal folds; Miranda-Ribeiro 1926) collected by B. Bicego in Bahia, but this was only discussed much later in Gallardo's (1964) review. However, the holotype of *L. macrosternum* (MZUSP 448, from a lot collected in 1896 by B. Bicego) is in fairly poor conditions of preservation and no longer exhibits such feature (Fig. 1), rendering us to rely solely on Miranda-Ribeiro's (1926) original description.

Cei (1950, 1962) and Gallardo (1964) analyzed several specimens belonging to the LCM complex and identified two clearly distinct morphotypes that co-occur in some regions of Brazil and Argentina: a large-sized morphotype with longer leg, single-lobed vocal sac, up to eight dermal longitudinal folds, and associated with humid areas in eastern South America (which is undoubtedly *Leptodactylus latrans*; referred therein as *L. ocellatus*); and a relatively smaller morphotype with shorter leg, bilobed vocal sac, 10 dermal longitudinal folds, and widely distributed across xeric environments in South America (features of specimens assigned to *L. chaquensis–L. macrosternum*; Gallardo 1964). Despite reaching similar conclusions regarding the distribution and specific limits of *L. latrans* (the larger morphotype), they did not agree on the identity and distribution of *L. chaquensis–L. macrosternum*.

Based on morphology and histological data, Cei (1962) identified the widespread smaller morphotype from the diagonal belt of open or seasonally dry formations (encompassing the Chaco, Cerrado, and Caatinga biomes; see Vanzolini 1968; Werneck 2011) and Amazonia (which he referred to as "forma amazônica" or Amazonian morph) as *L. chaquensis*, a claim that has recently been reinforced by acoustic evidence (Camurugi et al. 2017). Conversely, Gallardo (1964) concluded that the smaller morphotype from central, northern (e.g., northern Cerrado and Amazonia) and northeastern Brazil, also reaching the coast and Llanos of Venezuela, should be identified as *L. macro-*

Fig. 1.—Holotype of *Leptodactylus macrosternum*, MZUSP 448, from "Bahia province" (now, Bahia state), northeastern Brazil. (A) Dorsal, (B) ventral, and (C) lateral views of body. Scale = 1 cm. Photo provided by T. Grant, Museu de Zoologia, Universidade de São Paulo. A color version of this figure is available online.

sternum and elevated this name to full species status (originally described as a subspecies of "*Leptodactylus ocellatus*" by Miranda-Ribeiro 1926), also restricting the occurrence of *L. chaquensis* to Chaco and surrounding areas. At that time, the holotype of *L. macrosternum* was already in poor condition, and Gallardo (1964) based his conclusions on the analysis of topotypical specimens collected in Salvador (Bahia state) that differed from *L. latrans* (e.g., presence of bilobed vocal sac) and matched the original description of *L. macrosternum* (e.g., presence of 10 dermal longitudinal folds; Miranda-Ribeiro 1926). In many of his contributions on the identity and specific limits of *L. latrans–L. chaquensis*, Cei did not address the taxonomic status of *L. macrosternum* directly. After Gallardo's (1964) review, Cei (1970) corroborated the species status of *L. macrosternum* by means of biochemical and serological data, which also indicated a closer relationship between *L. chaquensis–L. macrosternum* in comparison with *L. latrans* (see also Cei 1962; Cei et al. 1967). Moreover, considering the shared morphological, histological, and physiological features between *L. chaquensis* and *L. macrosternum* (Gallardo 1964; Cei et al. 1967; Cei 1970), it is not surprising that these two taxa were recovered as sister groups in a recent total evidence phylogenetic analysis (de Sá et al. 2014), although it is still not clear how they can be precisely diagnosed morphologically, nor can their precise geographical ranges be delineated (De la Riva and Maldonado 1999; Heyer 2014). More recently, the taxonomic uncertainties related to *L. macrosternum* identity (especially because of the holotype poor preservation) led de Sá et al. (2014) to restrict its geographic range to the type locality until the relationships of the *L. latrans* group could be further evaluated.

As mentioned earlier, *Leptodactylus latrans* and *L. chaquensis–L. macrosternum* are distinguished by morphological (Cei 1950, 1962; Gallardo 1964; de Sá et al. 2014) and reproductive features (Cei 1948, 1950; Barrio 1966). The most comprehensive studies on the specific limits of the LCM complex are those of Cei (1950, 1962) and Gallardo (1964), which were mostly concordant regarding the distribution of *L. latrans* and the existence of a widespread smaller morphotype (*L. chaquensis–L. macrosternum*) that partially overlaps its distribution with that of *L. latrans*. Only one subsequent work attempted to establish specific limits of the LCM complex by assessing morphological variation for a set of specimens from sparse localities in South America (Heyer 2014). However, the existence of highly variable morphotypes and lack of genetic background hampered the recognition of species-specific traits at such a broad geographic scale. During the past decades, mitochondrial DNA has been used as a primer to establish genetic structure in zoological studies, especially if dealing with highly complex taxonomic groups with poorly understood specific limits (e.g., Fouquet et al. 2014; Gehara et al. 2014; Silva et al. 2020). Additionally, genetic information allows researchers to infer how morphological traits vary according to the genetic structure across the landscape (Posso-Terranova and Andrés 2018) and also test for specific limits (Pons et al. 2006; Funk et al. 2012; Barley et al. 2013).

Considering the intricate taxonomic history of the LCM complex, here we (1) assess the evolutionary lineages within the *Leptodactylus latrans* group (focusing on the LCM complex) and their geographic distribution, using samples obtained throughout their currently known geographic ranges; (2) test for species limits of populations/lineages using morphological, bioacoustic, and molecular data; (3) propose a multilocus molecular phylogeny including all species of the *L. latrans* group; and (4) update the taxonomic status of the LCM complex.

Materials and Methods

Taxon and Gene Sampling and Laboratory Procedures

Considering that specific limits of *Leptodactylus chaquensis–L. macrosternum* are not clear and that *L. latrans* may represent a species complex, our first strategy was to identify monophyletic evolutionary lineages through extensive mitochondrial DNA barcode sequencing. We amplified a 650 base-pair fragment of cytochrome c oxidase I (COI) mitochondrial gene (which is commonly used for such purposes; Hebert et al. 2003; Lyra et al. 2017) for all our newly sequenced 657 samples. Because cryptic species coexist along several localities in Brazil and Argentina (Cei 1962; Gallardo 1964), we sequenced from one to five individuals per locality to enhance the detectability of all lineages occurring in each locality. Additionally, we also gathered COI and 16S ribosomal RNA mitochondrial genes sequences available in GenBank for the *L. latrans* group, including that of the *L. latrans* neotype (MNRJ 30733; GenBank number KM091606) and all other sequences previously provided by Heyer and de Sá (2011) and de Sá et al. (2014). Our final genetic database (considering GenBank sequences) includes an extensive representation of the *L. latrans* group in South America (focusing on the LCM complex), with 728 terminals from 429 localities

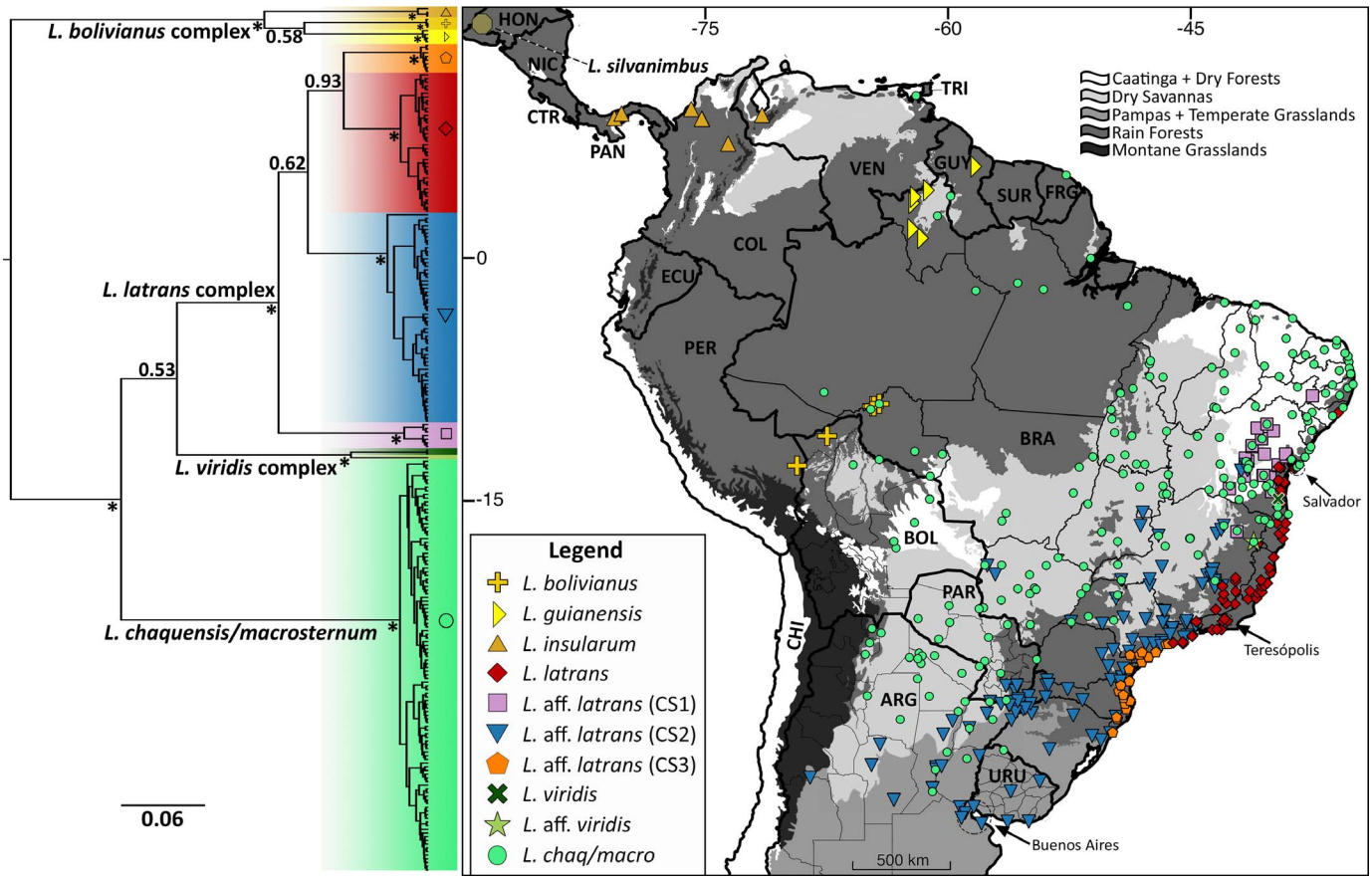

FIG. 2.—Geographic distribution of all genetic samples (mitochondrial + nuclear) from species belonging to the *Leptodactylus latrans* group in South America used herein (right); and COI mitochondrial gene tree recovered from a Bayesian inference analysis in BEAST (left). All clades highlighted are the major evolutionary lineages (putative species) recovered in both bGMYC and ABGD species delimitation analyses. Values on nodes indicate posterior probabilities. Asterisks on nodes denotes posterior probability = 1.0. Scale indicates rate of base substitutions per site. The municipalities of Salvador (Bahia state), Teresópolis (Rio de Janeiro state), and Buenos Aires (Buenos Aires province), relevant for the group taxonomic context, are indicated by arrows. *L. chaq/macro* = *L. chaquensis/macrosternum* lineage. South American country acronyms. ARG: Argentina, BOL: Bolivia, BRA: Brazil, CHI: Chile, COL: Colombia, CTR: Costa Rica, ECU: Ecuador, FRG: French Guiana, HON: Honduras, GUY: Guyana, NIC: Nicaragua, PAN: Panama, PER: Peru, PAR: Paraguay, SUR: Suriname, TRI: Trinidad and Tobago, URU: Uruguay, VEN: Venezuela. A color version of this figure is available online.

encompassing the entire currently know distribution of the *L. latrans* group (see Fig. 2 and Supplementary Material S1 in the Supplemental Materials available online, for all sampled localities and GenBank accession numbers). Additionally, we included samples from relevant localities considering the taxonomic history of LCM complex, such as *L. latrans* samples from the type locality, Teresópolis municipality, Rio de Janeiro state, samples from Salvador municipality, Bahia state and vicinities (*L. macrosternum* most likely type locality), and samples covering the Chaco (including *L. chaquensis* type locality, Tucumán Province).

We extracted DNA from muscle or liver tissues using ammonium (Maniatis et al. 1982) or sodium chloride (Bruford et al. 1992) salt precipitation methods. We conducted polymerase chain reaction (PCR) amplifications using Taq DNA Polymerase Master Mix (Ampliqon S/A, Denmark). For PCR protocols, we started with an initial denaturation cycle of 95°C for 3 min and finished with an extension cycle of 68°C for 5 min (specific annealing temperature and extension time for each primer pair are given in Table 1). In most occasions, we cleaned PCR products using enzymatic purifications (shrimp alkaline phosphatase and exonuclease I; Werle et al. 1994). We sent purified or unpurified PCR products to Macrogen Inc. (South Korea) for purification (when needed) and sequencing. We aligned all sequences using the MAFFT algorithm (Katoh et al. 2002) with the default parameters in Geneious v1.8.7 (Kearse et al. 2012). When needed, we pruned genes alignment to fit our shortest sequences prior to analyses.

Mitochondrial Evolutionary Lineages

To establish major mitochondrial evolutionary lineages (and therefore our putative species) based on the COI data set objectively, we implemented both tree-based and distance-based methods broadly used to delimit species based on single-locus mitochondrial DNA data sets. We used the Bayesian implementation of the generalized mixed Yule coalescent (GMYC) model to account for uncertainty in genealogy and model estimation with package bGMYC (Reid and Carstens 2012), in R v3.0.2 (R Core Team 2018). The GMYC method runs a model-based analysis to locate threshold points (or nodes) on the genealogy where there are transitions in branching rates, reflecting either inter- or intraspecific evolutionary processes, using ultrametric gene tree as input (Pons et al. 2006). Because the inclusion of identical sequences results in many zero length branches at

TABLE 1.—List of primers used in this study. COI = mitochondrial cytochrome c oxidase I; POMC = nuclear proopiomelanocortin; TYR = nuclear tyrosinase precursor.

Primer		Gene	Sequence	PCR Protocol	Reference
dgLCO1490	Forward	COI	GGTCAACAAATCATAAAGAYATYGG	[94 (30"), 48 (30"), 72 (40")] × 35	Meyer (2003)
dgHCO2198	Reverse	COI	TAAACTTCAGGGTGACCAAARAAYCA		
AnF1	Forward	COI	ACHAAYCAYAAAGAYATYGG		Lyra et al. (2017)
AnR1	Reverse	COI	CCRAARAATCARAADARRTGTTG		
16SA-L	Forward	16S	CGCCTGTTTATCAAAAACAT		Palumbi et al. (1991)
16SB-H	Reverse	16S	CCGGTCTGAACTCAGATCACGT		
Tyr I Lepto14	Forward	TYR	GTCSTGTCCAACTCTCCYGTG	[94 (30"), 58 (30"), 72 (40")] × 40	Fouquet et al. (2012)
Tyr E Lepto29	Reverse	TYR	CGTTGCTGGTTGGGTGGKTTC		
POMC_DRV_F1	Forward	POMC	ATATGTCATGASCCAYTTYCGCTGGAA	[94 (30"), 56 (30"), 72 (40")] × 40	Vieites et al. (2007)
POMC_DRV_R1	Reverse	POMC	GGCRTTYTTGAAWAGAGTCATTAGWGG		

the tip of the tree, which can cause the model to overpartition the data set (Reid and Carstens 2012), we maintained only unique haplotypes for the final BEAST gene tree (resulting in 235 terminals in the COI final alignment). To generate ultrametric trees used as input for the GMYC analysis, we ran the uncorrelated lognormal relaxed clock analyses for a 507 base-pair COI data set using BEAST v1.10.4 (Suchard et al. 2018), setting a fixed prior distribution of 0.01 for the *ucld.mean* parameter. For the bGMYC analysis, we used a post–burn-in sample of 100 trees to calculate the posterior distribution of the GMYC model. We set an upper bound for Yule and coalescent processes priors to 0.5 and 1.0, respectively, to obtain coalescence-to-Yule rates above 0, indicating a good model approximation to the reality of the data (Reid and Carstens 2012). We ran the bGMYC analysis for 100,000 generations, with a burn-in of 90,000 generations and a thinning interval of 100 samples. We used a threshold of 50% of conspecific probability to recognize genetic clusters delimited by the bGMYC model. We also implemented the automatic barcode gap discovery (ABGD) method, which relies on the overall pairwise differences of a given genetic distance matrix to automatically detect barcode gaps, using a range of intraspecific divergence priors, and sort sequences into candidate species (Puillandre et al. 2012). We used the same COI alignment employed in bGMYC and BEAST as input for ABGD. We set priors for minimum and maximum intraspecific divergence as 0.01 and 0.1, respectively, and relative gap width was set as 1.5. We used the default values for the remaining configuration settings. We selected the most constantly recovered groupings in the recursive partitions, as proposed by Puillandre et al. (2012).

TABLE 2.—Best-fitting partitioning scheme model of nucleotide substitution for COI gene tree and multilocus data set. COI = mitochondrial cytochrome c oxidase I; POMC = nuclear proopiomelanocortin; TYR = nuclear tyrosinase precursor; GTR = general time-reversible; F81 = Felsenstein (1981); TrN, TrNef = Tamura and Nei (1993); K80 = Kimura (1981).

Data set	Partition	Model
COI gene tree	COI first position	TrN + Γ
	COI second position	F81 + I
	COI third position	TrN + Γ
mtDNA + nuDNA	16S	GTR + Γ + I
	COI first position	TrN + Γ
	COI second position	F81 + I
	COI third position	TrN + Γ + I
	TYR and POMC first and second positions	F81 + I
	TYR and POMC third position	HKY + Γ + I

In search for all supported monophyletic clusters (posterior probability = 1.0), we generated a COI gene tree under a Bayesian framework with BEAST. We split the 507 base-pair COI alignment in three partitions, according to codon position (first, second, and third positions, 169 base pairs each), and used PartitionFinder2 (Lanfear et al. 2016) with the greedy algorithm, linked branch lengths and the Bayesian information criterion to select the best-fit partitioning scheme model of nucleotide substitution (Table 2). We then ran BEAST for 20 million generations, sampling every 2×10^3 generations, discarded the initial 25% generations and trees as burn-in, and assessed convergence (effective sample size > 200) with Tracer v1.7 (Rambaut et al. 2018). To generate the maximum credibility tree, we used TreeAnnotator v1.10.4 (Suchard et al. 2018; available at http://beast.community/treeannotator) and FigTree v1.4.2 (Rambaut 2014). We recognized major evolutionary lineages as those that: (1) were supported as candidate species by both distance and tree-based species delimitation analyses, (2) represented monophyletic groupings with significant support (posterior probability = 1.0), and (3) exhibited cohesive geographic distributions (e.g., distributed within a contiguous geographic range). This approach resulted in concordant sets of putative species, which we used in subsequent analyses (see Results).

For further examination of species boundaries and relationships, we sequenced fragments of the mitochondrial 16S gene (ca. 550 base-pair), and nuclear tyrosinase precursor (TYR, ca. 550 base-pair) and proopiomelanocortin (POMC, ca. 450 base-pair) genes for a subsample (115 specimens) of the COI data set representing both the genetic structure (including individuals from all divergent lineages) and geographic distribution (evenly sampling specimens along lineages geographic range). We provide all primer pairs and PCR protocols used for amplification of previously mentioned genes in Table 1.

Phylogenetic Relationships and Genetic Distances

To infer phylogenetic relationships and further investigate species boundaries, we created a final DNA alignment for 193 specimens (115 sequenced individuals plus GenBank-available sequences) encompassing all species currently included in the *Leptodactylus latrans* group (*L. bolivianus*, *L. chaquensis*, *L. guianensis*, *L. insularum*, *L. latrans*, *L. macrosternum*, *L. silvanimbus*, and *L. viridis*) and putative species identified early using the COI data set (see Results).

As outgroups, we used nine species representing the *L. fuscus* (*L. fuscus*, *L. longirostris*, and *L. mystaceus*), *L. pentadactylus* (*L. knudseni*, *L. labyrinthicus*, *L. pentadactylus*, and *L. rhodomystax*) and *L. melanonotus* species groups (*L. natalensis* and *L. podicipinus*). We built the full data set alignment based on the availability of the 16S rRNA gene because *L. latrans* neotype and *L. silvanimbus* lack the COI mitochondrial marker. The proportion of missing data for the whole data set is 30%. We split the full data set of 1945 base-pair into 10 partitions according to genome and transcript type (16S rRNA 520 base-pair; COI protein-coding mRNA 507 base-pair; TYR protein-coding nuDNA 511 base-pair; POMC protein-coding nuDNA 407 base-pair) and all protein-coding genes subdivided into codon position (first, second, and third). We used PartitionFinder2 with the greedy algorithm, linked branch lengths, and the Bayesian information criterion to select the best-fit partitioning scheme model of nucleotide substitution (Table 2).

We generated hypotheses of phylogenetic relationships among species of the *Leptodactylus latrans* group using maximum likelihood in RAxML v8.2.10 (Stamatakis 2014) and Bayesian inference in BEAST, implementing the best PartitionFinder2 scheme as substitution model prior. We obtained maximum-likelihood tree estimates with nodal support assessed via 1000 rapid bootstrap replicates. We considered nodal support significant or moderate for bootstrap values over 95% (Felsenstein and Kishino 1993) and 70% (Hillis and Bull 1993), respectively. For Bayesian inference, we ran BEAST analyses for 50 million generations, sampling every 5000 generations and discarding the initial 25% as burn-in. We assessed convergence (effective sample size $>$ 200) with Tracer v1.7, generated the maximum credibility tree with TreeAnnotator, and drew all phylogenetic trees using FigTree. We considered Bayesian posterior probability $>$0.95 as significant (Suchard et al. 2018). We regarded as valid those lineages recovered with significant nodal support, indicating reciprocal monophyly.

Additionally, we computed between-lineage mean distances using the Tamura-Nei (Tamura and Nei 1993) corrected *p*-distances with Molecular Evolutionary Genetics Analysis v6.0.6 (Tamura et al. 2013). For that, we employed the 507 base-pair COI alignment (235 terminals) and the 520 base-pair 16S alignment including all available sequences (184 terminals excluding outgroups). We defined groups by combining the results of both ABGD and bGMYC species delimitation methods (see below). GenBank accession numbers for all sequences are given in the Supplementary Material S1).

Morphology

We measured and analyzed 811 specimens belonging to the LCM complex, of which 273 corresponded to molecular vouchers (34% of our data set). Specimens without molecular data were assigned to the correct species based on combined information of morphology and geographic distribution (see Results). We excluded from subsequent analyses those individuals that occurred in sympatry zones and lacked molecular confirmation, were juveniles, or lacked any reliable diagnostic feature. We took the following measurements to the nearest 0.1 mm with digital calipers: snout–vent length (SVL), head width (between the center of tympanum membranes), head length (from the tip of the snout to the posterior margin of the tympanum), eye-to-snout distance (from the anterior margin of the eye to the tip of snout), eye-to-nostril distance (from the anterior margin of the eye to the posterior margin of the nostril), interocular distance (between the posterior margins of the eyes), eye diameter (taken horizontally between anterior and posterior margins of the eye), tympanum diameter (taken horizontally between anterior and posterior margins of the tympanum), hand length (from the wrist to the tip of Finger III), forearm length (from the elbow to the tip of Finger III), tibia length (from the outer edge of the knee to the outer edge of the heel), and foot length (from the distal border of the inner metatarsal tubercle to the tip of the Toe IV). We used the presence of thumb spines and vocal sacs/slits in males and presence of egg masses or absence of vocal slits in females for sex determination. Morphological nomenclature follows previous literature on Leptodactylidae (Heyer 1978; Heyer and de Sá 2011; de Sá et al. 2014). Specifically, nomenclature for dermal longitudinal folds (glandular crests on the dorsal surface of body and flank) follows de Sá et al. (2014), which are arranged as dorsal (Fold F1–3), dorsolateral (Fold F4), and lateral folds (Fold F5–6). Dorsal Fold F3 is also recognized as auxiliary fold (de Sá et al. 2014). Museum acronyms follow Sabaj (2016), and we provide a full list of specimens examined in Appendix I. Museum acronyms not included in Sabaj (2016) are amphibian collection of Universidade Federal de Uberlândia, Minas Gerais, Brazil (AAG-UFU); amphibian collection of Mapinguari Laboratory, Universidade Federal do Mato Grosso do Sul (MAP); and Universidade Federal do Triângulo Mineiro teaching collection, Uberaba, Minas Gerais, Brazil (UFTM).

Morphometry

To discriminate morphologically among the species sets (in the LCM complex) validated by our genetic data set, and to identify which variables contributed the most to their separation, we used a machine learning approach based on a random forest of decision trees (Breiman 2001). For this purpose, we created two data sets using only males: one data set with 177 individuals encompassing only measured individuals, the identities of which were confirmed by DNA barcoding (conservative approach), and another data set with 538 individuals encompassing both molecular and nonmolecular vouchers. The random forest algorithm implemented in the R package randomForest (Liaw and Wiener 2002) generates random classification trees by using bootstrap samples from the original data set to grow unpruned classification trees (usually 1000). Next, these trees are used to generate classifiers choosing the best splits based on a random sample of predictors. Finally, the algorithm uses these predictors aggregated to classify new data based on a majority rule. At each bootstrap step, it predicts the data not present in the bootstrap sample (out-of-the-bag samples) and aggregates these results at the end to generate an error estimate of the classification (for more detail see Liaw and Wiener 2002). The analysis also generates a measure of importance for each variable and a measure of the internal structure of the data. Variable importance is estimated based on the effect of permuting a variable while leaving others unchanged on prediction error. Our data set was inspected for univariate and multivariate outliers by using box plots and converting observations to Z

values, regarding those with $P(Z > |z|) < 0.0001$ as outliers. A few values (hand length for two individuals and eye-to-nostril distance for one individual) were substituted by NA values and imputed using missForest package in R (Stekhoven 2011). We detected three multivariate outliers (CFBH42701, CHUNB45658, and UFBA14331), which were dropped from further analyses.

Because classification error of preliminary analysis was high, we adjusted morphometric variables proportionally to body size favoring shape differences. For that, we defined body size as an isometric size variable (Rohlf and Bookstein 1987) following the procedure described by Somers (1986). We calculated an isometric eigenvector, defined a priori with values equal to $p^{-0.5}$, where p is the number of variables (Jolicoeur 1963), and obtained scores from this eigenvector, hereafter called Body Size, by postmultiplying the $n \times p$ matrix of $\log_{10}$-transformed data, where n is the number of observations, by the $p \times 1$ isometric eigenvector. Then, we removed the effect of size from the $\log_{10}$-transformed variables using Burnaby's method (Burnaby 1966). We postmultiplied the $n \times p$ matrix of the $\log_{10}$-transformed data by a $p \times p$ symmetric matrix L, defined as $L = I_p - V(V^TV)^{-1}V^T$, where I_p is a $p \times p$ identity matrix, V is the isometric size eigenvector defined above, and V^T is the transpose of matrix V (Rohlf and Bookstein 1987). This procedure lead to a better discrimination among groups, decreasing the out-of-the-bag estimates of error rate from 30–17% (results not shown).

We further assessed morphological variation and identified the best predictors of species/lineages with the guided regularized random forest analysis (Deng 2013). This approach is an enhanced regularized random forest method where importance scores of a previous run on a complete training data set are used to guide the predictor selection process. Importance scores are estimated by penalizing the selection of new predictors for splitting the decision tree when the gain (i.e., mean decrease in Gini impurity; Mingers 1989) is similar to that of features used in previous splits (Breiman 2001). To determine predictor importance in discriminating among species/lineages in the LCM complex, we implemented the guided regularized random forest analyses in the R package RRF (Deng 2013) on each imputed matrix, and calculated the average importance of each predictor across all runs. For each imputed matrix, we also calculated model accuracy based on 100 replicates of tenfold cross-validation (Breiman and Spector 1992), sequentially increasing the number of predictors based on their importance.

Bioacoustics

We recorded advertisement calls using Sennheiser K6/ME66 or K6/ME67 unidirectional microphones and digital recorders (Marantz PMD 670, 671; M-audio Microtrack 2; Tascam DR 40) set at sampling rates of 44.1 or 48.0 kHz and sample size of 16 bits. We deposited the recordings as uncompressed wave files in the acoustic repositories of AAG-UFU and CFBH collections, and Arquivos Sonoros da UFRN (ASUFRN). We provide additional information on sound recordings, including vouchers associated with calls, in Appendix II. We conducted the acoustic analysis in an expanded version (v0.9.6.1) of Soundruler (Gridi-Papp 2007), built as a package interfacing with Matlab v6.5.2 scripts (MathWorks, Natick, MA) through automated procedures that allow for unbiased quantification of acoustic traits. We present acoustic traits as averaged means for the males analyzed, and their corresponding standard deviation as standard deviations of the averaged mean values. We report ranges based on the total amplitude of values from the raw data set. We set parameters as follows: fast Fourier transform size = 1024 samples, fast Fourier transform overlap = 90%, window type = Hanning, contrast = 70%. Unless otherwise stated, we defined settings for automated recognition of signals as follows: detection smoothing = 400, resolution = 1; delineation smooth factor = 5, smoothing = 150, resolution = 1; critical amplitude ratio = –1 (disabled). For the "*Leptodactylus* aff. *latrans* CS1" lineage, we set the following parameters: detection smoothing = 500, resolution = 1; delineation smooth factor = 1, smoothing = 100, resolution = 1; critical amplitude ratio = 0.8. For the growl-type note of *L. macrosternum*, we set the following parameters: detection smoothing = 800, resolution = 1; delineation smooth factor = 1, smoothing = 50, resolution = 1; critical amplitude ratio = –1 (disabled).

We applied two band-pass filters (80-Hz high pass and 2000-Hz low pass) to sound files in Soundruler before conducting acoustic analyses to reduce background noise caused by rain, wind, roads, or insects and other frog species. We produced sonograms using seewave v2.1.0 (Sueur et al. 2008) and tuneR v1.3.2 (Ligges et al. 2017) in R v3.5.0 (R Core Team 2018), with the following settings: window = Hann, fast Fourier transform size = 1024 samples, fast Fourier transform overlap = 90% (except for the call of *Leptodactylus viridis*: fast Fourier transform size = 512 samples; fast Fourier transform overlap = 99%); the intensity of frequency components is indicated by their darkness in a relative 36-dB scale. We quantified the following acoustic traits: note length (time from 10% attack minus that at 10% decay, relative to call maximum amplitude, i.e., 100%), note rise time (time from beginning of call to point of maximum amplitude; given in %), dominant frequency (frequency with the greatest energy), frequency modulation (dominant frequency at 10% attack minus that at 10% decay, relative to the maximum amplitude of the note, i.e., 100%); pulse rate (pulse number minus 1, divided by the duration of peak-to-peak from first to last pulse of the note). The acoustic terminology used in call descriptions follows Littlejohn (2001).

RESULTS

Mitochondrial Evolutionary Lineages

We identified five major mitochondrial lineages belonging to the LCM complex with significant node supports in the Bayesian analysis (posterior probability = 1.0), cohesive geographic distributions (mostly nonoverlapping, with few sympatry zones), and supported as independently evolving species in the delimitation analyses (Figs. 2 and 3). Two lineages within *Leptodactylus viridis* and three lineages from the *L. bolivianus* complex were also well supported (Fig. 3), totaling 10 major evolutionary lineages in the *L. latrans* group (*L. silvanimbus* not included in the COI data set). These results support the following taxonomic arrangement:

Nominal *Leptodactylus latrans*.—We sampled 94 individuals assigned to the nominal lineage of *L. latrans*,

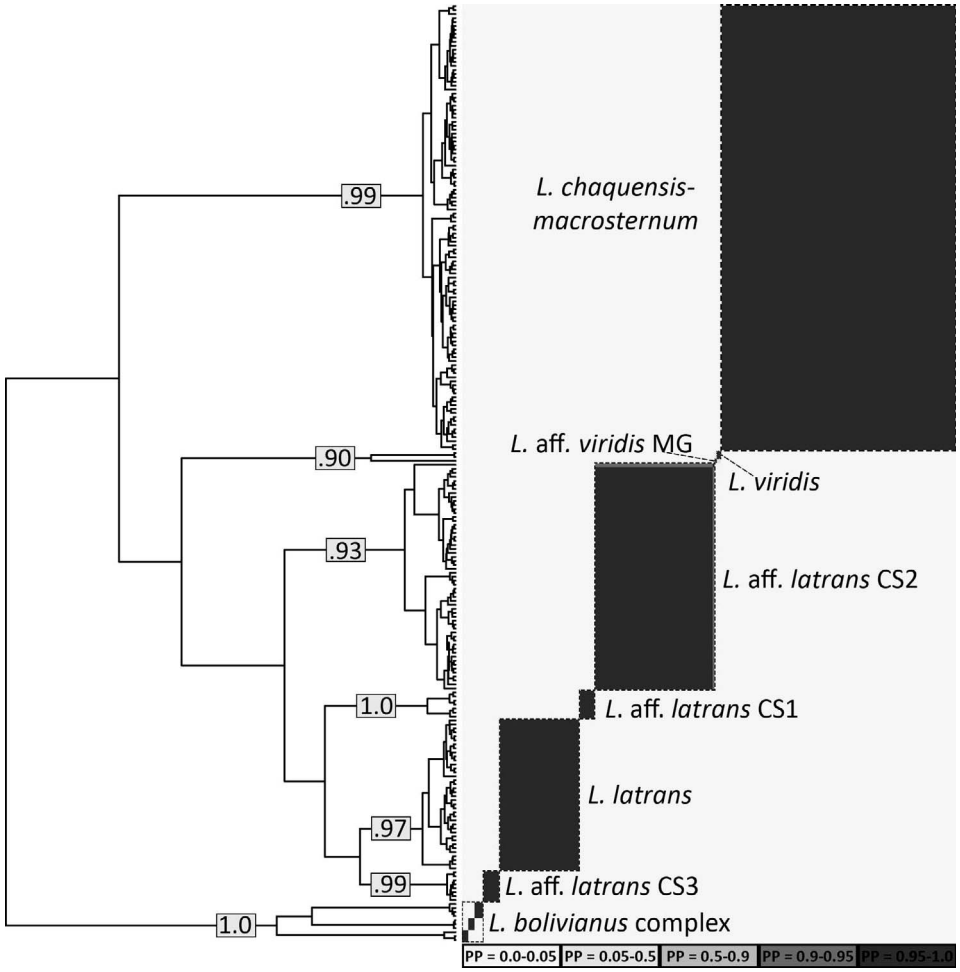

FIG. 3.—Summary of species delimitation analyses using Bayesian implementation of the generalized mixed Yule coalescent model for species in the *Leptodactylus latrans* group. The topology represents the maximum clade credibility cytochrome c oxidase I (COI) gene tree from BEAST. The genetic clusters identified by the automatic barcode gap discovery (ABGD) analysis are outlined with dashed contours. Numbers along branches are the posterior probability of species identities sampled from a posterior distribution of 100 trees generated in BEAST. The gray-scale plot is a sequence-by-sequence matrix colored by pair-wise posterior probabilities of conspecificity, where off-diagonal patterns indicate uncertainty of species limits owing to topological variation of phylogenetic tree. A color version of this figure is available online.

including samples from the type locality (Teresópolis municipality, Rio de Janeiro state; Fig. 2). Individuals belonging to this lineage are mostly distributed along the coastal Atlantic Forest, from Maceió municipality, Alagoas state to Bertioga municipality, São Paulo state. This lineage is found from sea level to higher-elevation zones (~600–900 m) in the Serra do Mar range of Rio de Janeiro state, and in the "Zona da Mata Mineira" region of southeastern Minas Gerais state.

The *Leptodactylus* aff. *latrans* CS1 lineage.—We sampled a total of 50 individuals assigned to the *L.* aff. *latrans* CS1 lineage. Individuals belonging to this lineage are restricted to Chapada Diamantina mountain range and vicinities, east of the São Francisco River in Bahia state, with single occurrence records in Minas Gerais and Pernambuco states.

The *Leptodactylus* aff. *latrans* CS2 lineage.—We sampled 163 individuals assigned to the *L.* aff. *latrans* CS2 lineage. Individuals belonging to this lineage are distributed from San Juan province, southwestern Chaco through the Humid Pampas in Argentina, Uruguay, and southern Brazil (all low-elevation areas below 100 m), and across the Atlantic Forest through high-elevation localities (west of Serra do Mar; reaching 1400 m) from Santa Catarina state to southern Chapada Diamantina in Bahia state. This taxon apparently exhibits a disjunct distribution in the Pantanal (Mato Grosso do Sul state), considering that the closest locality with taxa related to this population is located about 600 km (e.g., areas of Cerrado in western Minas Gerais).

The *Leptodactylus* aff. *latrans* CS3 lineage.—We sampled 31 individuals assigned to the *L.* aff. *latrans* CS3 lineage. Individuals belonging to this lineage are restricted to the southeastern coastal Atlantic Forest region from Santos municipality (São Paulo state) to northeastern Rio Grande do Sul state, associated with low-elevation areas (up to 500 m), east of the Serra do Mar mountain range.

The *Leptodactylus chaquensis/macrosternum* lineage.—Samples identified as *L. chaquensis* (Chaco) and *L. macrosternum* (Salvador municipality and vicinities) were clustered into a single clade. We sampled a total of 350 individuals assigned to a single geographically cohesive and broadly distributed lineage, with a range spanning more than

4000 km from southern Santa Fe province (Argentina) to the Guiana Shield of Roraima state (Brazil), also reaching the northern and northeastern Brazilian coast. This lineage is associated with biomes along the open diagonal in South America (Cerrado, Chaco, Pantanal, and Caatinga), as well as many areas of Amazonian and the Atlantic rainforests.

The *Leptodactylus bolivianus* complex.—Samples sequenced by us from Roraima and those from Rondônia states clustered with *L. guianensis* and *L. bolivianus*, respectively, and are within the known range of these species, whereas all our *L. insularum* samples were retrieved from GenBank. Accordingly, our delimitation analyses supported the existence of three distinct species, corroborating the recent taxonomic arrangement for the *L. bolivianus* complex (Heyer and de Sá 2011).

***Leptodactylus viridis*.**—We only sampled three specimens of *L. viridis*: two from Bahia state (the nominal lineage) and one from Minas Gerais state. Surprisingly, these populations are genetically and geographically (separated by the Jequitinhonha River) structured and the latter lineage was recovered as a putative new species (Fig. 3), which we regard as *L.* aff. *viridis*.

In the next section, we will treat the lineages within the LCM complex as follows: *Leptodactylus latrans* complex, formed by the nominal *L. latrans* and three candidate species CS1–3; *L. chaquensis/macrosternum*, formed by the species pair *L. chaquensis–L. macrosternum*, now treated as a single evolutionary entity (these groupings are depicted in Fig. 2).

Phylogenetic Relationships and Genetic Distances

Phylogenetic relationships.—Both Bayesian and maximum-likelihood approaches yielded phylogenies with identical topologies (Fig. 4), which overall matched the COI topology and the previously published phylogeny for the *Leptodactylus latrans* group (de Sá et al. 2014), except that de Sá et al. (2014) did not include representatives of *L.* aff. *viridis*, *L. guianensis*, or *L.* aff. *latrans* CS1 and CS3 lineages. In de Sá et al. (2014), their *L. macrosternum* (Lineages 1 and 2) and *L. chaquensis* were considered distinct entities, which instead clustered within a single lineage in our topology. Likewise, both *L. latrans* neotype and their *L. latrans* Lineage 1 clustered within our nominal *L. latrans* lineage, whereas their *L. latrans* Lineage 2 clustered within our *L.* aff. *latrans* CS2 lineage. However, differences in phylogenetic inference methods, molecular markers, partitioning schemes, and geographic sampling renders further comparisons of phylogenetic relationships and node support between de Sá et al. (2014) and our results inappropriate.

The Bayesian topology was highly supported (all ingroup nodes with posterior probability = 1.0), except for the relationships between *Leptodactylus silvanimbus* and other ingroups (posterior probability = 0.67). Likewise, we obtained moderate to significant bootstrap scores in the maximum-likelihood analysis, except for the phylogenetic relationships within the *L. bolivianus* complex clade (bootstrap score = 60). Compared to the COI data set, we also recovered as monophyletic the *L. bolivianus* complex (posterior probability = 1.0/bootstrap score = 100) and the clade formed by *L. viridis*, *L. chaquensis/macrosternum*, and *L. latrans* complex (posterior probability = 1.0/bootstrap score = 94). Within this last clade, *L. viridis* was recovered as sister to the clade containing *L. chaquensis/macrosternum* and the *L. latrans* complex (posterior probability = 1.0/bootstrap score = 75), and the *L. latrans* complex monophyly was highly supported (posterior probability= 1.0/bootstrap score = 96). All 10 mitochondrial lineages (putative species) recovered in the COI data set had high support values (posterior probability = 1.0/bootstrap score = 100) in both analyses (Bayesian and likelihood), therefore confirming that these clades are reciprocally monophyletic and supported as distinct evolutionary entities. A fully expanded version of Fig. 4 is presented in Supplementary Material S2 (in the Supplemental Materials available online).

Genetic distances.—The average genetic distance between species in the *Leptodactylus latrans* group was 8% and 14% for the 16S and COI mitochondrial genes, respectively. The lowest average genetic distances within the whole data set were between *L. latrans* and *L.* aff. *latrans* CS3 (~4 and 8% for 16S and COI, respectively), whereas the overall average genetic distance within the *L. latrans* complex varied between 4 and 9% and 8 and 16% for 16S and COI, respectively (Table 3). Within all lineages, the genetic distance did not exceed 2 and 5% for 16S and COI, respectively. Unexpectedly, this also occurred in the *L. chaquensis/macrosternum* lineage in which taxa are separated by almost 4000 km (e.g., from southern Chaco in Argentina to Guiana Shield populations in Brazil) and genetic distance for COI mitochondrial gene only varied between 2 and 3%. Moreover, the ABGD analyses identified that the most likely transition point between intra–interspecific genetic distances is around 5–6% for the COI data set (see Fig. 5).

Morphology

After establishing our evolutionary lineages, we searched for morphological/chromatic and morphometric traits that could support genetic clusters and aid in species identification within the LCM complex. Considering that species external morphology is conserved although exhibit highly variable polychromatic patterns, we attempted to identify which features are present or absent in each lineage qualitatively (a summary of these features is provided in Table 4).

Dermal longitudinal folds.—Dermal longitudinal folds (Fig. 6) have long been used as diagnostic characteristics in *Leptodactylus* (Heyer 1978; de Sá et al. 2014) and are useful for the recognition of species in the *L. latrans* group (Miranda-Ribeiro 1926; Gallardo 1964). For instance, all species belonging to the *L. bolivianus* complex lack Folds F1–F3, differing from species of the *L. latrans* complex and the *L. chaquensis/macrosternum* lineage (F1–F3 present; Fig. 7A; see Heyer and de Sá 2011; de Sá et al. 2014) and *L. viridis* (F1–F2 barely discernible or absent, and F3 absent; Fig. 7B; Jim and Spirandeli-Cruz 1979; de Sá et al. 2014). Gallardo (1964) mentioned that all specimens associated with *L. latrans* (referred therein as *L. ocellatus*) exhibited four dermal longitudinal folds on each side of the body, whereas *L. chaquensis* and *L. macrosternum* exhibited five. Upon the examination of >800 specimens and several pictures of live specimens of both clades (e.g., the *L. latrans* complex and *L. chaquensis/macrosternum*), we noticed that all individuals belonging to the *L. latrans* complex clade

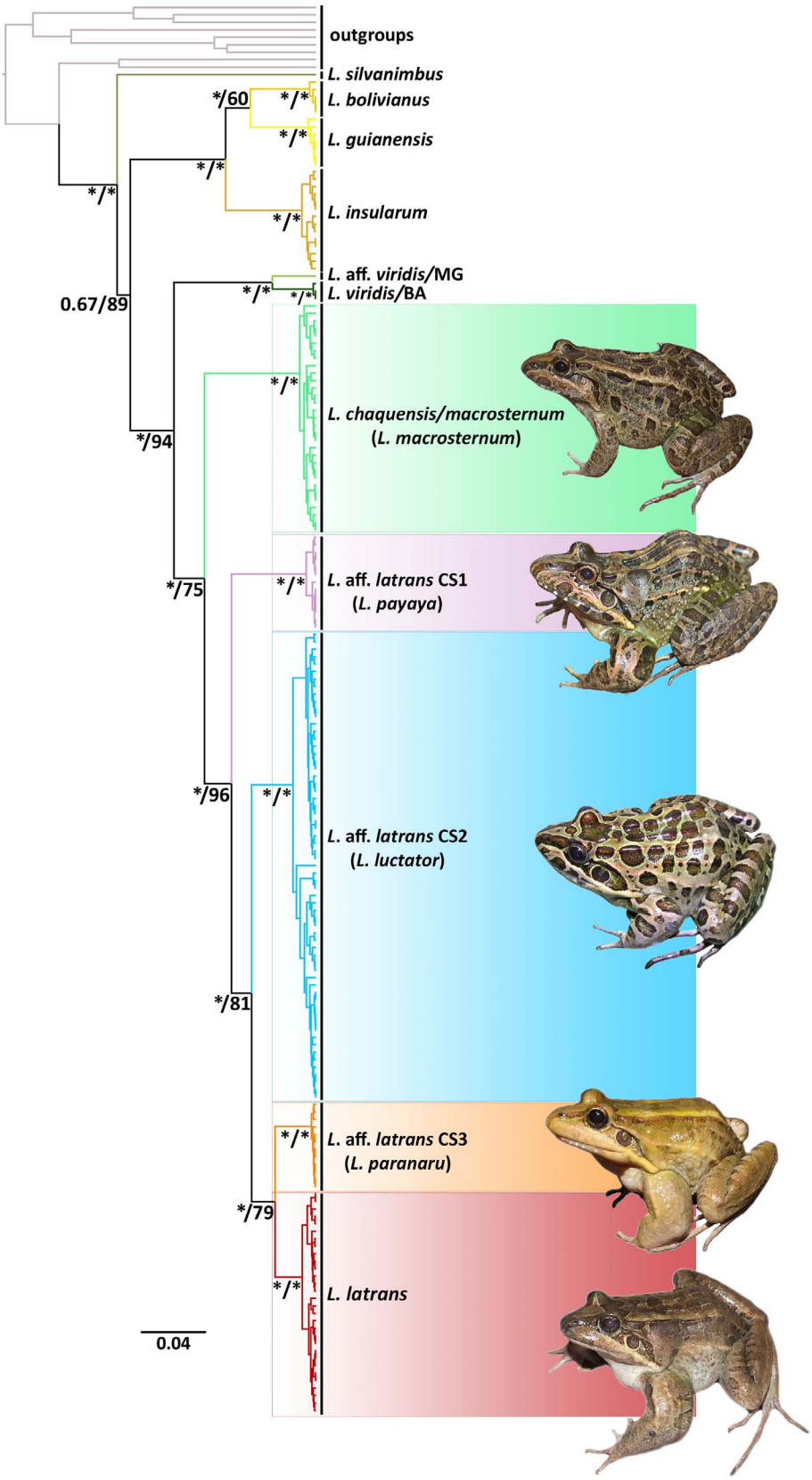

FIG. 4.—Phylogenetic relationships in the *Leptodactylus latrans* species group as estimated by a Bayesian inference (BEAST) and maximum-likelihood (RAxML) analyses of partitioned mitochondrial 16S rRNA, cytochrome c oxidase I (COI) mRNA, nuclear tyrosinase precursor (TYR), and proopiomelanocortin (POMC) genes. Values below nodes indicate Bayesian posterior probabilities and bootstrap values from maximum-likelihood analysis. Asterisks indicate posterior probabilities/bootstrap values = 1.0/100. Scale indicates rate of base substitutions per site. Colors on branches refer to the same evolutionary lineages recovered in the delimitation analyses. A color version of this figure is available online.

TABLE 3.—Average between-groups genetic distances of *Leptodactylus latrans* species group using the corrected *p*-distance Tamura-Nei model for the mitochondrial cytochrome c oxidase I (COI, below diagonal) and 16S (above diagonal) mitochondrial genes. The lower line is empty because no COI sequences were available for *L. silvanimbus*. Genetic distances among species in the *L. latrans* complex are highlighted in bold. Lineages are CS1–3 and CM (*chaquensis/macrosternum*).

		1	2	3	4	5	6	7	8	9	10	11
1	*L. guianensis*	—	0.07	0.09	0.17	0.16	0.16	0.17	0.15	0.19	0.18	0.22
2	*L. bolivianus*	0.13	—	0.06	0.13	0.13	0.13	0.14	0.12	0.16	0.16	0.18
3	*L. insularum*	0.15	0.16	—	0.14	0.14	0.14	0.15	0.11	0.15	0.15	0.15
4	*L. latrans*	0.21	0.21	0.26	—	**0.07**	**0.06**	**0.04**	0.08	0.15	0.14	0.19
5	*L. payaya* (CS1)	0.24	0.23	0.26	**0.15**	—	**0.09**	**0.06**	0.09	0.14	0.15	0.19
6	*L. luctator* (CS2)	0.2	0.2	0.24	**0.13**		—	**0.06**	0.09	0.15	0.15	0.18
7	*L. paranaru* (CS3)	0.21	0.21	0.27	**0.08**	**0.13**	**0.10**	—	0.09	0.17	0.16	0.18
8	*L. macrosternum* (CM)	0.19	0.18	0.2	0.2	0.18	0.17	0.17	—	0.15	0.13	0.18
9	*L. viridis*	0.19	0.23	0.24	0.2	0.18	0.19	0.18	0.19	—	0.06	0.19
10	*L.* aff. *viridis*	0.22	0.22	0.24	0.19	0.21	0.2	0.2	0.2	0.09	—	0.19
11	*L. silvanimbus*	—	—	—	—	—	—	—	—	—	—	—

exhibit eight well-developed dermal longitudinal folds (F2, F4, F5, and F6; Figs. 6 and 7C) and predominantly lack the auxiliary fold (F3; de Sá et al. 2014). If present, the auxiliary fold is short, not reaching the midlength of the body (Figs. 6A, 7C). Further, similarly to the Fold F1, the auxiliary fold (F3) is followed or formed entirely by a row of tubercles in the *L. latrans* complex (see Figs. 6A, 7C). In contrast, specimens of the *L. chaquensis/macrosternum* lineage exhibit eight well-developed dermal longitudinal folds (F2, F4, F5, and F6) and a long and well-discernible auxiliary row that extends from behind the eye to midlength of the body (see Fold F3; Fig. 6B), totaling 10 folds (not considering F1, which is formed by a row of tubercles). This auxiliary fold might be short or interrupted in some individuals of *L. macrosternum* (variation depicted in Fig. 7D–F). These results reinforce Gallardo's (1964) observations that the arrangement of dermal longitudinal folds (specifically the auxiliary fold) is useful for species recognition in the LCM complex. Moreover, the Fold F2 extends from the interocular ocellated blotch region (as depicted in Fig. 6A) or posterior to the interocular ocellated blotch region (as depicted in Fig. 6B) to the pelvic region. The lateral folds (F5–F6) can be either complete or interrupted. The lateral Fold F5 can be further characterized as long (extending from above arm insertion to groin; Fig. 6A) or short (extending from mid-length of body to groin; Fig 6B). Variation in the dermal folds F2, F5, and F6 was observed in specimens from all lineages in the LCM complex and are not useful to distinguish species. It is worth mentioning that these dermal structures seem to fade in preserved specimens, especially those already preserved for decades (e.g., the holotype of *L. macrosternum*). Therefore, it is desirable to assess this morphological feature from live (including pictures) or recently preserved specimens for a more accurate species identification.

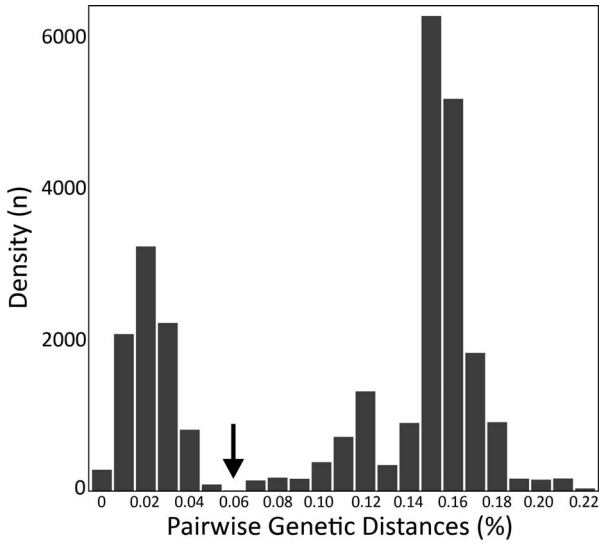

FIG. 5.—Pairwise genetic distances (x-axis) for all sequences of the COI data set from the *Leptodactylus latrans* species group showing the transition point (gap pointed by arrow) between intraspecific (left) and interspecific genetic (right) distances as identified by the automatic barcode gap discovery (ABGD) analysis. A color version of this figure is available online.

Thigh coloration.—Coloration of the thigh posterior surface in live specimens is highly variable within clades of the LCM complex. We found at least 15 distinct coloration hues varying among blue, gray, green, and yellow shades (some depicted in Fig. 8A–F). Nevertheless, we were able to associate exclusive color shades to evolutionary lineages in the LCM complex. The posterior thigh coloration of nominal *Leptodactylus latrans*, *L.* aff. *latrans* CS2 and CS3 lineages, ranges from blue/cyan to gray shades exhibiting either black blotches or well-marked maculated patches in the background (Fig. 8A,B), or without any black pigmentation. However, yellow shades on posterior thigh is an exclusive feature of *L.* aff. *latrans* CS2 (see Fig. 8F). The green coloration on posterior thigh (Fig. 8C) is a feature that has long been associated with the *L. chaquensis/macrosternum* lineage (Cei 1950; Gallardo 1964). However, we found that the shades of green on posterior thigh is a feature shared with specimens of the *L.* aff. *latrans* CS1 (Fig. 8D). This feature was also observed among specimens of the *L.* aff. *latrans* CS2 lineage (only observed in one unvouchered specimen from Minas Gerais state), but the green coloration is not as distinctive when compared to the brown shades on the dorsal surface of thigh, as exhibited in *L. chaquensis/macrosternum* and *L.* aff. *latrans* CS1 (Fig. 8C, D). Finally, *L.* aff. *latrans* CS1 only exhibited green/gray shades on posterior thigh with black blotches (not maculated patches) in the background (Fig. 8D,E).

Dorsal coloration.—Dorsal and dorsolateral body pigmentation is also a highly variable feature within and among the evolutionary lineages in the LCM complex. All

TABLE 4.—Summary of morphologic features relevant for species discrimination in the *Leptodactylus latrans* complex and *L. macrosternum*. Lineages are CS1–3 and CM (*chaquensis/macrosternum*). Ranges of body sizes (snout–vent length [SVL] in millimeters) are presented as range (mean ± SD). *n* = total number of measured individuals/measured individuals being molecular vouchers. Random Forest best predictors of morphometric variation expressed relative to head length and snout-to-vent length (SVL); presented as range (mean ± SD).

Variables	*L. latrans*	*L. payaya* (CS1)	*L. luctator* (CS2)	*L. paranaru* (CS3)	*L. macrosternum* (CM)
Male *n*	96/26	42/23	136/44	17/9	136/44
Female *n*	45/25	12/12	51/12	10/7	155/38
Male SVL	63.2–124.9 (95.8 ± 13.9)	58.5–96.9 (84.5 ± 8.2)	72.7–121.6 (95.1 ± 10.3)	78.9–126.3 (100 ± 12.7)	48.7–98.9 (74.4 ± 9.0)
Female SVL	61.4–104.7 (89.8 ± 8.2)	72.6–93.6 (83.3 ± 7.4)	73.9–115.8 (91.2 ± 7.8)	75.2–106.3 (88.7 ± 9.7)	55.9–90.8 (74.0 ± 7.3)
Number of folds on body	8	8	8	8	10
Auxiliary fold (F3)	Absent	Predominantly absent or short	Predominantly absent or short	Absent	Long and complete, interrupted or short
Posterior thigh coloration	Blue or gray	Green or gray	Yellow, blue, or gray	Blue or gray	Green or gray
Black pigmentation on posterior thigh	Strongly marked maculated, scattered blotches or absent	Scattered blotches or absent	Strongly marked maculated, scattered blotches or absent	Strongly marked maculated, scattered blotches or absent	Absent
Ocellated blotches on dorsum	Smooth or scattered and poorly marked	Scattered/evenly distributed and strongly marked	Scattered/evenly distributed and strongly marked	Smooth or scattered and poorly marked	Scattered/evenly distributed and strongly marked
Well-marked outline blotches on dorsum	Absent	Absent	Present	Absent	Present
Black pigmentation on underside thigh	Mottled or absent	Mottled or absent	Mottled, strongly marked maculated or absent	Mottled or absent	Absent
Yellow melanophores on belly and thigh	Absent	Absent	Present	Absent	Absent
Vocal sac	Single-lobed	Single-lobed	Single-lobed	Single-lobed	Bilobed
Male tympanum diameter/head length ratio	0.15–0.21 (0.19 ± 0.01)	0.18–0.23 (0.20 ± 0.01)	0.18–0.24 (0.21 ± 0.01)	0.14–0.20 (0.17 ± 0.02)	0.17–0.26 (0.22 ± 0.02)
Female tympanum diameter/head length ratio	0.14–0.21 (0.17 ± 0.01)	0.18–0.21 (0.20 ± 0.01)	0.18–0.24 (0.22 ± 0.01)	0.14–0.19 (0.17 ± 0.02)	0.18–0.27 (0.21 ± 0.01)
Male foot length/SVL ratio	0.48–0.65 (0.56 ± 0.03)	0.44–0.61 (0.54 ± 0.04)	0.44–0.62 (0.54 ± 0.03)	0.49–0.60 (0.55 ± 0.03)	0.42–0.60 (0.51 ± 0.03)
Female foot length/SVL ratio	0.51–0.65 (0.55 ± 0.03)	0.46–0.57 (0.52 ± 0.04)	0.46–0.63 (0.54 ± 0.03)	0.53–0.60 (0.55 ± 0.03)	0.39–0.60 (0.51 ± 0.04)

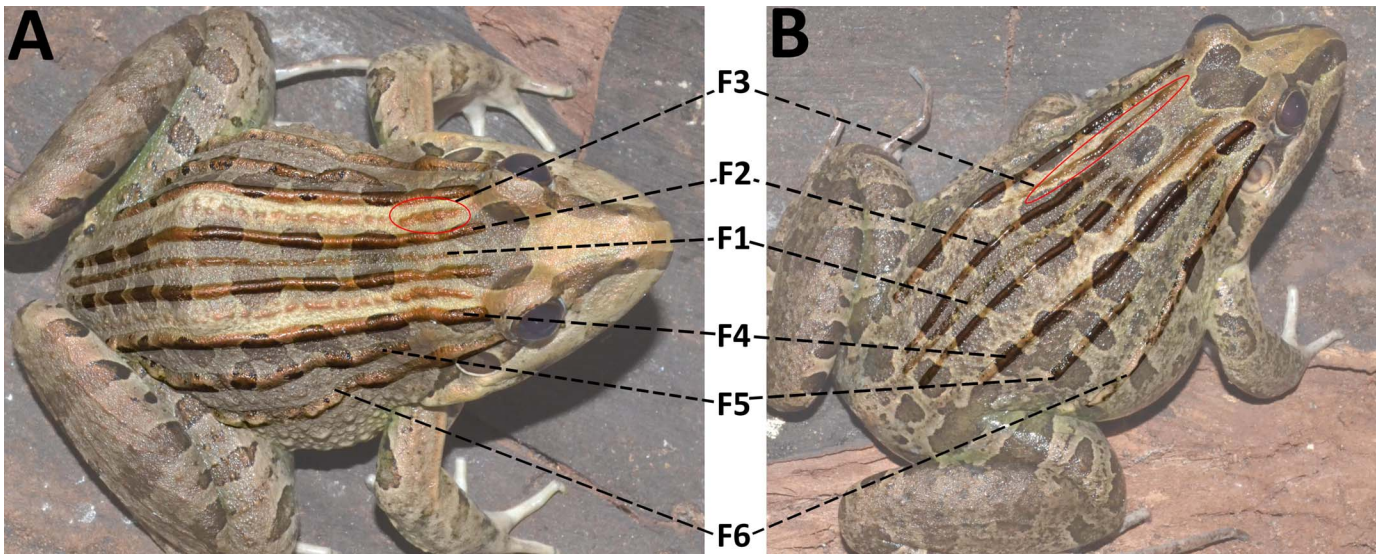

Fig. 6.—Dermal longitudinal folds depicting the variation on dorsal Fold F3 (or auxiliary fold, depicted by red circles): (A) short auxiliary fold followed by rows of tubercles in *Leptodactylus payaya* (CS1 lineage, CHUFPB 28193); and (B) long and complete auxiliary folds in *L. macrosternum* (*chaquensis/macrosternum* lineage, CHUFPB 28185) collected syntopically in Jacobina municipality, Bahia state, Brazil. F1–3 are dorsal, F4 is dorsolateral, and F5–6 are lateral folds as proposed by de Sá et al. (2014). A color version of this figure is available online.

specimens exhibit a conspicuous interocular ocellated blotch variable in shape and size. Such blotches are also present along the dorsal and dorsolateral regions of the body. We identified three main body pigmentation patterns related to the arrangement of the blotches for specimens in the LCM complex: (1) blotches overall absent, with only a few light brown and faded blotches or ocellated blotches scattered distributed on dorsum (smooth pattern, Fig. 9A); (2) light to dark brown blotches (with distinct shapes), or ocellated blotches sparsely or evenly distributed on dorsum (Fig. 9B); and (3) several well-marked dark brown ocellated blotches outlined by a light-cream colored ring evenly distributed on dorsum (Fig. 9C,D). As identified in posterior thigh coloration, we were also able to associate exclusive patterns of dorsal coloration with evolutionary lineages. For instance, we identified that *Leptodactylus latrans* and *L.* aff. *latrans* CS3 only exhibited patterns 1 and 2, with Pattern 1 mostly exclusive to these lineages. Only two out of hundreds examined specimens of *L.* aff. *latrans* CS2 (AAG-UFU 1680; Fig. 7C), and an unvouchered individual from Araguari, Minas Gerais exhibited Pattern 1. Likewise, Pattern 3 was only observed in specimens of the *L.* aff. *latrans* CS2 and *L. chaquensis/macrosternum* lineages. The *L.* aff. *latrans* CS1 lineage only exhibited Pattern 2.

Ventral coloration.—We considered the coloration of the ventral surface of thigh as part of the ventral color patterns described here. Patterns are also highly variable within and among lineages. Overall, ventral pigmentation can be entirely light beige lacking black pigmentation (as depicted in Fig. 10A,B) or mottled with dark gray/brown patches and blotches distributed along belly and thigh surfaces (as depicted in Fig. 10C,D). Two distinct patterns were only observed in representatives of the *Leptodactylus* aff. *latrans* CS2 lineage: (1) a gray or light beige mottled pigmentation pattern, with several circular yellow melanophores from the gular region to the belly, and (2) a well-marked black maculated patch along the ventral surface of the thigh (both depicted in Fig. 10E,F). The latter coloration pattern is mostly observed among specimens from southernmost populations (e.g., Argentina, Uruguay, and southern Brazil) and Pantanal populations of the lineage CS2. Moreover, *L. chaquensis/macrosternum* does not exhibit patterns depicted in Figs. 10D–F, as pigmentation is mostly light beige on belly and underside surfaces of thigh, lacking any black pigmentation (Fig. 10B).

Thumb spines.—The number and shape of thumb spines has also been used as a diagnostic trait for some species of the *Leptodactylus latrans* group. For instance, both *L. bolivianus* and *L. guianensis* exhibit one thumb spine on each hand (Heyer and de Sá 2011), distinguishing them from *L. insularum*, which has two spines on each thumb, and the spine shape is the main external character that distinguishes morphologically the two former species (Heyer and de Sá 2011). However, males of all clades in the LCM complex always exhibit two spines on hand. We found three distinct shapes for thumb spines in the LCM complex: (1) thumb spines with triangular shape and pointed tips (Fig. 11A), (2) thumb spines longer than wide with rounded tips (e.g., conical shape, Fig. 11B,D), (3) thumb spines wider than long with flattened and slightly rounded tips (e.g., rectangular shape, Fig. 11C). These patterns are variable within and among individuals, as well as among lineages. Therefore, thumb spine features do not constitute unique traits of any of the lineages within the LCM complex.

Vocal sac.—As proposed by Gallardo (1964), the vocal sac morphology is a useful characteristic that helps distinguish species belonging to the *Leptodactylus latrans* complex and *L. chaquensis/macrosternum*, but it is barely evident externally, especially in preserved specimens. All males from the *L. latrans* complex exhibit a single-lobed vocal sac that do not expand laterally, whereas males from the *L. chaquensis/macrosternum* lineage exhibit a bilobed vocal sac that slightly expands laterally (Fig. 11D; see also Santos and Cechin 2008). Moreover, throat coloration of adult

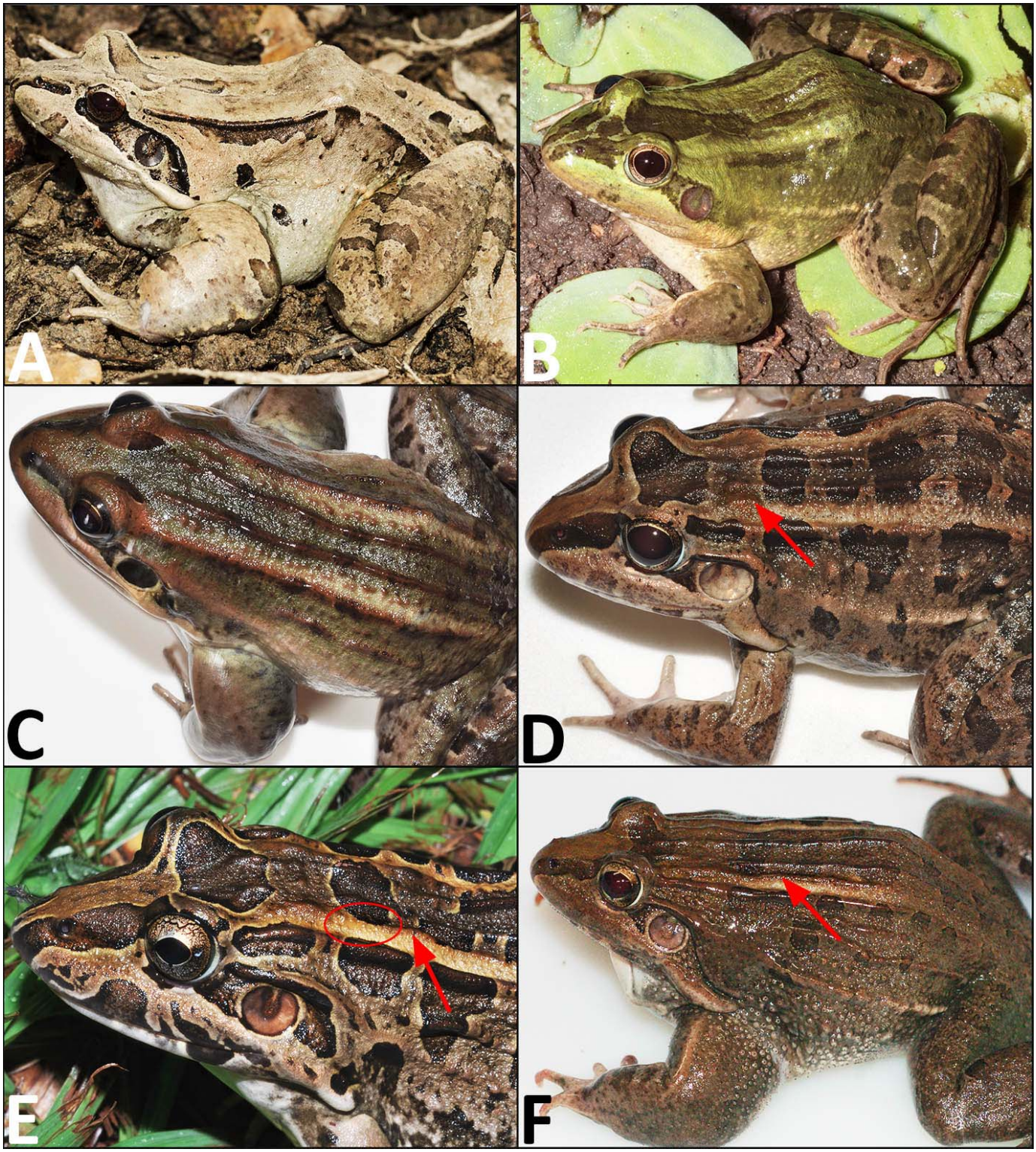

FIG. 7.—Variation of dermal longitudinal folds in species of the *Leptodactylus latrans* group. Dorsal folds (F1–F3) absent or barely discernible in (A) *L. guianensis* (INPA-H036479 from Serra da Mocidade, Roraima), photo by Haroldo Palo, Jr.; and (B) *L. viridis* (CFBH29605), photo by P. Peloso. Dorsal folds well discernible: (C) with developed row of tubercles in *L. luctator* (CS2 lineage, AAG-UFU1680). Auxiliary fold variation (F3, indicated by arrows) in *Leptodactylus macrosternum*: (D) short (AAG-UFU5273), (E) long and interrupted (depicted by circle, unvouchered from Araguari, Minas Gerais), and (F) long and complete (unvouchered from Belém, Pará). See Appendix I for locality data of analyzed vouchers. A color version of this figure is available online.

males is also useful for lineage discrimination. The anterior throat is homogeneously dark gray in male specimens of the *L. latrans* complex (Fig. 11A–C; see also Fig. 10C), whereas the homogeneous dark gray pigmentation or brown–gray blotches are absent in *L. chaquensis/macrosternum* (Fig. 11D).

Morphometric variation.—Both morphometric data sets yielded identical results regarding variable importance

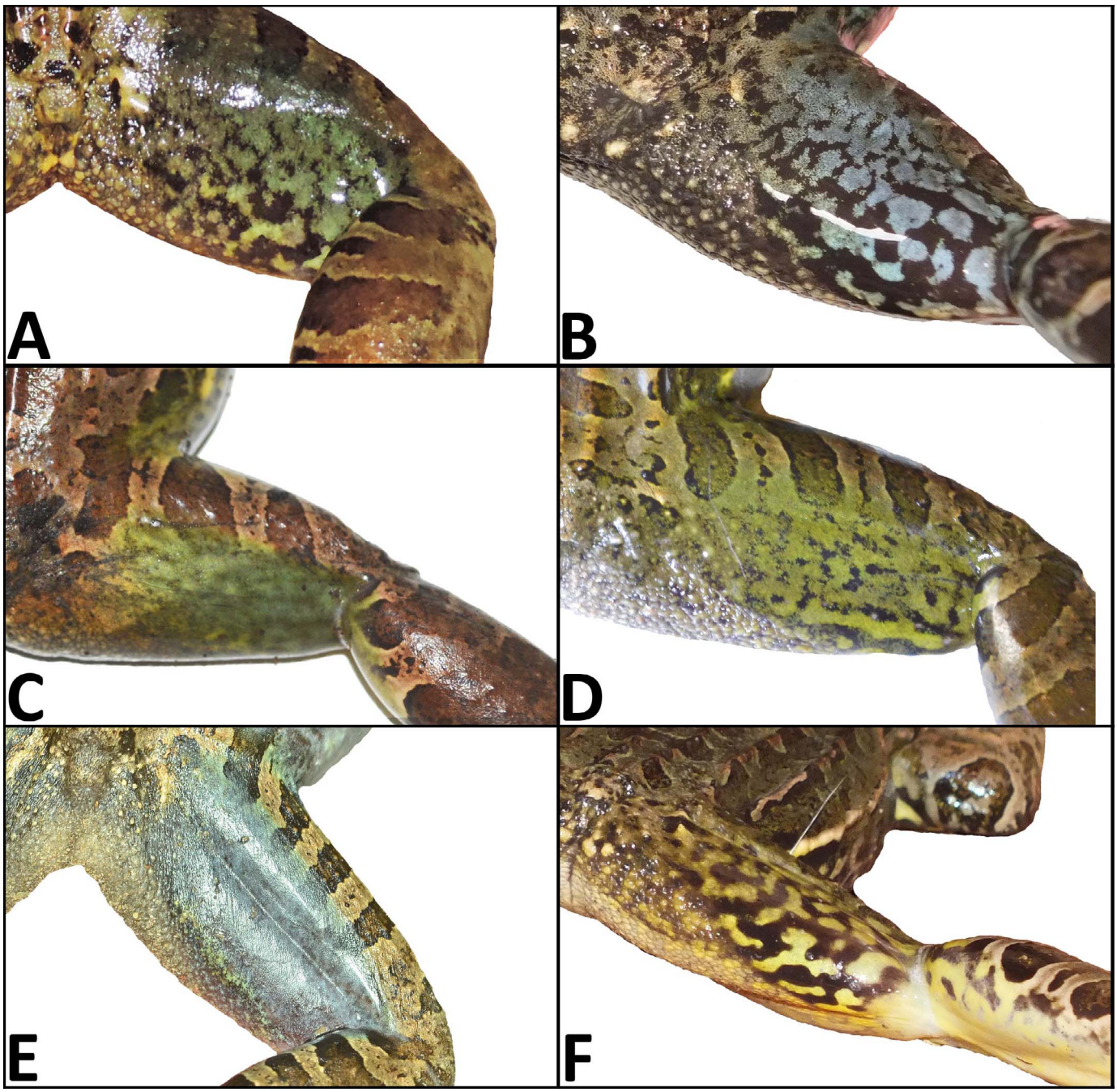

Fig. 8.—Thigh posterior surface coloration patterns: Blue/cyan shades: (A) *Leptodactylus latrans* (MZFS 5138), photo by F. Camurugi; (B) *L. latrans* (CFBH 42703). Green shade: (C) *L. macrosternum* (*chaquensis/macrosternum* lineage, CHUFPB 28815), and (D) *L. payaya* (CS1 lineage, CHUFPB 28192). Gray shade: (E) *L. payaya* (CS1 lineage, UFBA14300), photo by R.O. Abreu. Yellow shade: (F) *L. luctator* (CS2 lineage, CFBH42813). See Appendix I for locality data of analyzed vouchers. A color version of this figure is available online.

to discriminate among groups. Therefore, we present the following results based on the full data set (538 individuals). Across lineages, the guided regularized random forest results revealed a cross-validation error ranging from 0.46–0.17 (corresponding to using the single best predictor to using all predictors). The guided regularized random forest model based on the two best predictors (body size, tympanum diameter) had an accuracy of ~42%, based on 100 replicates of tenfold cross-validation. Overall, our results highlight great similarity in morphometric characteristics among genetic lineages (Fig. 12), except for the *Leptodactylus chaquensis/macrosternum* lineage that can be discriminated with low classification error (3%). Conversely, our method did not fully discriminate the four lineages of the *L. latrans* complex based on morphometric traits, exhibiting moderate (15 and 17% in *L. latrans* and *L.* aff *latrans* CS2 lineage, respectively) to high (71 and 100% in *L.* aff. *latrans* CS1 and CS3 linages, respectively) values of classification error (Fig. 12C). The best predictors that most contributed to the separation between species were body size, adjusted tympanum diameter, and adjusted foot length (Fig. 12B). The selection of body size on explaining morphometric

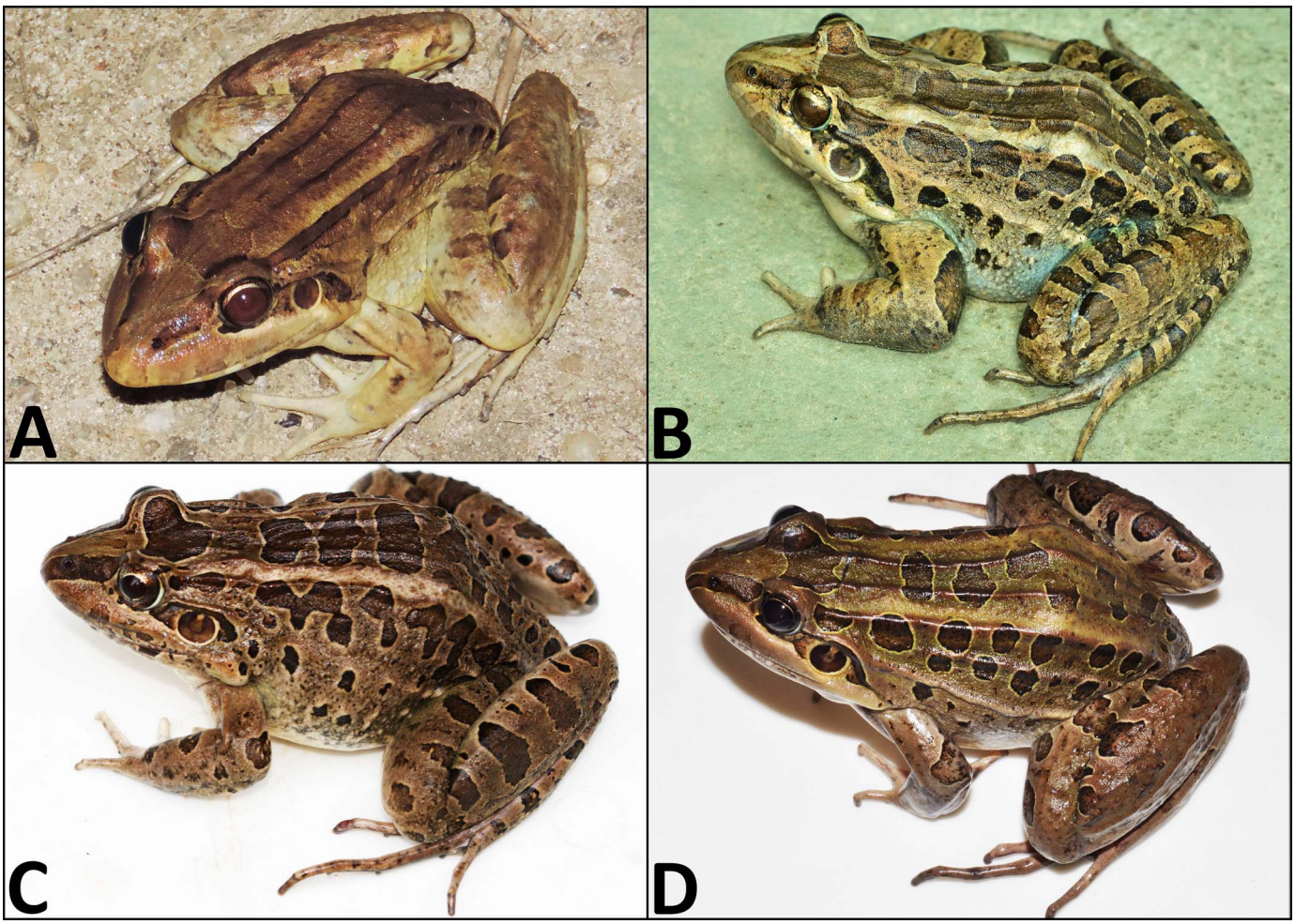

FIG. 9.—Dorsal coloration patterns. (A) *Leptodactylus latrans* (unvouchered from Terra Nova, Bahia) without ocellated blotches on dorsum (smooth, Pattern 1), photo by F. Camurugi; (B) *L. payaya* (CS1 lineage, UFBA 14300) with light to dark-brown ocellated blotches evenly distributed on dorsum (Pattern 2), photo by R.O. Abreu; (C) *L. macrosternum* (*chaquensis/macrosternum* lineage, UFTM teaching collection from Conceição das Alagoas, Minas Gerais); and (D) *L. luctator* (CS2 lineage, AAG-UFU 1173) exhibiting dark-brown ocellated blotches outlined by light coloration (Pattern 3). See Appendix I for locality data of analyzed vouchers. A color version of this figure is available online.

variation is linked to larger SVL reached by *L. latrans* and *L.* aff. *latrans* CS2 and CS3 lineages compared to *L.* aff. *latrans* CS1 and *L. chaquensis/macrosternum* (Table 4). Specimens of *L.* aff. *latrans* CS1 and *L. chaquensis/macrosternum* never exceed SVLs of 96.9 and 98.9 mm, respectively, whereas the other three lineages grow up to 121.6–126.3 mm in SVL (Table 4). The selection of tympanum diameter is related to the proportionally larger tympanum diameter in males of *L. chaquensis/macrosternum* and some males of *L.* aff. *latrans* CS2 if compared to *L. latrans* and *L.* aff. *latrans* CS1 and CS3 males of similar sizes (Fig. 12A). Although there is an overlap in relative size of the tympanum, only specimens of *L. chaquensis/macrosternum* have a tympanum diameter/head length ratio greater than 0.24 (Table 4). Similarly, ratios for foot length/SVL also overlap among lineages, but this character will distinguish some specimens of *L. latrans* and *L.* aff. *latrans* CS2 from those of remaining lineages. For instance, ratios over 0.60 would likely be *L. latrans* or *L.* aff. *latrans* CS2 rather than one of the other lineages, while ratios below 0.44 would likely be *L. chaquensis/macrosternum* (Table 4). Future studies addressing morphometric variation in the group could focus on ontogenetic and geographic variation within the genetic lineages to explore differences related to these traits (e.g., Heyer and de Sá 2011). Overall, differences in body size, tympanum diameter, and foot length also apply to females. A fully expanded table of descriptive morphometric variables is presented in Supplementary Material S3 (in the Supplemental Materials available online).

Advertisement Calls

Lineages within the *Leptodactylus latrans* complex have such similar calls that some of them could not be distinguished acoustically from each other based on any of the temporal and spectral traits analyzed in this study. Calls are single, low-pitched notes, emitted at irregular intervals (Fig. 13A–D). A major difference (detectable by the human ear) is related to the call envelope: the presence of weak/irregular amplitude modulations in the calls of *L.* aff. *latrans* CS2 and CS3 lineages (Fig. 13B,D, respectively), resembling a harsh sound. These amplitude modulations were detected qualitatively, but quantification was not possible because amplitude oscillations are usually weak and irregular within calls and among individuals. In contrast, amplitude modu-

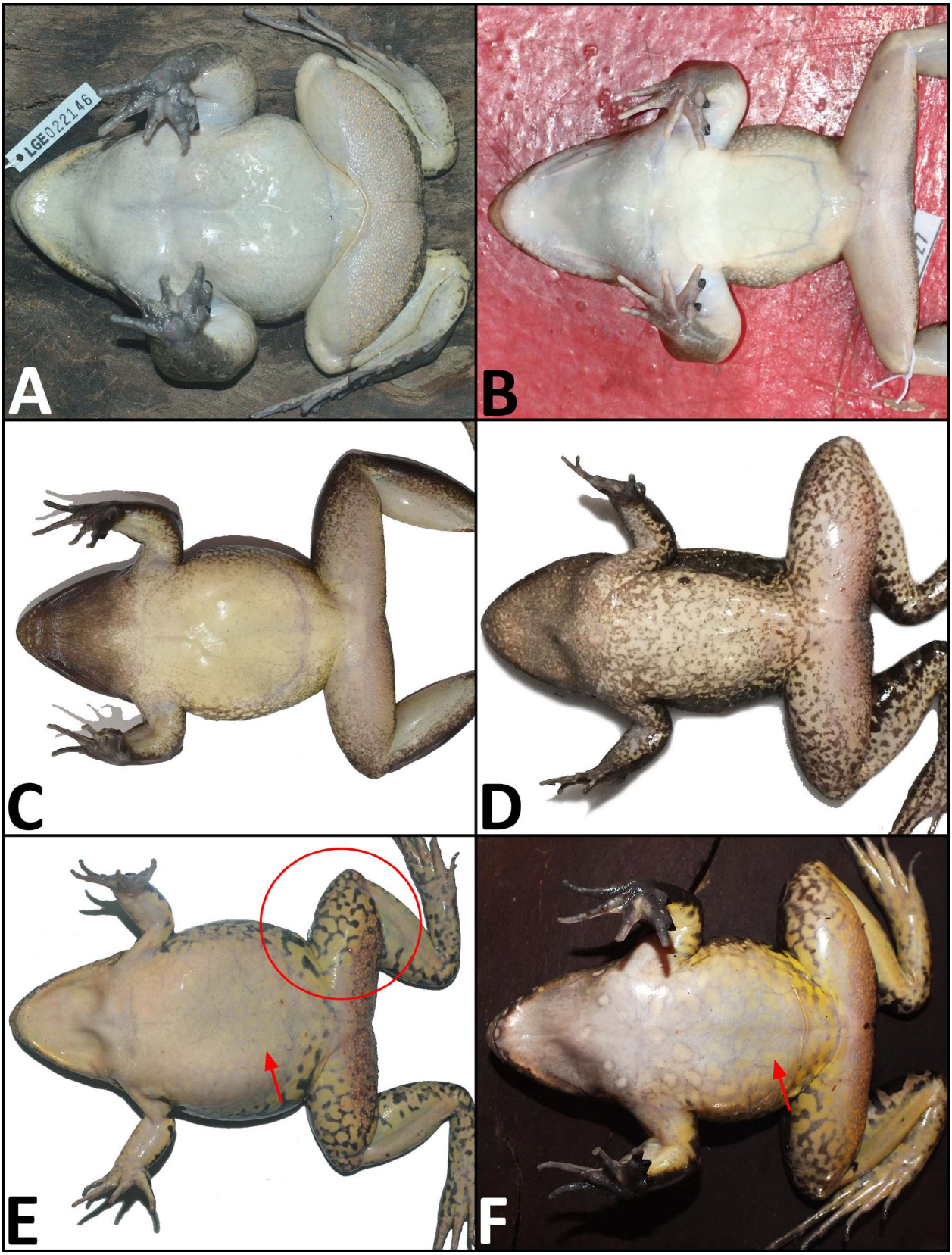

Fig. 10.—Ventral coloration patterns. Lacking black pigmentation: (A) *Leptodactylus luctator* (CS2 lineage, LGE 22146), and (B) *L. macrosternum* (*chaquensis/macrosternum* lineage, INPA-H 038801 from Médio Solimões, Amazonas), photo by L. Moraes. (C) *L. payaya* (CS1 lineage, CHUFPB28184), and (D) *L. latrans* (CFBH 42766) exhibiting sparse and densely pigmented mottled patterns, respectively. (E) *L. luctator* (CS2 lineage, LGE 22149) exhibiting black maculated patches along thigh surface (within red circle) and faded yellow melanophores on belly (arrow), and (F) *L. luctator* (CS2 lineage, CFBH 42814) exhibiting evident yellow melanophores on belly (arrow). See Appendix I for locality data of analyzed vouchers. A color version of this figure is available online.

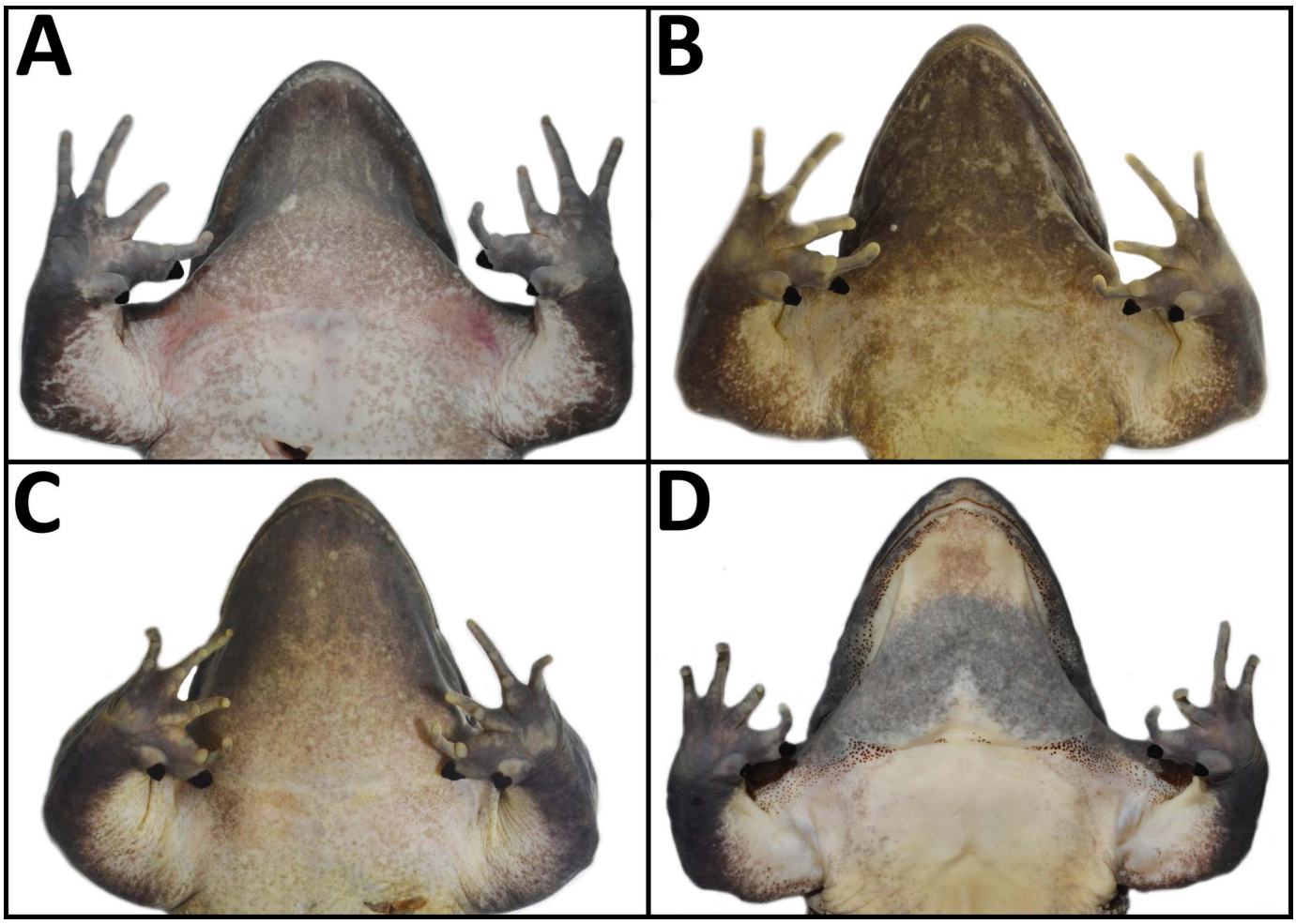

Fig. 11.—Vocal sac, throat coloration, and thumb spine morphology. Single-lobed vocal sac: (A) *Leptodactylus latrans* (CFBH 42765) exhibiting triangular thumb spines, (B) *L. payaya* (CS1 lineage, CHUNB 53238) exhibiting conical thumb spines,; (C) *L. luctator* (CS2 lineage, CHUFPB 28151) exhibiting rectangular thumb spines. Bilobed vocal sac: (D) *L. macrosternum* (*chaquensis/macrosternum* lineage, CFBH 26142) exhibiting conical thumb spines. See Appendix I for locality data of analyzed vouchers. A color version of this figure is available online.

lations were almost always absent in the call of nominal *L. latrans* (only one individual among nine recorded individuals exhibited weak irregular amplitude modulations), which sounds like a hoot-sound instead (Fig. 13A). A third pattern is the presence of more homogeneous and well-marked amplitude modulations along the call, an acoustic pattern exclusive to CS1 lineage, which is regarded herein as a partly fused multipulsed call (Fig. 13C). These major patterns are described in detail in the Taxonomic Account section. The calls of the *L. chaquensis/macrosternum* lineage are complex, including three distinct note types: grunts, growls, and trills (see Heyer and Giaretta 2009; Camurugi et al. 2017; Fig. 14A–C). Despite being more complex, the calls of this lineage are highly stereotyped throughout South America, from northern Argentina, the Cerrado of central Brazil, northern Atlantic Forest, and Amazonia (Heyer and Giaretta 2009; Tárano 2010; Camurugi et al. 2017). A quantitative description and comparative sounds are provided in the next section.

With respect to the other species of the *Leptodactylus latrans* group, calls of the three species recognized in the *L. bolivianus* complex (*L. bolivianus*, *L. guianensis*, and *L. insularum*) were described in Heyer and de Sá (2011). All three species have stereotyped whistle-like calls defined as single, nonpulsed notes with upsweep frequency modulation (Fig. 14D). The call of the Honduran *L. silvanimbus* (Heyer et al. 1996a) is unique in the *L. latrans* group by being broad-bandwidth and lacking frequency modulation, giving the impression of a honk-like sound (Fig. 14E). The bubbling call of *L. viridis* was described by Rocha et al. (2016) and can also be regarded as unique mainly because of its brief duration (<50 ms) and strong frequency upsweep (Fig. 14F). Because of the low availability of calls for the *L. latrans* group, we are aware that acoustic variation is most likely negatively biased, although support all genetic lineages in the LCM complex as distinct species. For this reason, we restricted the acoustic analysis to major temporal and spectral traits and did not perform between-group statistical comparisons (see Discussion section).

Taxonomic Nomenclature Reappraisal

Currently, there are 15 names (emendations or incorrect spelling not included) available in the synonym of *Leptodactylus latrans* (Lavilla et al. 2010; Frost 2020). Considering that our results corroborate the existence of four distinct species in the *L. latrans* complex (three unnamed) and that

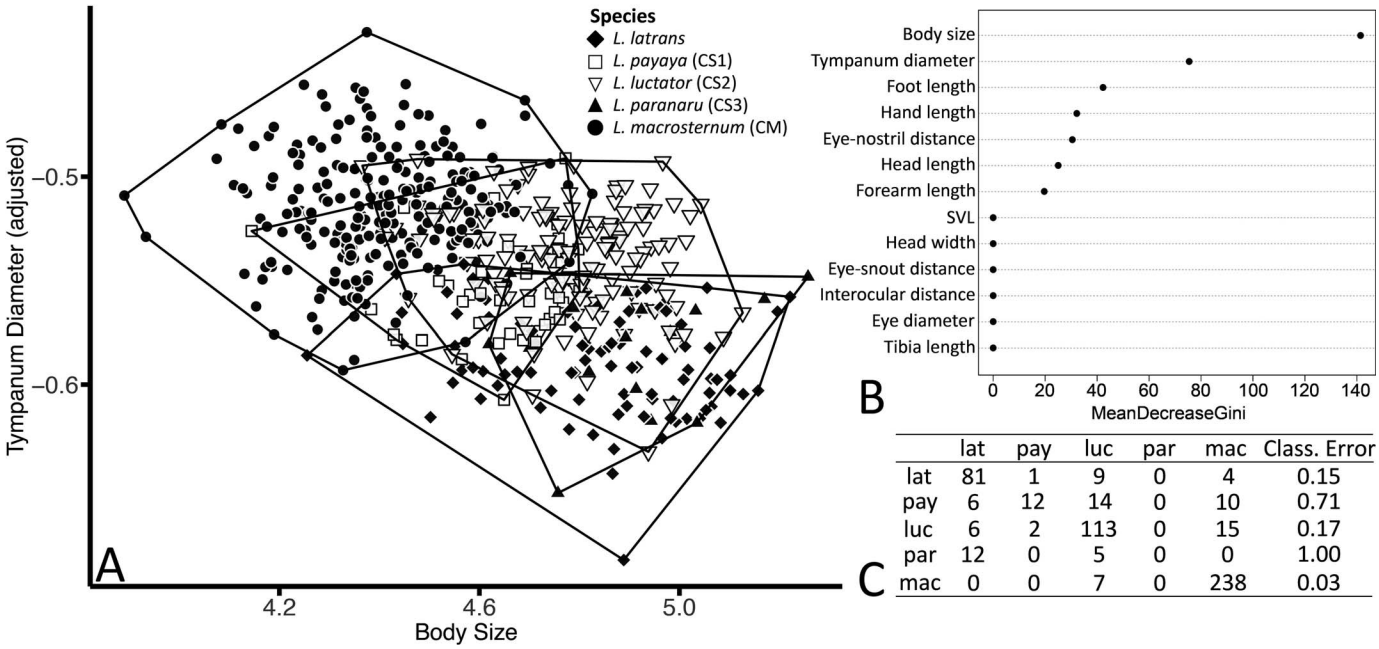

FIG. 12.—Random forest results for species in the *Leptodactylus latrans* complex and *L. macrosternum* based on morphometric variables. (A) Variation in body size and tympanum diameter, the two best predictors of differences among species/lineages. (B) Dot charts of variable importance scores based on mean decrease of guided regularized random forest models. The higher the mean decrease in Gini accuracy, the higher the predictor importance. (C) Confusion matrix showing individual classification error. Species abbreviations are the first three letters of the specific epithet shown in letter A legend. Lineages are CS1–3 and CM (*chaquensis/macrosternum*). A color version of this figure is available online.

L. chaquensis and *L. macrosternum* correspond to a single species, a reassessment of the nomenclature of this clade is needed. Although morphologically cryptic, the geographic ranges of lineages in the *L. latrans* complex are mostly nonoverlapping among each other, with few sympatric zones throughout their distribution (Fig. 2), enabling the association of previously available names with lineages if geographic information is available. Therefore, we discuss the validity of some names previously regarded as *L. latrans* synonyms (Lavilla et al. 2010), and others that do not require any further discussion are listed in the Taxonomic Account section.

***Rana pygmaea* Spix 1824.**—Spix (1824) described a juvenile leptodactylid specimen collected from Bahia province (which is now part of Bahia state) that differed from *Rana pachypus* mainly in body size. There was much discussion about the true identity of this taxon (see Hoogmoed and Gruber 1983), which has been considered as a juvenile of *R. pachypus* by Peters (1872) and subsequently a synonym of *Leptodactylus latrans* (Hoogmoed and Gruber 1983), or an allied species to *L. mystacinus* (Miranda-Ribeiro 1926, 1927). Although geographic information is not accurate, Spix (1824:26) explicitly distinguishes specimens collected along "locis humidis" (possibly a reference to sites located within the limits of the Atlantic Forest) as he did with *R. pachypus*, from those that were collected along the interior or mountainous regions, which might be the case of *R. pygmaea*. According to Vanzolini (1981), Spix's expedition crossed several municipalities in the inlands of Bahia (e.g., Caetité, Maracás), where three distinct lineages of the LCM complex occur in sympatry/syntopy (e.g., *L. chaquensis/macrosternum*, *L.* aff. *latrans* CS1 and CS2 lineages). Additionally, the *R. pygmaea* illustration provided by Spix (1824) does not exhibit the interocular ocellated blotch (Plate VI, Fig. 2 in Spix 1824), a conspicuous feature exhibited by all species in the *L. latrans* group (even in postmetamorphic individuals; FMM, personal observation). For instance, the ocellated blotch was depicted by him in adult and juvenile *R. pachypus* illustrations (see Plate II, Fig. 1 and Plate III, Fig. 2 in Spix 1824), but not in *R. pygmaea*. The only feature depicted in *R. pygmaea* illustration that is shared by all species in the *L. latrans* group is the dark brown transversal bars in the dorsal surface of thigh and tibia, a feature also observed in other leptodactylid frogs (e.g., species in the *L. fuscus* group) that occur in interior of Bahia, such as *L. mystaceus* and *L. mystacinus* (Leite et al. 2008) among others. Considering Spix's (1824) vague description and illustration and that the type specimen is now considered lost (Glaw and Franzen 2006), it is not possible to unambiguously assign this name to any species of the *L. latrans* group. Therefore, *R. pygmaea* is here regarded as a nomen dubium (a name of unknown or doubtful application; ICZN 1999), and associated with a species inquirenda (a species of doubtful identity needing further investigation; International Commission on Zoological Nomenclature [ICZN] 1999).

***Rana pachypus octolineatus* Mayer 1835.**—Lavilla et al. (2010) mentioned that this name was subjectively included as a synonym of *Rana pachypus* (and thereafter *R. ocellata*) by Tschudi (1838). There is no information regarding the geographic origin of the type series (and how many individuals compose it), which is presumably lost (Lavilla et al. 2010). Lavilla et al. (2010) further mentioned that Tschudi's decision to keep *R. pachypus octolineatus* in the synonymy of *Leptodactylus latrans* remains valid until the type specimens are found. Nevertheless, even if specimens were located, it is unlikely that one could correctly assign it to any of the four *L. latrans* lineages

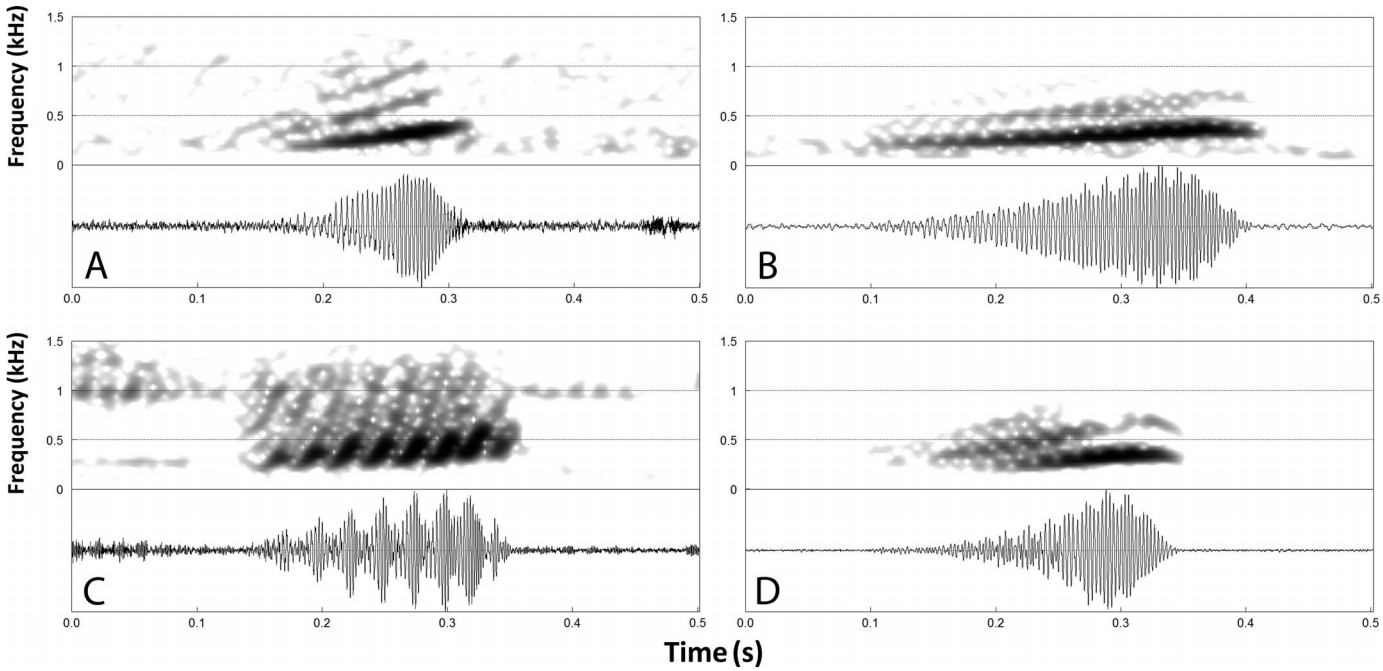

FIG. 13.—Advertisement calls (spectrogram and oscillogram from top to bottom) of species in the *Leptodactylus latrans* complex. (A) nonpulsed note with a smooth envelope of *L. latrans* topotype (CFBH 42772) recorded from Teresópolis, Rio de Janeiro, Brazil (recording ASUFRN668); (B) nonpulsed note of *L. luctator*, with weak amplitude modulations (CS2 lineage, unvouchered), recorded from Uberlândia, Minas Gerais, Brazil (recording Leptod_luctator-UberlandiaMG8aAAGm); (C) an eight-pulse note of *L. payaya* holotype (CS1 lineage, CHUFPB 28187) recorded from Jacobina, Bahia, Brazil (recording ASUFRN674); and (D) nonpulsed note of *L. paranaru* holotype, exhibiting amplitude modulations (CS3 lineage, CFBH 42804), recorded from Peruíbe, São Paulo, Brazil (recording ASUFRN671). Figures are equally scaled. A color version of this figure is available online.

(considering their cryptic morphology and sympatric condition along some localities in Brazil). Considering the impossibility to undoubtedly associate the name with a specific lineage, and to avoid taxonomic confusion with other currently well-known species names, *R. pachypus octolineatus* is here considered a nomen dubium, and associated with a species inquirenda.

***Rana luctator* Hudson 1892.**—The name *Rana luctator* was first assigned to *Leptodactylus ocellatus* (= *L. latrans* complex) by Serié (1935) and later confirmed by Gallardo (1964). This specimen was collected around the vicinity of Buenos Aires municipality by Hudson (1892), and lost at some point in the course of his expedition. Nevertheless, he clearly intended to investigate its taxonomic identity, and explicitly stated that it might be a new species to science:

> Believing that I had discovered a frog differing in structure from all known species, and possessing a strange unique instinct of self-preservation, I carried my captive home, intending to show it to Dr. Burmeister, the director of the National Museum at Buenos Ayres. Unfortunately, after I had kept it some days, it effected its escape by pushing up the glass cover (Hudson 1892:76).

Hudson did not provide a proper morphological description of the taxon but the illustration on page 77 (by J. Smid) overall resembles *Leptodactylus latrans*, except that it shows a frog with palmate feet (character absent among members of the genus *Leptodactylus*). Anyhow, he described an aggressive behavior exhibited by this specimen that is worthy of note. He explicitly stated that the frog attempted to clasp his fingers as he tried to capture it: "Before I was sufficiently near to make a grab, it sprang straight at my hand, and, catching two of my fingers round with its fore legs, administered a hug so sudden and violent as to cause an acute sensation of pain" (Hudson 1892:76).

Then, he continues describing his encounter with this frog mentioning what would be a male with hypertrophied arms: "I then noticed the enormous development of the muscles of the fore legs, usually small in frogs, bulging out in this individual, like a second pair of thighs, and giving it a strangely bold and formidable appearance" (Hudson 1892:76).

Considering all these statements (exhibiting clasping behavior and hypertrophied arms), it is certain that the referred specimen can only be associated with a member of the *Leptodactylus latrans* group among all anurans occurring in Buenos Aires province. This name fits all requirements of the ICZN (Articles 5, 8, 10, 11 and 12; ICZN 1999), which consider as valid those names without an associated type-specimen provided in scientific works published before 1999. Because the only lineage occurring in this region is *L.* aff. *latrans* CS2 (*L. chaquensis/macrosternum* does not occur in that region; see Fig. 2), *Rana luctator* is the first available name applicable to this candidate species and has priority over other names that are also available for this lineage such as: *Cystignathus oxycephalus* Philippi 1902 (type locality: "ad Montevideo," Uruguay), *L. ocellatus* var. *reticulata* Cei 1948 (type locality: "Arroyo, Isla Apipé, Ituzaingó [Corrientes]" and "Puerto Bemberg [Misiones]," Argentina), and *L. ocellatus* var. *bonairensis* Cei 1949 (type locality: "Río Colorado y Bahía Blanca," Argentina), whose types are from regions where only *L.* aff. *latrans* CS2 lineage occurs. Based on this evidence, we formally revalidate *R. luctator* (Hudson 1892) as *L. luctator* (Hudson 1892) comb. nov.

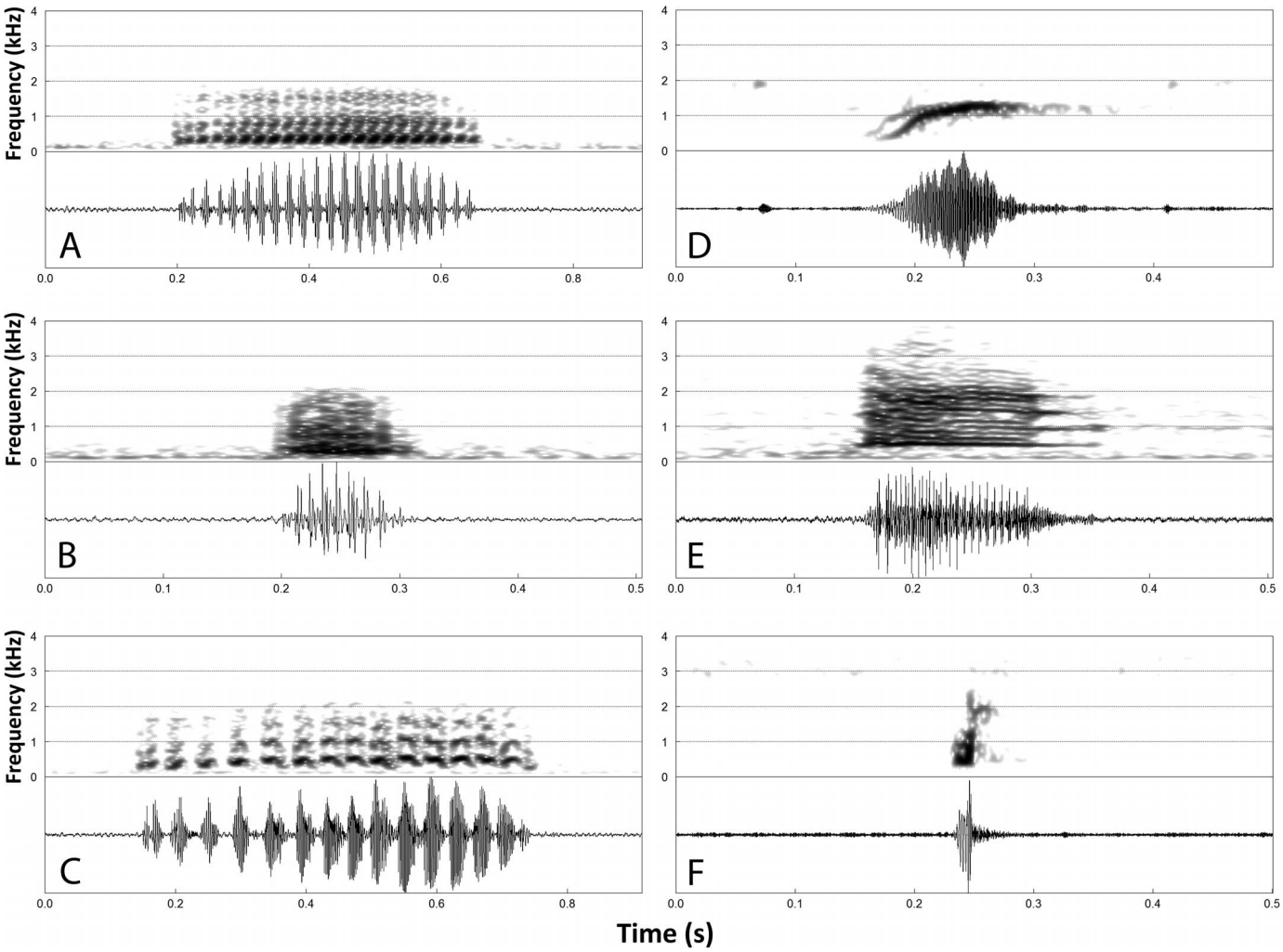

Fig. 14.—Advertisement calls (spectrogram and oscillogram from top to bottom) of species in the *Leptodactylus latrans* species group. (A–C) The three distinct note types (growl, grunt, and trill, respectively) of the vocal repertoire of *L. macrosternum* (*chaquensis/macrosternum* lineage, AAG-UFU 4108) recorded from Araguari, Minas Gerais, Brazil (recording Leptod_macrosternumAraguariMG2bAAGm); (D) nonpulsed, frequency-modulated call of *L. insularum* (unvouchered) recorded from Guárico province, Venezuela, by Z. Tárano (recording from Tárano 2010); (E) broad-bandwidth call of *L. silvanimbus* (unvouchered) recorded from Ocotepeque province, Honduras (recording USNM Tape 317, cut 6); and (F) nonpulsed, frequency-modulated call of *L. viridis* (UFMG 15127) recorded from Carlos Chagas, Minas Gerais, Brazil, by P.C. Rocha (recording CBUFMG 139). A color version of this figure is available online.

The *Leptodactylus chaquensis/macrosternum* case.—As mentioned previously, information regarding the type locality of *Leptodactylus macrosternum* is vague, but it is certain that the specimens collected by the naturalist B. Bicego (and later described by Miranda-Ribeiro 1926) were obtained somewhere around the vicinities of Salvador municipality (Brazilian state of Bahia; Bokermann 1966). We now have enough evidence supporting the sympatric/syntopic occurrence of *L. latrans* and the smaller morphotype (= *L. chaquensis/macrosternum*) in some localities of Bahia coastal zone, especially in the vicinities of Salvador (Fig. 2). Hence, it is very likely that B. Bicego collected within sympatry zones in Bahia, although only a single individual among 13 was described by Miranda-Ribeiro (1926) as the morphotype *L. ocellatus macrosternum*. Nevertheless, Miranda-Ribeiro's (1926) description states that *L. ocellatus* (now *L. latrans*) and *L. ocellatus macrosternum* are distinguished by the arrangement of dermal longitudinal folds, a feature that we now confirm and that was also highlighted by Gallardo (1964) as diagnostic between these two morphologically similar species. Later, Cei (1950) described the Chacoan population from Argentina as *L. chaquensis*, but he did not mention differences in the arrangement of dermal folds and focused on reproductive and physiological features in order to distinguish *L. chaquensis* from *L. latrans*. We showed earlier in our study that the widespread lineage distributed across xeric environments of South America (including Chacoan and Bahia populations) consists of a single species, because of the low genetic differentiation (which agrees with the overall intraspecific divergence reported for the *L. latrans* group; Fig. 5) and the absence of morphological/morphometric and acoustic variation. In summary, the name *L. macrosternum* is the first available and valid name to be applied correctly to populations of the widespread lineage found across the open diagonal in South America, rendering *L. chaquensis* Cei 1950 a junior synonym of *L. macrosternum* Miranda-Ribeiro 1926.

In the following section we provide an updated taxonomic account and formally name and describe the lineages CS1

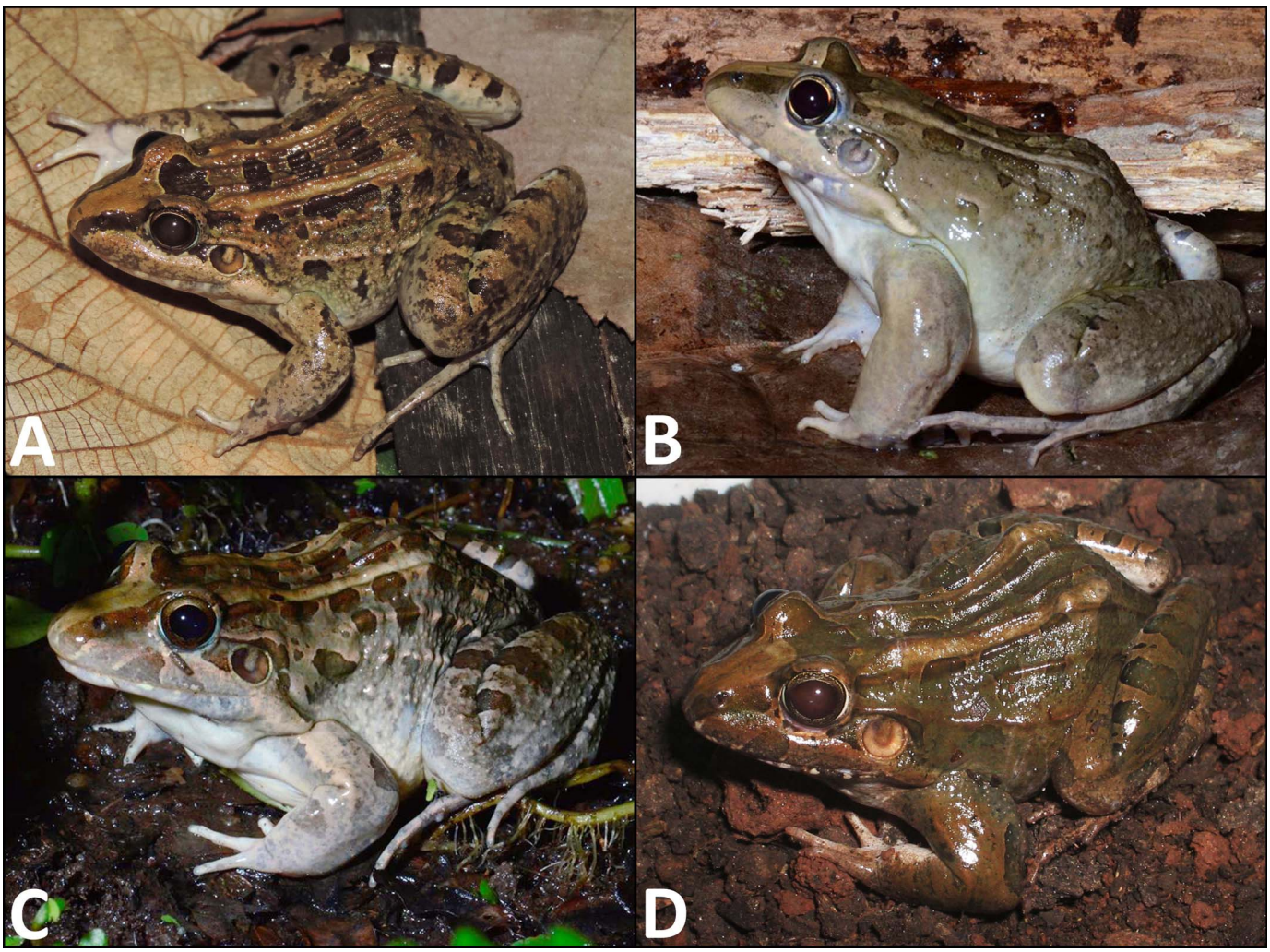

FIG. 15.—Representatives of *Leptodactylus macrosternum*: (A) adult male (MZFS 5141) from Terra Nova, Bahia, Brazil (Salvador vicinities), photo by F. Camurugi; (B) adult male (MAP-T 379) from Óbidos municipality, Pará, Brazil (Amazonia); (C) adult male (unvouchered) from Macaíba, Rio Grande do Norte, Brazil (Caatinga); and (D) adult male (LGE 14821) from Nueve de Julio, Chaco, Argentina (Chaco). Note the long dermal auxiliary fold (F3) of *L. macrosternum* (a diagnostic characteristic), which is absent in species of the *L. latrans* complex. A color version of this figure is available online.

and CS3 as new species, which could not be linked to any of the available names included in the synonymic list of *Leptodactylus latrans*. There is more than one century of published literature using the names related to the *L. latrans* group, specifically those assigned to the LCM complex. Because members of this species group are widely distributed in South America and easily detected in nature, they are cited in virtually any species list. Therefore, in the cases of *L. latrans*, *L. luctator*, and *L. macrosternum* (which exhibit broad geographic ranges), we list only those synonyms originally published as species descriptions.

Updated Taxonomy and New Species Descriptions

Leptodactylus macrosternum Miranda-Ribeiro 1926 (Figs. 1 and 15)

Leptodactylus ocellatus macrosternum Miranda-Ribeiro (1926:147). Holotype juvenile (MZUSP 448, sex undetermined) collected by Mr. Beniamino Bicego in June 1896 around the vicinities of Salvador municipality, "Bahia province" (= Bahia state), Brazil. Gallardo (1964:379–382; Bokermann 1966:73).

Leptodactylus ocellatus macrosternus Miranda-Ribeiro 1927:125 [misspelling].

Leptodactylus ocellatus var. *typica* Cei 1948:308–312. Syntypes not designated (presumably FML) from Tucumán, Argentina (senior synonym of *Leptodactylus chaquensis* by implication in the original and subsequent literature). Opinion 2044 (International Trust for Zoological Nomenclature [ITZN] 2003:173) suppressed this name for purposes of synonymy.

Leptodactylus chaquensis (Cei 1950:417). Syntypes FML 979 (containing two male specimens) from "Simoca y Río Colorado (Tucumán) y Manantiales (Corrientes)," Argentina. [not examined; **new synonymy**]. Lavilla (1992:85; Hayward 1963:507; Gallardo 1964:382–383).

Diagnosis.—Assigned to the *Leptodactylus latrans* species group by phylogenetic placement and the following combination of features: (1) adult male SVL = 48.7–98.9 mm ($\bar{X}$ = 74.4 mm) and adult female SVL = 55.9–90.8 mm ($\bar{X}$ = 74.0 mm), (2) adult males with a pair of black keratinized

TABLE 5.—Comparative data for the three note types in the acoustic repertoire of *Leptodactylus macrosternum* ("*chaquensis/macrosternum*" lineage). Data are given as mean ± SD (range). The following traits were quantified from three note types (growls, trills, and grunts): note length (NL), note rise time (NRT), pulse number (PP), pulse rate (PR), dominant frequency (DF), and linear frequency modulation (LFM); *n* = number of males recorded (number of calls/pulses analyzed); NA = not applicable.

Trait	Growl, *n* = 2 (21 / 455)	Trill, *n* = 1 (6 / 87)	Grunt, *n* = 1 (5 / NA)
NL (ms)	435.5 ± 64.6 (316–591)	593.8 ± 44.0 (537–667)	102.9 ± 14.6 (81–117)
NRT (%)	47.8 ± 5.4 (26–63)	70.3 ± 7.8 (59–78)	39.0 ± 8.5 (27–48)
PP/note	21.8 ± 1.0 (15–27)	14.5 ± 0.5 (14–15)	NA
PR/s	52.0 ± 5.4 (48–57)	24.0 ± 1.7 (22–26)	NA
DF (Hz)	388.5 ± 24.2 (366–445)	480.9 ± 22.2 (452–495)	314.4 ± 19.3 (280–323)
LFM (Hz)	–14.2 ± 86.4 (–215 to 188)	71.8 ± 64.8 (0–172)	–60.3 ± 23.6 (–86 to –43)

thumb spines on hand, (3) adult males with chest spicules (no spines), (4) two pairs of complete and well-developed dorsal longitudinal folds (Folds F2 and F4) extending from behind the eye or posterior interocular region to the pelvic region, (5) pair of auxiliary folds (Fold F3) long extending from behind eye to mid-length of the body, (6) bilobed vocal sac in adult males, (7) toes and fingers laterally fringed, (8) single longitudinal row of spicules on posterior surface of tibia, (9) vocal repertoire made up of three distinct note types, (10) growl note type with dominant frequency ranging from 366–445 Hz ($\bar{X}$ = 389 Hz).

Coloration of the holotype in preservative.—The overall holotype coloration is completely faded (Fig. 1), without any recognizable pigmentation pattern.

Measurements of holotype (in millimeters).—SVL 65. The poor preservation conditions of the holotype prevent us from taking reliable morphometric measurements.

Variation.—Most of the variation is related to the auxiliary Fold F3 (which may be short, interrupted or long and complete; Fig. 7D–F) and to the posterior thigh coloration (in life), which is usually distinctively green without black pigmentation in the background, while some individuals may exhibit gray shades. In life, body dorsal coloration is overall reddish brown (Fig. 15A–C), but may also exhibit green shades (Fig. 15D). Variation in morphological features other than those reported above are mentioned in the Morphology section of Results.

Advertisement call.—Redescription is based on a small sample of calls recorded by us (*n* = 2 males) to allow direct comparisons with calls of species in the *Leptodactylus latrans* complex. Previous descriptions can be found in Heyer and Giaretta (2009) and Camurugi et al. (2017). See Appendix II for locality and recording information. Descriptive statistics (mean and standard deviation) are given in Table 5. The call is composed of up to three distinct note types (referred as growl, grunt, and trill; sensu Heyer and Giaretta 2009), which differ from each other in temporal (note duration, pulse number and rate) and frequency (dominant frequency and frequency modulation) traits, as well as differences in their envelopes (Table 5; Fig. 14A–C). Call notes are given at highly variable rates as single notes, in sequences of the same note type (mainly growl and trill notes) or combinations of more than one note type. The growl note type (Fig. 14A) is the most commonly emitted by males of *L. macrosternum*, which led Camurugi et al. (2017) to classify this note into a main reproductive context (i.e., advertisement call note). The growl-type note (*n* = 21) has pulses (*n* = 455) separated by brief silence gaps in between (in most cases) or partly fused in a few cases. Growl notes have their rise time at 26–63% of their length. Note length ranges from 316–591 ms. Each note is composed of 15–27 pulses, emitted at a rate of 48–57/s. The dominant frequency ranges from 366–445 Hz. Notes have modest frequency modulation, either positive or negative, which ranges from –215 to 188 Hz. The grunt-type note (*n* = 5) has a few amplitude modulations throughout its length that could not be accurately quantified in the time domain, even though note subunits were visualized in the frequency domain (Fig. 14B). Grunt notes have their rise time at 27–48% of their length. Note length ranges from 81–117 ms. The dominant frequency ranges from 280–323 Hz. Notes have subtle negative frequency modulation ranging from –86 to –43 Hz. The trill-type note (*n* = 6) has complete pulses (*n* = 87), separated by silent gaps in between along the note (Fig. 14C). Trill notes have their rise time at 59–78% of their length. Note length ranges from 537–667 ms. Pulse number is 14–15, emitted at a rate of 22–26/s. The dominant frequency ranges from 452–495 Hz. Notes have modest positive frequency modulation or lack modulation, which ranges from 0–172 Hz.

Comparisons with other species (characteristics from other species are given within parentheses).—*Leptodactylus macrosternum* differs from *L. silvanimbus*, the three species of the *L. bolivianus* complex (*L. bolivianus*, *L. guianensis*, and *L. insularum*), and *L. viridis* by exhibiting well-developed and complete dorsal longitudinal folds F1 and F2, extending from behind the eye to the pelvic region (absent in *L. silvanimbus*, *L. bolivianus*, *L. guianensis*, and *L. insularum*, Heyer and de Sá 2011; Fig. 7A; and barely discernible or absent in *L. viridis*, Jim and Spirandeli-Cruz 1979; Fig. 7B). The bilobed vocal sac differentiates male *L. macrosternum* from those of *L. latrans* (single-lobed vocal sac, Gallardo 1964; de Sá et al. 2014). Also, the anterior throat coloration is light beige in *L. macrosternum* male, differing from those of *L. latrans* (homogeneously dark gray). The presence of two thumb spines distinguishes male *L. macrosternum* from those of *L. bolivianus*, *L. guianensis*, and *L. viridis* (one thumb spine; Jim and Spirandeli-Cruz 1979; Heyer and de Sá 2011). By exhibiting a long auxiliary fold extending from behind the eye to mid-length of the body (Fig. 6B), *L. macrosternum* differs from *L. latrans* (absent or, if present, short and restricted to the anterior third of body length; as depicted in Fig. 6A). The presence of a single longitudinal row of spicules on the posterior surface of tibia differentiates *L. macrosternum* from *L. viridis* (three longitudinal rows of spicules; Jim and Spirandeli-Cruz 1979). By its larger body size (SVL = 48.7–98.9 mm, $\bar{X}$ = 75.3 mm), *L. macrosternum* differs from *L. silvanimbus* (SVL = 35.8–55.0 mm, $\bar{X}$ = 47.8 mm; de Sá et al. 2014) and *L. viridis* (SVL range = 63.0–70.9 mm; de Sá et al. 2014; Supplemen-

tary Material S3). In opposite, the overall smaller body size (with maximum SVL reaching 98.9 mm) distinguishes *L. macrosternum* from *L. latrans* and the three species of the *L. bolivianus* complex (combined maximum SVL = 104.6–124.9 mm; Table 4; de Sá et. al. 2014). The relatively larger tympanum diameter and shorter foot length distinguishes *L. macrosternum* from *L. latrans* (Table 4). Additionally, *L. macrosternum* differs from *L. viridis* by the overall reddish-brown body coloration in life (body coloration in life predominantly green; Fig 7B; Jim and Spirandeli-Cruz 1979; de Sá et al. 2014). In life, coloration of groin and posterior thigh is generally distinctly green (not distinctly green in *L. latrans*). Moreover, *L. macrosternum* does not exhibit black pigmentation on the belly and on the posterior and underside surface of the thigh, distinguishing it from *L. latrans* (present). The presence of evident dark brown and outlined ocellated blotches on dorsum distinguishes *L. macrosternum* from *L. latrans* (smooth or faded and without outlined ocellated blotches).

The complex call of *Leptodactylus macrosternum*, made up of three distinct note types, distinguishes this species from all congeners of the *L. latrans* group, which have single-note calls. Additionally, *L. macrosternum* is the only species in this species group having notes formed by complete pulses (growls and trills; Fig. 14A,C, respectively). The rarest note type recorded, the grunt-type note (Fig. 14B), is not markedly pulsed as are growls and trills. This note type also differs from those of congeners in the *L. latrans* group by the absence of frequency upsweep (present in species of the *L. bolivianus* and *L. latrans* complexes; Heyer and de Sá 2011). Furthermore, grunt notes' duration (81–117 ms) and dominant frequency (280–323 Hz) is shorter and lower-pitched, respectively, in comparison with calls of *L. silvanimbus* (ca. 150 ms and 500 Hz on average; Heyer et al. 1996a), and longer and lower-pitched, respectively, in comparison with calls of *L. viridis* (16–31 ms and 560 Hz on average; Rocha et al. 2016).

Leptodactylus macrosternum exhibits from 69–92 base-pair (from 507) differences in the COI mitochondrial gene (or approximately 17–20% of genetic distance) in comparison with other species of the *L. latrans* group. This clade is supported as a distinct evolutionary entity with significant support in all phylogenetic (posterior probability = 1.0/bootstrap score = 100) and delimitation (bGMYC; ABGD) analyses.

Geographic distribution.—*Leptodactylus macrosternum* is broadly distributed across the open diagonal of South America (Figs. 2 and 16). Its range spans more than 4000 km from southern Santa Fe province in Argentina, to the Brazilian Guiana Shield in Roraima state, to the Llanos of Venezuela (Dixon and Staton 1976; Gorzula and Señaris 1998; Barrio-Amorós 2004) and Guyana savannas (Cole et al. 2013), also reaching the coastal region of Bahia state in Salvador municipality, and all northeastern and northern Brazilian coast. Although not sampled by us, there are records of *L. macrosternum* (referred as *L. chaquensis* therein) for the three states of southern Brazil: Rio Grande do Sul (Santos and Cechin 2008; Teixeira et al. 2017), Santa Catarina (Machado et al. 2014) and Paraná (Oda et al. 2014). Moreover, one of the *L. macrosternum* samples provided by de Sá et al. (2014) from Trinidad and Tobago also clustered with what we now regard as *L. macrosternum*, reinforcing the occurrence of this taxon on a continental island off South America coast (referred as *L. ocellatus* by Murphy 1997).

Remarks.—Although we did not observe any strong genetic differentiation throughout the entire distribution of what we now regard as *Leptodactylus macrosternum*, Cei (1970) found significant serological differences of *L. macrosternum* between samples from São Paulo state in southeastern Brazil and northwestern Argentina (regarded as *L. chaquensis*), which led him to corroborate the species status of *L. macrosternum* (as proposed by Gallardo 1964). This source of information has been employed previously as a good diagnostic feature corroborating the taxonomic status of several *Leptodactylus* species (see Cei et al. 1967; Maxson and Heyer 1988). Although voucher information is available (housed at Butantan Institute collection under accession 2538–2539), we did not have access to these specimens or any precise geographic information. Anyhow, we are now aware that four distinct lineages occur in São Paulo state (*L. macrosternum*, *L. latrans*, and *L.* aff. *latrans* CS2 and CS3 lineages). Therefore, the existence of serological differences may be explained by erroneous identification (e.g., the specimens assigned to *L. macrosternum* actually correspond to some of our unnamed lineages) or may reflect an ecological specialization related to biome (Cerrado vs. Chacoan populations) and should be better explored in future research.

Leptodactylus latrans (Steffen 1815)
(Fig. 17)

Rana latrans Steffen (1815:13). Holotype or type series not stated (presumably lost), from "Brasilia" (= Brazil).

Rana gibbosa Raddi (1823:67). Holotype not stated (although presumably at MZUF), from Rio de Janeiro, Brazil. Bokermann (1965:9–12).

Rana fusca Raddi (1823:68). Holotype deposited at MZUF (voucher not stated) from "Rio-janeiro" (= Rio de Janeiro state), Brazil (Bokermann 1966:88).

Rana pachypus Spix (1824:26). Syntypes ZSM (10 specimens; presumed lost), ZMB, and ZMH (presumably) from "Habitat in locis humidis Provinciae Rio de Janeiro" (= Rio de Janeiro state), (Var. 1) from "locis humidis Bahiae" (= Bahia state), and (Var. 2) from "locis aquosis Parae" (= Pará state), Brazil. Hoogmoed and Gruber (1983:356; designated ZSM 122/0/1 as lectotype; not examined); Glaw and Franzen (2006:176); Tschudi (1838:78); Duméril and Bibron (1841:396); Peters (1872:225).

Rana pygmaea Spix (1824:30). Holotype or type series not designated, although figured a specimen [Plate VI, Fig. 2] from "Provincia Bahiae" (= Bahia state), Brazil [**nomen dubium**]. Günther (1858:27); Peters (1872:225); Boulenger (1882:247); Hoogmoed and Gruber (1983:355); Heyer (1973:26).

Rana pachybrachion Wied-Neuwied (1824:671). Holotype or type series not designated, from "Brasiliens" (= Brazil). [Possible emendation or misspelling of *P. pachypus* by Vanzolini and Myers (2015:75–76).]

Rana macrocephala Wied-Neuwied (1825:544). Holotype or type series not designated, from "Urwäldern an der Lagoa d'Arara unweit des Flusses Mucuri" (= Lagoa

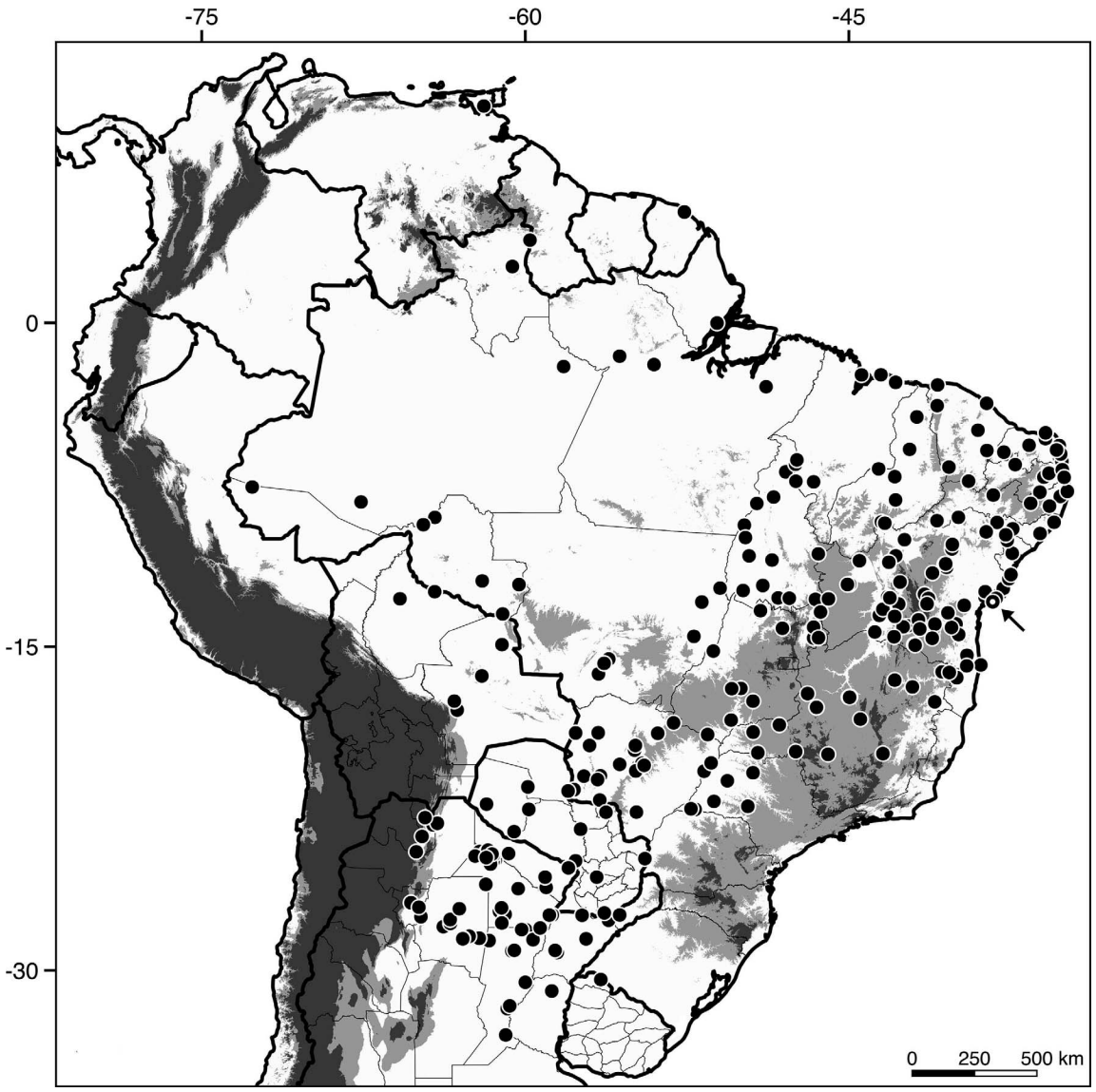

Fig. 16.—Geographic distribution of examined specimens and molecular samples of *Leptodactylus macrosternum* in South America. Arrow and dotted symbol denote the species type locality. Areas above 500 and 1000 m are shaded gray. A color version of this figure is available online.

d'Arara, Mucuri river, southern Bahia state), Brazil. Bokermann (1966:89).

Rana pachypus octolineatus Mayer (1835:24). Holotype, type series and locality not stated. [**nomen dubium**].

Leptodactylus ocellatus: Girard (1853:420); Girard (1858:29–31). Gallardo (1964:378–379; in part, misidentification).

Leptodactylus serialis Girard (1853:421). Holotype or type series not designated, from "Rio de Janeiro, Rio de Janeiro, Brazil." Cochran (1961:64), implied that USNM 7389 (2 specimens) are syntypes [not examined]. Girard (1858:29); Boulenger (1882:247); Jiménez de la Espada (1875:48).

Leptodactylus caliginosus Girard (1853:422). Holotype or type series not designated, from "Rio de Janeiro, [Rio de Janeiro], Brazil." Cochran (1961:64), implied that USNM 7357 (2 specimens) are syntypes [not examined]. Girard (1858:31–33); Nieden (1923:490); Lutz (1930:2, 22).

Cystignathus pachypus (Spix): Günther (1858:27).

Cystignathus caliginosus (Girard): Günther (1858:28); Burmeister (1861:532).

Leptodactylus pachypus (Spix): Jiménez de la Espada (1875:48).

Leptodactylus pygmaeus (Spix): Miranda-Ribeiro (1927:119); Flower (1928:25).

Leptodactylus latrans (Steffen): Lavilla et al. (2010:8). Designated a Neotype male (MNRJ 30733) from "Vale dos Agriões (22°25′S, 42°58′W, approximately 900 m, datum = WGS84), municipality of Teresópolis, state of Rio de Janeiro, Brazil" [not examined; they also provided Neotype coloration and measurements].

Rana pacybrachion: Vanzolini and Myers (2015:75–76; misspelling).

Diagnosis.—Assigned to the *Leptodactylus latrans* species group by phylogenetic placement and the following combination of features: (1) adult male SVL = 63.2–124.9 mm ($\bar{X}$ = 95.8 mm) and adult female SVL = 61.4–104.7 mm

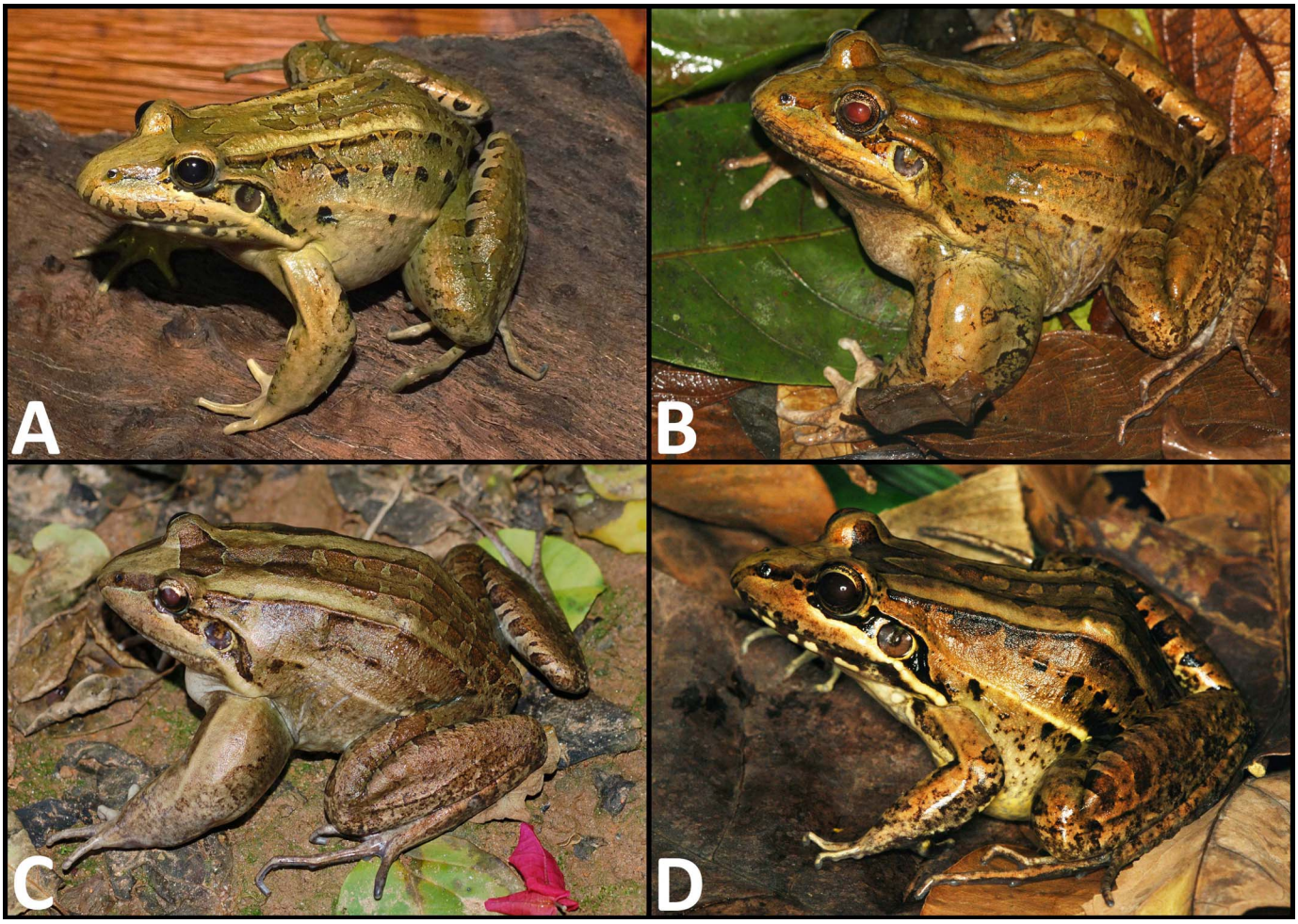

FIG. 17.—Representatives of nominal *Leptodactylus latrans*: (A) adult male (CFBH 42763) from Teresópolis municipality, Rio de Janeiro, Brazil; (B) adult male (AAG-UFU 6148) from Santa Teresa municipality, Espírito Santo, Brazil; (C) unvouchered adult male from Ubatuba municipality, São Paulo, Brazil; and (D) adult female (UFBA 15099) from Salvador municipality, Bahia, Brazil (photo by R.O. Abreu). A color version of this figure is available online.

($\bar{X}$ = 89.8 mm); (2) adult males with a pair of black keratinized thumb spines on hand; (3) adult males with chest spicules (no spines); (4) two pairs of complete and well-developed dorsal longitudinal folds (Folds F2 and F4) extending from behind the eye or posterior interocular region to the pelvic region; (5) pair of auxiliary folds (Fold F3) absent or, if present, are short and restricted to the anterior third of the dorsum; (6) single-lobed vocal sac in adult males; (7) toes and fingers laterally fringed; (8) single longitudinal row of spicules on posterior surface of tibia; (9) advertisement call as single, nonpulsed notes with smooth envelope (amplitude modulations absent); (10) dominant frequency ranging from 280–455 Hz ($\bar{X}$ = 356 Hz).

Variation.—We observed that the distribution of ocellated blotches along the dorsal region varies from smooth (ocellated blotches absent, Fig. 17B) to a sparsely scattered pattern (see Fig. 17A,C,D). The ocellated blotches are mostly restricted to dorsal and dorsolateral regions, whereas lateral regions mostly lack this feature. The supralabial light stripe that extends from below the eyes to the forelimb region (passing under the tympanum) can be well marked (Fig. 17D) or poorly marked (Fig. 17A–C). A supratympanic dark stripe extending from below the eye to the forelimb insertion (posteriorly behind tympanum) can be well marked (Fig. 17A,D) or poorly marked (Fig. 17B). Similarly, the supratympanic dark stripe may form a triangular-shaped feature posterior to the tympanum, which can be black (Fig. 17D), light to dark brown (Fig. 17A,C), or indistinct/absent (Fig. 17B). Some specimens may exhibit green shades along body dorsum, instead of the overall reddish-brown body coloration in life (Fig. 17A–D). All other variations in morphological features are mentioned in the Morphology section of Results.

Advertisement call.—Description is based on calls of nine males (n = 100 calls), of which three (n = 46 calls) are topotypes. See Appendix II for locality and recording information. Descriptive statistics (mean and standard deviation) are given in Table 6. Calls are given at irregular intervals. The call is composed of single, nonpulsed notes with rise time at 28–82% of their length (Fig. 13A). Note length ranges from 124–248 ms. Frequency range is mostly distributed across the first three harmonics, and the second harmonic often has more energy at the very onset, when the fundamental frequency is still barely detectable, but almost all sound energy is contained in the fundamental harmonic throughout the note. The dominant frequency always coincides with the fundamental harmonic, ranging from 280–445 Hz. Notes have a modest frequency upsweep,

TABLE 6.—Advertisement call traits for the species in the *Leptodactylus latrans* complex clade. Data are given as mean ± SD (range). The following traits were quantified from notes of the advertisement call: note length (NL), note rise time (NRT), pulse number (PP), pulse rate (PR), dominant frequency (DF), and linear frequency modulation (LFM); *n* = number of males recorded (number of calls/pulses analyzed); NA = not applicable.

Trait	*L. latrans*, *n* = 9 (100/NA)	*L. payaya* (CS1), *n* = 4 (49/416)	*L. luctator* (CS2), *n* = 8 (134/NA)	*L. paranaru* (CS3), *n* = 4 (37/NA)
NL (ms)	174.9 ± 29.7 (124–248)	191.9 ± 14.9 (158–245)	282.4 ± 58.4 (158–413)	181.0 ± 17.6 (129–241)
NRT (%)	53.5 ± 11.9 (28–82)	66.1 ± 9.2 (56–86)	67.6 ± 8.9 (45–85)	72.5 ± 8.1 (59–82)
PP/note	NA	8.4 ± 1.3 (6–10)	NA	NA
PR/s	NA	50.8 ± 8.1 (42–62)	NA	NA
DF (Hz)	355.7 ± 39.6 (280–445)	470.1 ± 69.2 (398–633)	342.8 ± 29.2 (280–409)	339.7 ± 14.3 (323–366)
LFM (Hz)	152.2 ± 58.4 (43–301)	359.8 ± 116.3 (94–609)	160.3 ± 52.0 (43–281)	–27.1 ± 32.4 (–141 to 47)

ranging from 43–301 Hz. An exception to this description is restricted to variation in the envelope of calls recorded from a topotype, in which we detected irregular amplitude modulations along the note. Without any other information, it is difficult to interpret the possible sources of variation related to such changes in the amplitude envelope. We are aware that the calling rate in the *Leptodactylus latrans* complex, for instance, depends much on the motivation state of nearby calling males, the presence of neighboring calling males and receptive females, among other factors. Call envelope might also be modulated as a result of the combination of the extrinsic factors mentioned above and intrinsic factors (e.g., within-male variation/plasticity) and/or simply reflect interfering structures in the environment that could have affected sound propagation.

Comparisons with other species (characteristics from other species are given within parentheses).—*Leptodactylus latrans* differs from *L. silvanimbus*, the three species of the *L. bolivianus* complex (*L. bolivianus*, *L. guianensis*, and *L. insularum*), and *L. viridis* by exhibiting well-developed and complete dorsal longitudinal folds F1–F2 that extend from behind the eye to the pelvic region (absent in *L. silvanimbus*, *L. bolivianus*, *L. guianensis*, and *L. insularum*, Heyer and de Sá 2011; Fig. 7A; and barely discernible or absent in *L. viridis*, Jim and Spirandeli-Cruz 1979; Fig. 7B). The presence of two thumb spines distinguishes males of *L. latrans* males from those of *L. bolivianus*, *L. guianensis* and *L. viridis* (one thumb spine; Jim and Spirandeli-Cruz 1979; Heyer and de Sá 2011). The presence of a single longitudinal row of spicules on the posterior surface of tibia distinguishes *L. latrans* from *L. viridis* (three longitudinal rows of spicules; Jim and Spirandeli-Cruz 1979). By its larger body size (SVL = 63.2–124.9 mm, $\bar{X}$ = 93.8 mm), *L. latrans* differs from *L. silvanimbus* (SVL = 35.8–55.0 mm, $\bar{X}$ = 47.8 mm; de Sá et al. 2014) and *L. viridis* (SVL range = 63.0–70.9 mm; de Sá et al. 2014; Supplementary Material S3). Additionally, *L. latrans* differs from *L. viridis* by the overall reddish-brown body coloration in life (body coloration predominantly green; Fig. 7B; Jim and Spirandeli-Cruz 1979; de Sá et al. 2014).

Leptodactylus latrans is further distinguished from congeners of the *L. latrans* group by acoustic traits. The three species of the *L. bolivianus* complex (*L. bolivianus*, *L. guianensis*, and *L. insularum*) have well-marked frequency upsweep in their calls, in contrast to modest frequency modulation in the call of *L. latrans*. In addition, calls in the *L. bolivianus* complex always have higher dominant frequencies (combined range = 600–1130 Hz; Heyer and de Sá 2011) than the call of *L. latrans* (range = 280–445 Hz). *Leptodactylus silvanimbus* has a broad-band call without frequency sweeps, differing in both features from the call of *L. latrans*, which is relatively more well tuned and with a frequency upsweep (Fig. 14E; Heyer et al. 1996a). *Leptodactylus viridis* has a short-length call (16–31 ms; Fig. 14F; Rocha et al. 2016) relative to the call of *L. latrans* (124–248 ms).

Leptodactylus latrans has 32–110 base-pair (from 507) differences in the COI mitochondrial gene (or approximately 8–26% of genetic distance) in comparison to the other species of the *L. latrans* group. This clade is supported as a distinct evolutionary entity with significant support in all phylogenetic (posterior probability = 1.0/bootstrap score = 100) and delimitation (bGMYC; ABGD) analyses.

Geographic distribution.—*Leptodactylus latrans* is endemic to the Atlantic Forest and occurs along the Brazilian coastal zone from Pernambuco (Cei 1962; Gallardo 1964; Roberto et al. 2017) to northern São Paulo state in Bertioga municipality, also occupying higher altitudinal zones (~700–900-m elevation) in Rio de Janeiro state and the "Zona da Mata Mineira," the Atlantic Forest in eastern Minas Gerais. In São Paulo state, we only recorded this species along coastal areas (below 100-m elevation) east of the Serra do Mar mountain range (Figs. 2 and 18).

Remarks.—Because *Leptodactylus latrans* is the only species restricted to the Atlantic Forest from northern São Paulo state to Salvador municipality in Bahia state, all species names whose type localities are assigned to the same region were kept as synonyms of *L. latrans*: *Rana gibbosa* Raddi 1823 (type locality: Rio de Janeiro, Brazil), *R. fusca* Raddi 1823 (type locality: "Rio-Janeiro," Brazil). Junior homonym of *R. fusca* (Schneider 1799; Lavilla et al. 2010), *R. pachypus* Spix 1824 (type locality: "Habitat in locis humidis Provinciae Rio de Janeiro" [Var. 1]; while [Var. 2] from "locis humidis Bahiae" is a junior synonym of *R. fusca* Schneider 1799; Peters 1872), *L. serialis* Girard 1853 (type locality: "Rio de Janeiro," Rio de Janeiro, Brazil), and *L. caliginosus* Girard 1853 (type locality: "Rio de Janeiro," Rio de Janeiro, Brazil).

Lavilla et al. (2010) and Vanzolini and Myers (2015) mentioned that *Rana pachybrachion* is possibly an incorrect subsequent spelling or emendation of *R. pachypus* (Spix

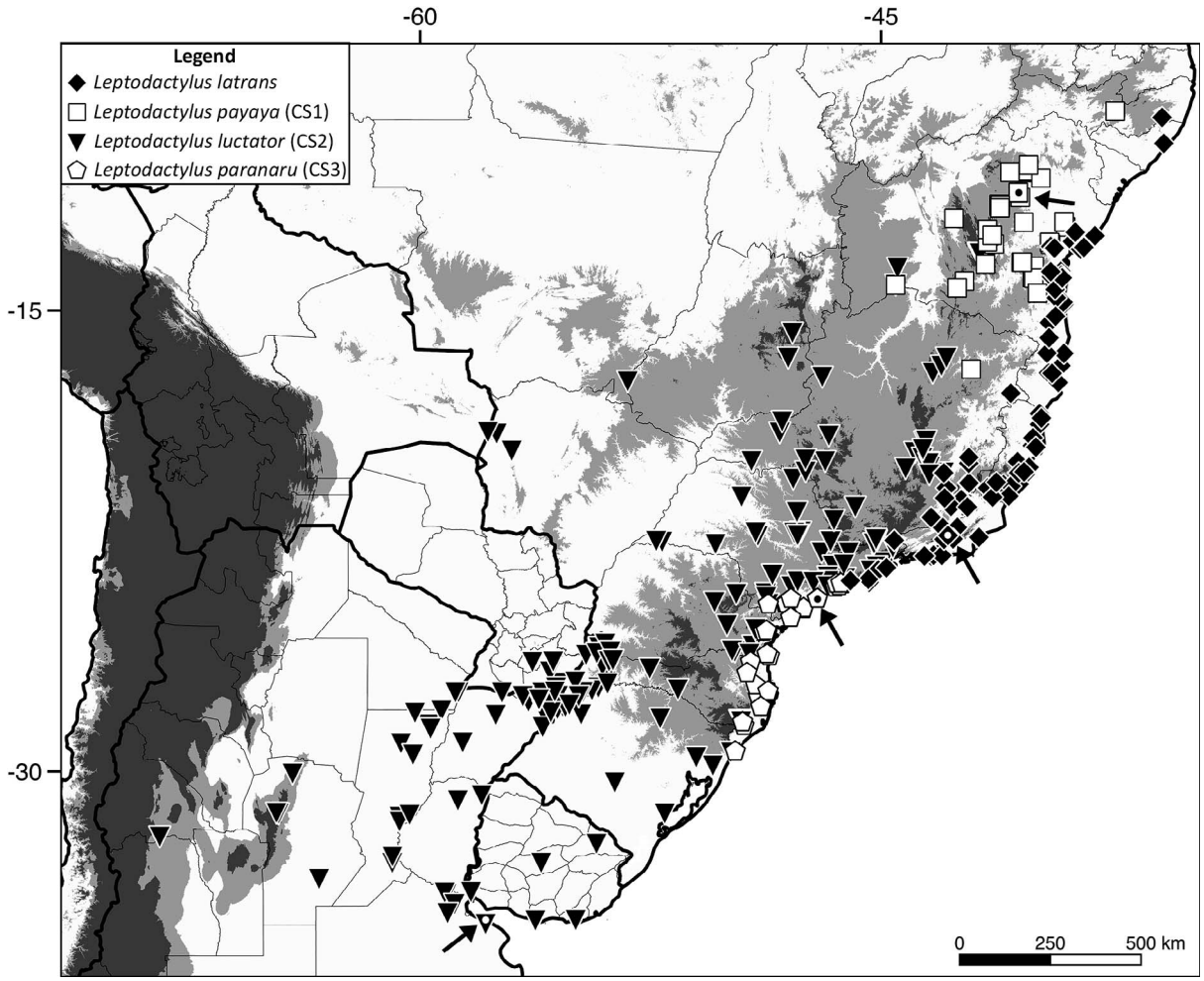

FIG. 18.—Geographic distribution of examined specimens and molecular samples of species in the *Leptodactylus latrans* complex. Arrow and dotted symbol denote each species type locality. Areas above 500 and 1000 m are shaded gray.

1824). Vanzolini and Myers (2015) further argued that Wied-Neuwied obtained specimens of *R. pachypus/pachybrachion* from Espírito Santo and Jucu rivers (which are now part of Espírito Santo state). As mentioned previously, *Leptodactylus latrans* is the only lineage occurring along this state and, therefore, this name is here kept as a synonym of *L. latrans*.

As mentioned in Lavilla et al. (2010) and Vanzolini and Myers (2015), *Rana macrocephala* might correspond to *Ceratophrys aurita* (Raddi 1823) instead of *Leptodactylus*, but the holotype is currently lost. The specimen described by Wied-Neuwied was collected from southern Bahia state, Lagoa d'Arara, lower Mucuri river (Vanzolini and Myers 2015), and was tentatively placed in the synonymy of *L. ocellatus* by Bokermann (1966), because of its geographic distribution and description. In any case, *L. latrans* is the only lineage occurring in southernmost Bahia and, therefore, this name is kept as a synonym of *L. latrans*.

Leptodactylus luctator (Hudson 1892), comb. nov.
(Figs. 19, 20)

Rana luctator Hudson (1892:78). Holotype not designated, from the vicinities of "Buenos Ayres" (= Buenos Aires municipality), Argentina. Gallardo (1964:373–384); Lavilla (1992:87).

Cystignathus oxycephalus Philippi (1902:105–106), his Plate VII; Fig. 3. Syntypes MNHNC (two specimens) from "ad Montevideo. Arrechavaleta" (= Montevideo province), Uruguay [**new synonymy**]. Klappenbach (1968:150).

Cystignathus oxicephalus: Philippi (1902:124) [misspelling].

Leptodactylus ocellatus var. *reticulata* Cei (1948:308–312). Syntypes not designated (presumably FML) from "Arroyo, Isla Apipé, Ituzaingó (Corrientes)" and "Puerto Bemberg (Misiones)," Argentina [**new synonymy**].

Leptodactylus ocellatus var. *bonairensis* Cei (1949:127–132). Syntypes not designated, from "Río Colorado y Bahía Blanca," (= Bahía Blanca municipality, southern Buenos Aires province) Argentina [**new synonymy**]. Cei (1950:416); Gorham (1966:133).

Leptodactylus ocellatus. Cei (1950:411–413); Gallardo (1964:378–379) [in part, misidentification].

Neotype.—LGE 22146, an adult male collected by D. Barrasso in March 2019 at Villa Elvira, La Plata municipality, Buenos Aires province, Argentina (34°58′36"S; 57°52′10"W; 14-m elevation; on all cases datum = WGS84).

Diagnosis.—Assigned to the *Leptodactylus latrans* species group by phylogenetic placement and the following combination of features: (1) adult male SVL = 72.7–121.6

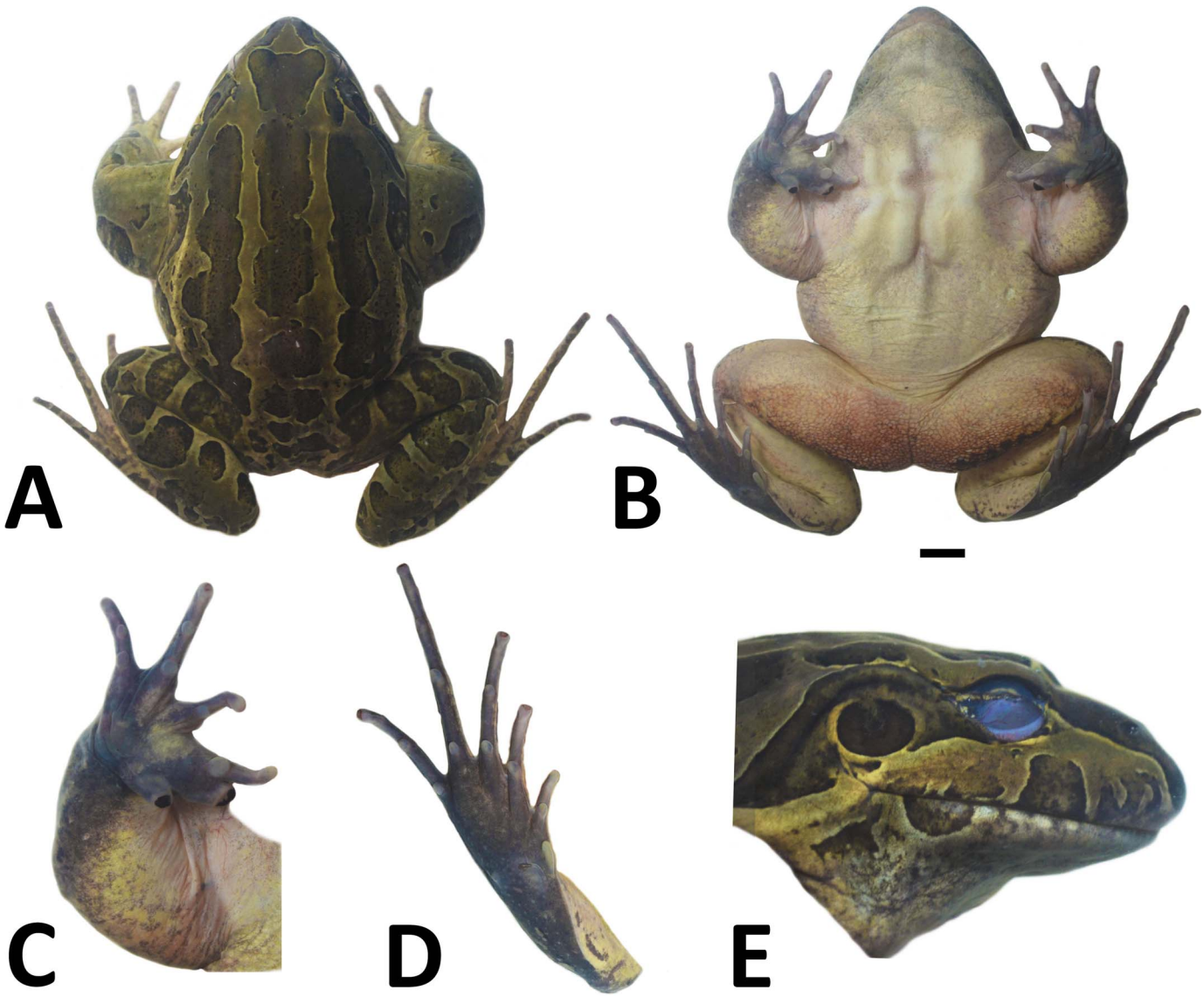

Fig. 19.—Neotype of *Leptodactylus luctator* (LGE 22146). (A) Dorsal and (B) ventral views of body. Views of (C) hand, (D) foot, and (E) head. Scale = 1 cm. Figures C, D, and E not to scale. A color version of this figure is available online.

mm ($\bar{X}$ = 95.0 mm) and adult female SVL = 73.9–115.8 mm ($\bar{X}$ = 91.2 mm); (2) adult males with a pair of black keratinized thumb spines on hand; (3) adult males with chest spicules (no spines); (4) two pairs of complete and well-developed dorsal longitudinal folds (Folds F2 and F4) extending from behind the eyes or posterior interocular regions to the pelvic region; (5) pair of auxiliary folds (Fold F3) absent or, if present, are short and restricted to the anterior third of the dorsum; (6) single-lobed vocal sac in adult males; (7) toes and fingers laterally fringed; (8) single longitudinal row of spicules on posterior surface of tibia; (9) advertisement call as single, nonpulsed notes with weak/irregular amplitude modulations; (10) dominant frequency ranging from 280–409 Hz ($\bar{X}$ = 343 Hz).

Neotype description.—Adult male, with strongly hypertrophied arm. Robust build; head slightly wider than long (head length/width ratio about 93%), head length 34% of SVL, and head width 37% of SVL. Snout rounded from above (Fig. 19A), obtuse in profile (Fig. 19E); canthus rostralis indistinct and rounded; loreal region oblique, slightly concave. Nostril closer to tip of snout than to eyes. Eye protuberant; eye diameter 21% of head length; eye to nostril distance larger than eye and tympanum diameters. Tympanum circular, annulus distinct, thick; distance from tympanum to eye smaller than tympanum diameter. Upper eyelid, head, and dorsal skin smooth; a thick supratympanic fold from posterior corner of eye, arching downwards posteriorly to tympanum, and reaching dorsal region of arm insertion; a thick, longitudinally elongated buccal fold posteriorly to mouth commissure; eight dermal longitudinal folds, four on each side of the body: Fold F2 from posterior interocular region to urostyle region; Fold F4 extends dorsolaterally from posterior corner of eye to groin; Fold F1 (formed by small tubercles) poorly developed, mostly restricted to posterior region of dorsum; Fold F5 slightly shorter than Fold F6, interrupted and extending from above shoulder region to groin; Fold F6 complete, from posterior corner of eye to groin. Ventral skin, dorsal, and ventral

FIG. 20.—Representatives of *Leptodactylus luctator*: (A) neotype, adult male (LGE 22146) from La Plata municipality, Buenos Aires, Argentina; (B) adult male (MZFS 4438) from Piatã municipality, Bahia, Brazil; (C) adult male (voucher MAP1530) from Corumbá municipality, Mato Grosso do Sul, Brazil; and (D) adult male (CFBH 42813) from Buri municipality, São Paulo, Brazil. A color version of this figure is available online.

surfaces of arm smooth; patch formed by small keratinized spicules overall absent on throat and along the ventrolateral region of body; granular seat patch under thighs; cloacal region without expanded fringes; dorsal surface of thigh and tibia with many small pointed spicules; on dorsal tibia surface these spicules align forming a longitudinal row. Vocal sac barely discernible externally, subgular, and single-lobed. Vocal slits present on each side of tongue; vomerine teeth in two transverse series almost contacting medially, laying between and just posterior to choanae. Tongue large, free, slightly notched posteriorly. Hand (Fig. 19C) with slender fingers, not webbed, and with rounded and not expanded tips; weak lateral fringes without small keratinized spicules along their edges; finger lengths III < V < II < IV; subarticular tubercles rounded, and proximal tubercles more developed than distal ones; few rounded supernumerary tubercles present but not very developed; outer metacarpal tubercle large and cordiform; inner metacarpal tubercle small and rounded; a large and rounded keratinized black spine on thumb, lateral to proximal subarticular tubercle of Finger II; a large and rounded keratinized spine on strongly developed prepollex. Leg robust, with long tibia and foot, representing about 48 and 54% of SVL, respectively. Foot (Fig. 19D) with slender toes and only basally webbed; lateral fringes without small keratinized spicules along edge; toe lengths I < II < V < III < IV; toe tips rounded; subarticular tubercles large and rounded; sole of foot with several distinct keratinized spicules; outer metatarsal tubercle very small, rounded and poorly developed; inner metatarsal tubercle large, elliptical, and slightly elevated; sole of tarsus with several evenly distributed keratinized spicules; inner tarsal fold developed, approximately the length of the tarsus.

Coloration of neotype.—In life, dorsal surface of body (dorsum and flanks) and limbs overall light brown with well-delimited dark brown blotches (Fig. 20A); on body, blotches are arranged longitudinally, running over dermal folds from behind eyes to cloacal region, while blotches are arranged transversally on thigh upper side and tibia posterior surfaces. Arm with small dark brown blotches, except for a larger circular blotch on elbow. Anterior surface of arm and groin beige. Posterior surface of thigh yellow mustard with brown maculated patches on the background. Dermal longitudinal folds (F1–F5) dark brown, and F6 whitish. Dark brown stripe from snout, passing through nostrils, to the anterior corner of the eye. Upper half of the loreal region light brown, while the lower half with dark brown blotches on the upper lip. Dark brown stripe running over the supratympanic fold. Tympanic membrane homogeneously dark gray. Throat homogeneously pigmented in light gray. Ventral surface of arm, leg, and belly beige; underside surface of

thigh with small and nonevident yellow melanophores. Ventral surface of hand, foot, and tarsus overall dark gray.

Measurements of neotype (in millimeters).—SVL 99.7, head width 37.1, head length 34.4, eye–snout distance 17.1, eye–nostril distance 9.2, interocular distance 21.9, eye diameter 9.5, tympanum diameter 6.1, hand length 23.3, forearm length 42.8, tibia length 47.7, foot length 51.9.

Variation.—We observed that the most predominant ocellated blotch patterns along the dorsal region are patterns 2 and 3 (Fig. 20). The supralabial light stripe that extends from below eyes to the forelimb insertion (passing under the tympanum) can be well marked (Fig. 20B–D) or indistinct (Fig. 20A). A supratympanic dark stripe extending from below the eye to the forelimb insertion (posteriorly behind tympanum) is generally well marked and varies between black and brownish shades. Similarly, the supratympanic dark stripe may form a triangular-shaped mark posterior to the tympanum, which can be black (see Fig. 1B in Teixeira et al. 2017), light to dark brown (Fig. 20C,D) or indistinct/absent (Fig. 20A,B). Some specimens may exhibit green shades along body dorsum (Fig. 20B,C), instead of the overall reddish-brown body coloration in life. All other variations in morphological features are mentioned in the Morphology section of Results.

Advertisement call.—Description is based on calls of eight males (n = 134 calls; Table 6). See Appendix II for locality and recording information. Descriptive statistics (mean and standard deviation) are given in Table 6. Calls are given at irregular intervals. The call is made up of single, nonpulsed notes with rise time at 45–85% of their length (Fig. 13B). Although defined as nonpulsed, this species has weak/irregular amplitude modulations along the note, in contrast to the smooth envelope of nominal *L. latrans*. Note length ranges from 158–413 ms. Frequency range is mostly distributed across the first three harmonics, being that the second harmonic often has more energy at the very onset, when the fundamental frequency is hardly detected, but almost all sound energy is contained in the fundamental harmonic throughout the note. The dominant frequency always coincides with the fundamental harmonic, ranging from 280–409 Hz. Notes have modest frequency upsweep ranging from 43–281 Hz.

Comparisons with other species (characteristics from other species are given within parentheses).—*Leptodactylus luctator* differs from *L. silvanimbus*, the three species of the *L. bolivianus* complex (*L. bolivianus*, *L. guianensis*, and *L. insularum*), and *L. viridis* by exhibiting well-developed and complete dorsal longitudinal folds F1 and F2, extending from behind the eye to the pelvic region (absent in *L. silvanimbus*, *L. bolivianus*, *L. guianensis*, and *L. insularum*, Heyer and de Sá 2011; Fig. 7A; and barely discernible or absent in *L. viridis*, Jim and Spirandeli-Cruz 1979; Fig. 7B). The single-lobed vocal sac distinguishes males of *L. luctator* from those of *L. macrosternum* (bilobed vocal sac; Gallardo 1964). Also, the anterior throat is homogeneously dark gray in *L. luctator* males, differing from those of *L. macrosternum* (anterior throat light beige). The presence of two thumb spines differentiates males of *L. luctator* from those of *L. bolivianus*, *L. guianensis*, and *L. viridis* (one thumb spine; Jim and Spirandeli-Cruz 1979; Heyer and de Sá 2011). *Leptodactylus luctator* lacks the long auxiliary dorsal fold (or if present is short and restricted to the body's anterior third; Fig. 6A) distinguishing it from *L. macrosternum* (long auxiliary fold extending from behind the eye to midlength of the body; Fig. 6B). The presence of a single longitudinal row of spicules on the posterior surface of tibia differentiates *L. luctator* from *L. viridis* (three longitudinal rows of spicules; Jim and Spirandeli-Cruz 1979). By its larger body size (SVL = 72.7–121.6 mm, $\bar{X}$ = 94.0 mm), *L. luctator* differs from *L. macrosternum* (SVL = 48.7–98.9 mm, $\bar{X}$ = 74.3 mm), *L. silvanimbus* (SVL = 35.8–55.0 mm, $\bar{X}$ = 47.8 mm; de Sá et al. 2014), and *L. viridis* (SVL range = 63.0–70.9 mm; de Sá et al. 2014; Supplementary Material S3). Additionally, *L. luctator* differs from *L. viridis* by the overall reddish-brown body coloration in life (body coloration predominantly green; Fig. 7B; Jim and Spirandeli-Cruz 1979; de Sá et al. 2014). In life, *L. luctator* exhibits yellow melanophores on belly, groin, and on the posterior and underside surface of the thigh (absent in *L. latrans* and *L. macrosternum*). Moreover, *L. luctator* exhibits a black and well-marked maculated patch on the underside surface of thigh, distinguishing it from *L. latrans* (absent or exhibiting a mottled pattern) and *L. macrosternum* (absent). The presence of evident dark brown and outlined ocellated blotches on dorsum distinguishes *L. luctator* from *L. latrans* (smooth or faded and without outlined ocellated blotches).

Leptodactylus luctator is further distinguished from congeners of the *L. latrans* group based on acoustic traits. From the closest related species (i.e., *L. latrans* complex clade), *L. luctator* differs in having nonpulsed notes with weak/irregular amplitude modulations, which is nonpulsed with a smooth envelope in *L. latrans* (amplitude modulations absent). The single-note call of *L. luctator* differs from the extended vocal repertoire of *L. macrosternum* made up of three distinct note types (referred to as *L. chaquensis* in Heyer and Giaretta 2009, Camurugi et al. 2017). The three species of the *L. bolivianus* complex (*L. bolivianus*, *L. guianensis*, and *L. insularum*) have well-marked frequency upsweep in their calls, in contrast to the modest frequency modulation in the call of *L. luctator*. Besides, calls in the *L. bolivianus* complex always have higher dominant frequencies (combined range = 600–1130 Hz; Heyer and de Sá 2011) than the call of *L. luctator* (range = 280–409 Hz). *Leptodactylus silvanimbus* has a broad-band call without frequency sweep, differing in both features from the call of *L. luctator*, which is relatively more well tuned and with a frequency upsweep (Heyer et al. 1996a; Fig. 14E). *Leptodactylus viridis* has a very short-length call (16–31 ms; Fig. 14F; Rocha et al. 2016) in comparison with that of *L. luctator* (158–413 ms).

Leptodactylus luctator exhibited from 42–106 base-pair (from 507) differences in the COI mitochondrial gene (or approximately 10–24% of genetic distance) in comparison to the other species of the *L. latrans* group. This clade is supported as a distinct evolutionary entity with significant support in all phylogenetic (posterior probability = 1.0/bootstrap score = 100) and delimitation (bGMYC; ABGD) analyses.

Geographic distribution.—This is the most geographically widespread taxa among species in the *Leptodactylus latrans* complex (Figs. 2 and 18). It occurs in five countries of South America from low-elevation and coastal zones (e.g., Argentina and Uruguay) to high-elevation areas (e.g., above 1000 m) in eastern South America. It is distributed from

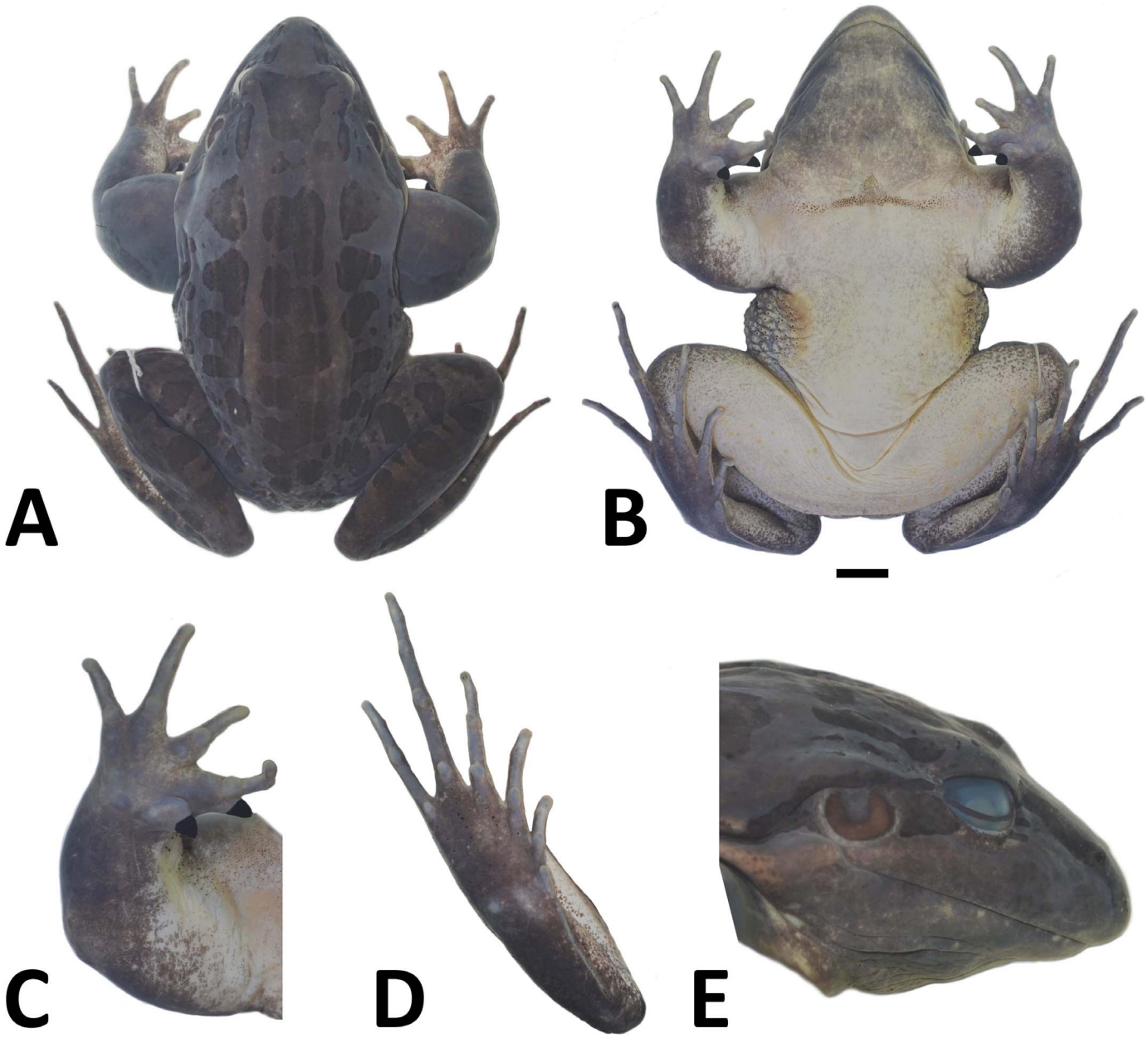

Fig. 21.—Holotype of *Leptodactylus payaya* (CHUFPB 28187). (A) Dorsal and (B) ventral views of body. Views of (C) hand, (D) foot, and (E) head. Scale = 1 cm. Figures C, D, and E not to scale. A color version of this figure is available online.

southwestern Chaco in San Juan Province, through the Pampas of Argentina and Uruguay, across the Atlantic Forest from southeastern Paraguay and southern Brazil in Rio Grande do Sul through high altitudinal zones in Santa Catarina, Paraná, and São Paulo states (west of the Serra do Mar mountain range), also reaching rocky outcrop fields (known as "campos rupestres") within the Espinhaço mountain range in Minas Gerais and Bahia states. This species also occurs in areas under the influence of Cerrado (e.g., Federal District and Mato Grosso, Goiás, and western Minas Gerais states) and apparently exhibits a disjunct distribution in areas under the influence of Pantanal in Mato Grosso do Sul state, with a single record in the easternmost region of Bolivia (see De la Riva and Maldonado 1999). According to Cei (1950, 1962), the distribution of populations related to this species extends to the southernmost regions of Buenos Aires Province (e.g., Bahía Blanca municipality; Cei 1950), but we did not have access to samples from these regions to confirm their specific identity.

Remarks.—Because all our samples belonging to the *Leptodactylus latrans* complex from Uruguay (Montevideo municipality) and Argentina (Corrientes, Misiones and Buenos Aires provinces) cluster within the CS2 lineage (now *L. luctator*), we regard *Cystignathus oxycephalus* Philippi 1902 (type locality: "ad Montevideo," Uruguay), *L. ocellatus* var. *reticulata* Cei 1948 (type locality: "Arroyo, Isla Apipé, Ituzaingó [Corrientes]" and "Puerto Bemberg [Misiones]," Argentina), and *L. ocellatus* var. *bonairensis* Cei 1949 (type locality: "Río Colorado y Bahía Blanca," Argentina) as synonyms of *L. luctator*. Although we did not

Fig. 22.—Representatives of *Leptodactylus payaya*: (A) holotype, adult male (CHUFPB 28187); (B) paratopotype, adult male (CHUFPB 28189); (C) paratopotype, adult male (CHUFPB 28184); and (D) paratopotype, adult female (CHUFPB 28193), all from Chapada Diamantina, Jacobina municipality, Bahia state, Brazil. A color version of this figure is available online.

have access to samples from Bahía Blanca, southern Buenos Aires, it is unlikely that populations are genetically structured if compared to sequences from northern Buenos Aires, given the climatic similarity and lack of major geographic barriers (mountains or rivers) along these two regions. Still, genetic information is desirable to confirm our taxonomic decision on the southernmost populations of *L. luctator*.

Leptodactylus ***payaya*** sp. nov.
(Figs. 21 and 22)

Leptodactylus latrans: Magalhães et al. (2015:247, 261), their Fig. 9G [in part, misidentification].

Leptodactylus macrosternum: Pedrosa et al. (2014:4–5), their Fig. 3A [misidentification].

Leptodactylus ocellatus: Juncá (2005:344), her Table 2 (in part); Nunes and Juncá (2006:152, 154), their Fig. 5 [misidentification].

Holotype.—CHUFPB 28187, an adult male collected by F.M. Magalhães and W. Pessoa on 16 March 2018 at Chapada Diamantina, Jacobina municipality, Bahia state, Brazil (11°9′38.66"S, 40°32′6.60"W; 467-m elevation).

Paratopotypes.—CHFUPB 28184, 28186, 28188–92, adult males, and CHUFPB 28193, adult female, all collected with the holotype.

Diagnosis.—Assigned to the *Leptodactylus latrans* species group by phylogenetic placement and the following combination of features: (1) adult male SVL = 58.5–96.9 mm ($\bar{X}$ = 84.3 mm) and adult female SVL = 72.6–93.6 mm ($\bar{X}$ = 84.6 mm); (2) adult males with a pair of black keratinized thumb spines on hand; (3) adult males with chest spicules (no spines); (4) two pairs of complete and well-developed dorsal longitudinal folds (Folds F2 and F4) extending from behind the eye or posterior interocular region to the pelvic region; (5) pair of auxiliary fold (Fold F3) absent or, if present, are short and restricted to the anterior third of the

dorsum; (6) single-lobed vocal sac in adult males; (7) toes and fingers laterally fringed; (8) single longitudinal row of spicules on the posterior surface of tibia; (9) advertisement call as a single type of partly fused, multipulsed note; (10) dominant frequency ranging from 398–633 Hz ($\bar{X} = 470$ Hz).

Holotype description.—Adult male; arm strongly hypertrophied. Robust build; head slightly wider than long (head length/width ratio about 95%), head length 35% of SVL, and head width 36% of SVL. Snout rounded from above (Fig. 21A), obtuse in profile (Fig. 21E); canthus rostralis indistinct and rounded; loreal region oblique, slightly concave. Nostril closer to tip of snout than to eye. Eye protuberant; eye diameter 19% of head length; eye to nostril distance larger than eye and tympanum diameters. Tympanum circular, annulus distinct, thick; distance from tympanum to eye smaller than tympanum diameter. Upper eyelid, head, and dorsal skin smooth; a thick supratympanic fold from posterior corner of eye, arching downwards posteriorly to tympanum, and reaching dorsal region of arm insertion; a thick, longitudinally elongated buccal fold posteriorly to mouth commissure; eight dermal longitudinal folds, four on each side of body: Fold F2 from posterior interocular region to urostyle region; Fold F4 extends dorsolaterally from posterior corner of eye to groin; Fold F1 (formed by small tubercles) poorly developed and not discernible in preservative; Fold F5 slightly shorter than Fold F6, interrupted, from above shoulder region to groin; Fold F6 complete, from posterior corner of eye to groin; ventral skin, dorsal and ventral surfaces of arm smooth; a patch formed by small keratinized spicules from wrist to throat region, where more densely grouped spicules form a triangular shaped feature posteriorly to throat. Patch of keratinized spicules on each side of ventrolateral region of body, extending from below arm to groin; a granular seat patch under thighs; cloacal region without expanded fringes; dorsal surface of thigh and tibia with many small pointed spicules; on dorsal tibia surface spicules align forming longitudinal row. Vocal sac barely discernible externally, subgular, and single lobed. Vocal slits present on each side of tongue; vomerine teeth in two transverse series almost contacting medially, laying between and just posterior to choanae. Tongue large, free, slightly notched behind. Hand (Fig. 21C) with slender fingers, not webbed, and with rounded and not expanded tips; weak lateral fringes with small keratinized spicules along their edges; finger lengths III < V < II < IV; subarticular tubercles rounded, and proximal tubercles more developed than distal ones; few rounded supernumerary tubercles present but not very developed; outer metacarpal tubercle large and cordiform; inner metacarpal tubercle small and rounded; a large and triangular keratinized black spine on thumb, lateral to proximal subarticular tubercle of Finger II; a large, triangular, keratinized spine on strongly developed prepollex. Leg robust with long tibia and foot, representing about 49 and 47% of SVL, respectively. Foot (Fig. 21D) with slender toes and only basally webbed; lateral fringes with small keratinized spicules along edges; toe lengths I < II < V < III < IV; toe tips rounded; subarticular tubercles large and rounded; sole of foot with several distinct keratinized spicules; outer metatarsal tubercle very small, rounded and poorly developed; inner metatarsal tubercle large, elliptical, slightly elevated; sole of tarsus with several evenly distributed keratinized spicules; inner tarsal fold developed, approximately the length of tarsus also exhibiting keratinized spicules along its edge.

Coloration of holotype.—In life, dorsal surface of body (dorsum and flanks) and limbs overall reddish brown with well-marked dark brown circular blotches (Fig. 22A); on body, blotches are sparsely scattered on dorsum, and on posterior members blotches are arranged transversally on thigh and mostly indistinct on tibia. Arm mostly lacking dark brown blotches; anterior surface of arm, groin, and thigh posterior surface with green shades; posterior surface of thighs without strongly marked black maculated patches. Dermal longitudinal folds (F1–F5) dark brown, and F6 whitish. Dark brown stripe between nostrils and anterior corner of eye. Loreal region homogeneously reddish brown, with a light brown stripe above lip, running over the buccal fold posteriorly to mouth commissure, reaching arm insertion. Thin dark brown stripe running over the supratympanic fold. Tympanic membrane homogeneously dark gray. Throat homogeneously pigmented in dark gray; ventral surface of arm, leg, and belly beige. Ventral surface of hand, foot, and tarsus overall dark gray.

Measurements of holotype (in millimeters).—SVL 95.0, head width 34.5, head length 32.8, eye–snout distance 16.2, eye–nostril distance 9.0, interocular distance 19.4, eye diameter 7.5, tympanum diameter 6.3, hand length 22.1, forearm length 40.1, tibia length 46.3, foot length 44.7.

Variation.—The supralabial light stripe that extends from below eyes to the forelimb region (passing under the tympanum) can be indistinct (Fig. 22A) or well marked (Fig. 22B–C). A supratympanic dark stripe extending from below eye to the forelimb (posteriorly behind tympanum) can also be indistinct (Fig. 22A) or well marked (Fig. 22B,C). Similarly, the supratympanic dark stripe may form a triangular-shaped mark posterior to the tympanum, which can be black (Fig. 22C), light to dark brown (see Fig. 22B), or poorly defined (Fig. 22A,D). All other variations in morphological features are mentioned in the Morphology section of Results.

Etymology.—The specific epithet *payaya* is a reference to the Payayás indigenous ethnicity (a masculine noun in Portuguese) that once inhabited the Chapada Diamantina region in northeastern Brazil (Puntoni 2002). The region corresponds to the new species type locality. There are still descendants of the Payayá people fighting for conservation by developing projects related to the reforestation of river banks in Chapada Diamantina. The specific epithet *payaya* is treated as a noun in apposition.

Advertisement call.—Description is based on calls of four males ($n = 49$ calls and 416 pulses; Table 6), including the holotype. See Appendix II for locality and recording information. Descriptive statistics (mean and standard deviation) are given in Table 6. Calls are given at irregular intervals. The call consists of single, multipulsed (partly fused) notes with rise time at 56–86% of their length (Fig. 13C). Note length ranges from 158–245 ms. Pulse number is 6–10, which are emitted at a rate of 42–62/s. Frequency range is mostly distributed across the first three harmonics, being that the fundamental harmonic always has more sound energy along the call. The dominant frequency ranges from 398–633 Hz. Notes have frequency upsweep ranging from 94–609 Hz and oscillatory frequency modulations associated

with pulsing (incomplete amplitude modulations along the note).

Comparisons with other species (characteristics from other species are given within parentheses).—*Leptodactylus payaya* differs from *L. silvanimbus*, the three species of the *L. bolivianus* complex (*L. bolivianus*, *L. guianensis*, and *L. insularum*), and *L. viridis* by exhibiting well-developed and complete dorsal longitudinal folds F1 and F2, extending from behind the eye to the pelvic region (absent in *L. silvanimbus*, *L. bolivianus*, *L. guianensis*, and *L. insularum*, Heyer and de Sá 2011; Fig. 7A; and barely discernible or absent in *L. viridis*, Jim and Spirandeli-Cruz 1979; Fig. 7B). The single-lobed vocal sac differentiates males of *L. payaya* from those of *L. macrosternum* (bilobed vocal sac; Gallardo 1964). Also, the anterior throat is homogeneously dark gray in *L. luctator* males, differing from those of *L. macrosternum* (anterior throat light beige). The presence of two thumb spines differentiates males of *L. payaya* from those of *L. bolivianus*, *L. guianensis*, and *L. viridis* (one thumb spine; Jim and Spirandeli-Cruz 1979; Heyer and de Sá 2011). *Leptodactylus payaya* lacks the long auxiliary dorsal fold (or if present is short and restricted to the body's anterior third; Fig. 6A) distinguishing it from *L. macrosternum* (long auxiliary fold extending from behind the eye to midlength of the body; Fig. 6B). The presence of a single longitudinal row of spicules on the posterior surface of tibia distinguishes *L. payaya* from *L. viridis* (three longitudinal rows of spicules; Jim and Spirandeli-Cruz 1979). By its larger body size (SVL = 58.5–96.9 mm, $\bar{X}$ = 84.4 mm), *L. payaya* differs from *L. silvanimbus* (SVL = 35.8–55.0 mm, $\bar{X}$ = 47.8 mm; de Sá et al. 2014), and *L. viridis* (SVL range = 63.0–70.9 mm; de Sá et al. 2014; Supplementary Material S3). In opposite, the overall smaller body size (with maximum SVL reaching 96.9 mm) distinguishes *L. payaya* from *L. latrans*, *L. luctator*, and the three species of the *L. bolivianus* complex (combined maximum SVL = 104.6–124.9 mm; de Sá et. al. 2014; Table 4). Additionally, *L. payaya* differs from *L. viridis* by the overall brownish body coloration in life (body coloration predominantly green; Fig. 7B; Jim and Spirandeli-Cruz 1979; de Sá et al. 2014). In life, coloration of groin and posterior surface of thigh is generally distinctly green (groin and posterior thigh are not distinctly green in *L. latrans* and *L. luctator*). Moreover, *L. payaya* only exhibits mottled black blotches on the posterior surface of thigh, distinguishing it from *L. latrans* and *L. luctator* (exhibit well-marked black maculated patches) and *L. macrosternum* (black pigmentation absent). Moreover, *L. payaya* also lacks maculated black patches on the underside surface of thigh, distinguishing from *L. luctator* (present). The presence of evident dark brown ocellated blotches (without an outline) on dorsum differentiates *L. payaya* from *L. latrans* (smooth or faded ocellated blotches) and *L. luctator* (outlined ocellated blotches present).

Leptodactylus payaya is further distinguished from congeners of the *L. latrans* group based on acoustic traits. By having multipulsed notes (unique feature within the *L. latrans* complex), *L. payaya* differs from *L. latrans* and *L. luctator*, as well as the members of the *L. bolivianus* complex, *L. silvanimbus*, and *L. viridis* (nonpulsed notes; Fig. 11; Heyer et al. 1996a; Heyer and de Sá 2011; Rocha et al. 2016). The single-note call of *L. payaya* differs from the extended vocal repertoire of *L. macrosternum* made up of three distinct note types (referred as *L. chaquensis* in Heyer and Giaretta 2009; Camurugi et al. 2017).

Leptodactylus payaya has from 52–108 base-pair (from 507) differences in the COI mitochondrial gene (or approximately 13–24% of genetic distance) in comparison to the other species of the *L. latrans* group. This clade is supported as a distinct evolutionary entity with significant support in all phylogenetic (posterior probability = 1.0/ bootstrap score = 100) and delimitation (bGMYC; ABGD) analyses.

Geographic distribution.—This species is distributed across open fields of the Chapada Diamantina mountain range and surrounding areas in Bahia state, east of the São Francisco River, with single records west of this river in Côcos municipality, Bahia and in Caatinga/Atlantic Forest ecotonal areas from Minas Gerais and Pernambuco states (Figs. 2 and 18).

Leptodactylus ***paranaru*** sp. nov.
(Figs. 23 and 24)

Leptodactylus latrans: Wachlevski and Rocha (2010:603); Zina et al. (2012:254) [misidentification].
Leptodactylus ocellatus: Silva et al. (2000:27); Bertoluci et al. (2007:368); Narvaes et al. (2009:120) [in part, misidentification].

Holotype.—CFBH 42804, an adult male collected by F.M. Magalhães and F.M. Lanna on 27 January 2018 at Peruíbe municipality, São Paulo state, Brazil (24°22′43.42"S, 47°4′31.04"W; 14-m elevation).

Paratopotypes.—CFBH 42805 and 42807, adult males collected along with the holotype. CFBH 12455, an adult female collected by M.T. Thomé and K. Zamudio on 25 February 2006; CFBH 24121, an adult male collected by R.J. Sawaya, F.E. Barbo, and M.G. Rodrigues on 01 October 2008; and CFBH 38572, an adult male collected by F.R Silva and A.Z. Boaratti on 11 December 2014.

Diagnosis.—Assigned to the *Leptodactylus latrans* species group by phylogenetic placement and the following combination of features: (1) adult male SVL = 78.9–126.3 mm ($\bar{X}$ = 100.0 mm) and adult female SVL = 75.2–106.3 mm ($\bar{X}$ = 89.9 mm); (2) adult males with a pair of black keratinized thumb spines on hand; (3) adult males with chest spicules (no spines); (4) two pairs of complete and well-developed dorsal longitudinal folds (Folds F2 and F4) extending from behind eye or posterior interocular region to pelvic region; (5) pair of auxiliary folds (Fold F3) absent or, if present, short and restricted to anterior third of the dorsum; (6) single-lobed vocal sac in adult males; (7) toes and fingers laterally fringed; (8) single longitudinal row of spicules on posterior surface of tibia; (9) advertisement call as single, nonpulsed notes with weak/irregular amplitude modulations; (10) dominant frequency 323–366 Hz ($\bar{X}$ = 340 Hz).

Holotype description.—Adult male; arm strongly hypertrophied. Robust build; head slightly wider than long (head length/width ratio about 91%), head length 37% of SVL, and head width 40% of SVL. Snout rounded from above (Fig. 23A), obtuse in profile (Fig. 23E); canthus rostralis slightly marked and rounded; loreal region oblique, slightly concave. Nostril closer to tip of snout than to eye. Eye protuberant; eye diameter 21% of head length; eye to

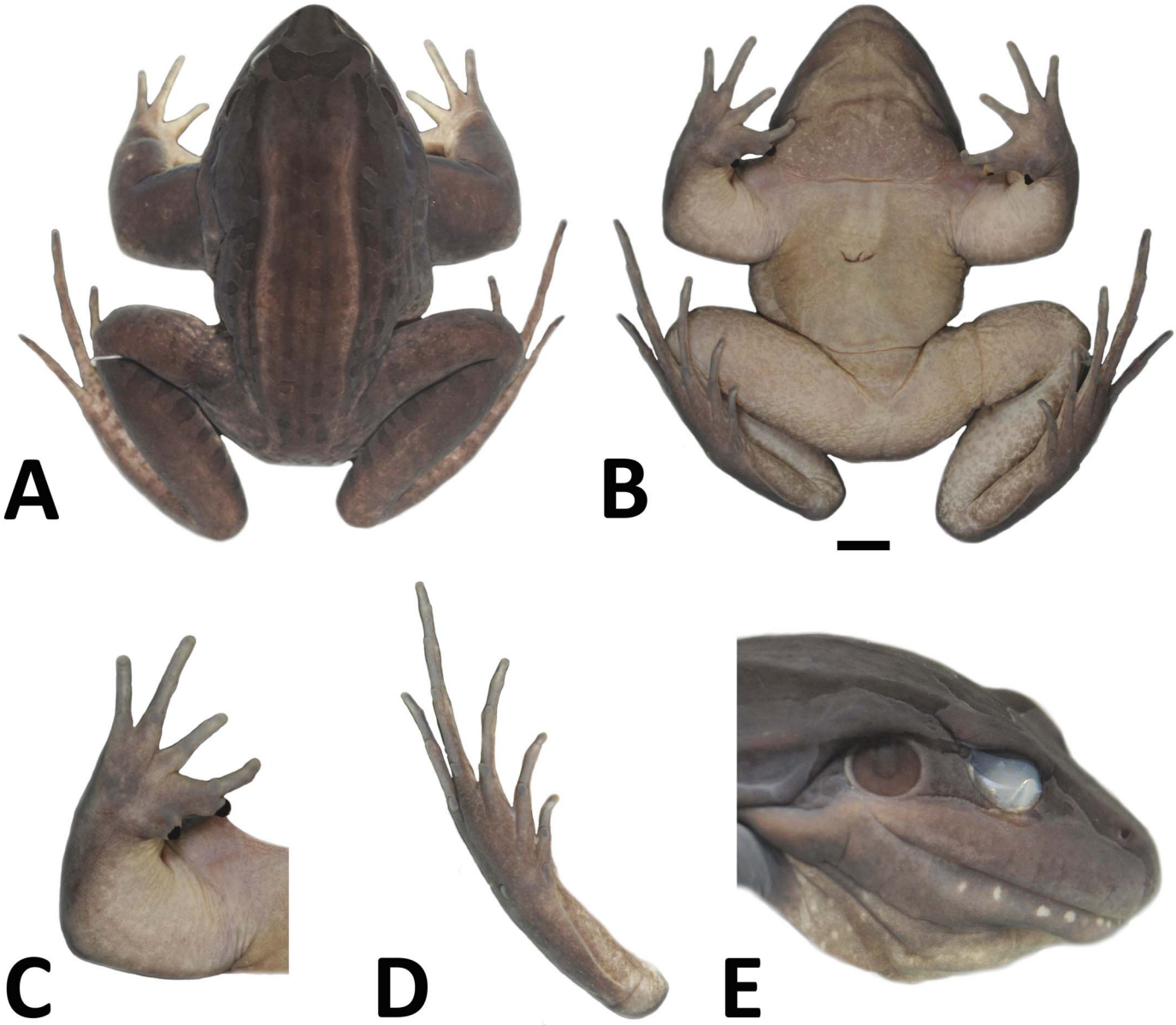

Fig. 23.—Holotype of *Leptodactylus paranaru* (CFBH 42804). (A) Dorsal and (B) ventral views of body. Views of (C) hand, (D) foot, and (E) head. Scale = 1 cm. Figures C, D, and E not to scale. A color version of this figure is available online.

nostril distance larger than eye and tympanum diameter. Tympanum circular, annulus distinct, thick; distance from tympanum to eye smaller than tympanum diameter. Upper eyelid, head, and dorsal skin smooth; a thick supratympanic fold from posterior corner of eye, arching downwards posteriorly to tympanum, and reaching dorsal region of arm insertion; a thick, longitudinally elongated buccal fold posteriorly to mouth commissure; eight dermal longitudinal folds, four on each side of body: Fold F2 from posterior interocular region to urostyle region; Fold F4 dorsolaterally from posterior corner of eye to groin; Fold F1 (formed by small tubercles) poorly developed and not discernible in preservative; Fold F5 slightly shorter than Fold F6, interrupted and extending from above shoulder region to groin; Fold F6 interrupted, from posterior corner of eye to groin; ventral skin, dorsal and ventral surfaces of arm smooth; very few keratinized small spicules from wrist to throat region. A patch of keratinized spicules on each side of ventrolateral region of body, from below arm to groin; a granular seat patch under thighs; cloacal region without expanded fringes; dorsal surface of thigh and tibia with many small pointed tubercles or spicules; on dorsal tibia surface these spicules align forming a longitudinal row. Vocal sac barely discernible externally, subgular, and single-lobed; no lateral vocal folds. Vocal slits present; vomerine teeth in two transverse series, almost contacting medially, laying between and just posterior to choanae. Tongue large, free, slightly notched behind. Hand (Fig. 23C) with slender fingers, not webbed, and with rounded and not expanded tips; weak lateral fringes without keratinized spicules along their edges; finger lengths III < V < II < IV; subarticular tubercles rounded, and proximal tubercles more developed than distal ones; few rounded supernumerary tubercles present but not very developed; outer metacarpal tubercle large and

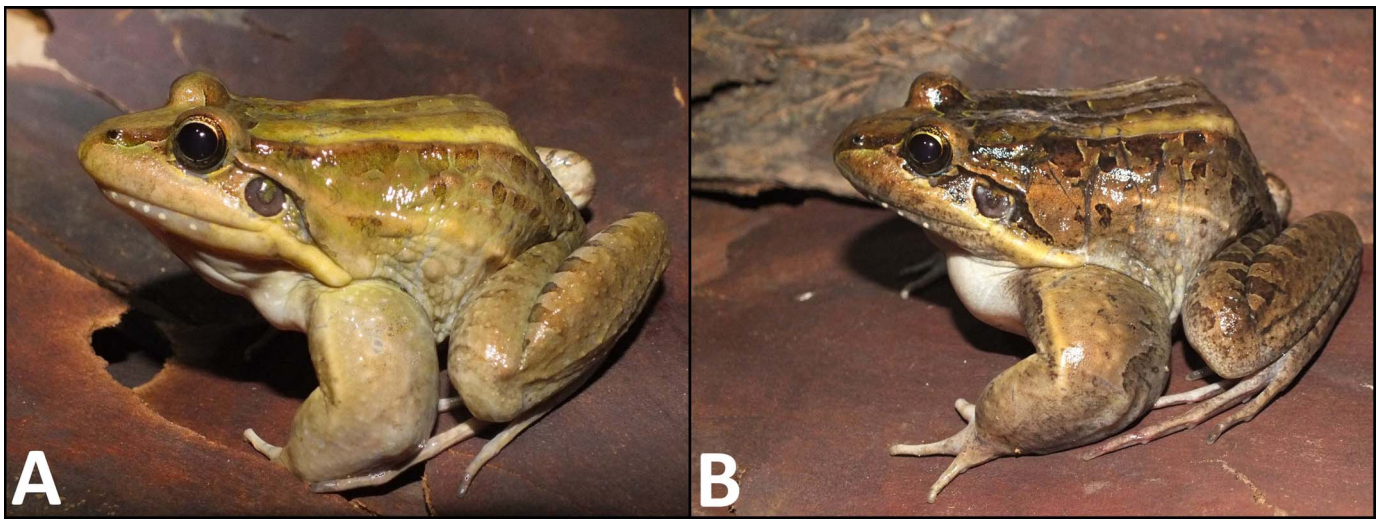

Fig. 24.—Representatives of the *Leptodactylus paranaru*: (A) holotype, adult male (CFBH 42804); and (B) paratopotype, adult male (CFBH 42807) from Peruíbe municipality, São Paulo, Brazil. A color version of this figure is available online.

cordiform; inner metacarpal tubercle small and rounded; a large and slightly rectangular keratinized black spine on thumb, lateral to proximal subarticular tubercle of Finger II; a large and triangular keratinized spine on strongly developed prepollex. Leg robust; tibia and foot long, representing about 55% and 60% of SVL, respectively. Foot (Fig. 23D) with slender toes and only basally webbed; lateral fringes without keratinized spicules along their edges; toe lengths I < II < V < III < IV; toe tips rounded; subarticular tubercles large and rounded; sole of foot with several distinct keratinized spicules; outer metatarsal tubercle very small, rounded and poorly developed; inner metatarsal tubercle large, elliptical, slightly elevated; sole of tarsus with several evenly distributed keratinized spicules; inner tarsal fold developed, approximately the length of tarsus without keratinized spicules along edge.

Coloration of holotype.—In life, dorsal surface of body (dorsum and flanks) and limbs overall light brown with greenish shades (Fig. 24A); on body, poorly marked brown circular blotches sparsely scattered along dorsum and upperside thigh, and arranged transversally on tibia posterior surface. Arm mostly lacking brown blotches; posterior surface of thighs with blue shades and well-marked black macular patches on the background. Dermal longitudinal folds (F1 –F5) brown, and F6 whitish. Dark brown stripe between nostrils and anterior corner of eye. Loreal region homogeneously light brown, forming a stripe that runs above lip, over the buccal fold posteriorly to mouth commissure, reaching arm insertion; lower lip with few white spots. Thin dark brown stripe running over the supratympanic fold. Tympanic membrane homogeneously dark gray. Throat homogeneously pigmented in dark gray; ventral surface of arm, leg, and belly beige. Ventral surface of hand, foot, and tarsus overall dark gray.

Measurements of holotype (in millimeters).—SVL 87.2, head width 35.2, head length 31.9, eye–snout distance 16.0, eye–nostril distance 9.2, interocular distance 22.2, eye diameter 8.3, tympanum diameter 6.8, hand length 23.2, forearm length 41.6, tibia length 48.3, foot length 52.1.

Variation.—We observed that the distribution of ocellated blotches along the dorsal region vary from a smooth to a faded and sparsely scattered pattern (Fig. 24). The ocellated blotches are mostly restricted to the dorsal and dorsolateral regions, while body lateral regions mostly lack this feature. The supralabial light stripe that extends from below eyes to the forelimb insertion (passing under the tympanum) can be well marked or barely distinct (Fig. 24). A supratympanic dark stripe extending from below eye to the forelimb insertion (posteriorly behind tympanum) can be well marked (Fig. 24B) or poorly marked (Fig. 24A). Similarly, the supratympanic dark stripe may form a triangular-shaped mark posterior to the tympanum, which can be light to dark brown (Fig. 24B) or indistinct/absent (Fig. 24A). In life, some specimens may exhibit green shades along body dorsum (Fig. 24A), instead of the overall reddish-brown body coloration (Fig. 24B). All other variations in morphological features are mentioned in the "Morphology" section of Results.

Etymology.—The specific epithet *paranaru* is the combination of two Tupi-Guarani (an indigenous linguistic family from South America) masculine nouns: for some spoken indigenous languages, mainly from the Tupi and Guarani lineages, "paranã" can be understood as sea (Freitas 1936; Rodrigues 1953), while "aru" means frog (Boudin 1978), meaning "sea frog." This name is to be treated as a noun in apposition and a reference to the new species restricted occurrence along the Brazilian southeastern coastal zone, which can be found at fresh or brackish water bodies a few meters from the shore (e.g., referred to as *L. ocellatus* in Narvaes et al. 2009; Zina et al. 2012).

Advertisement call.—Description is based on calls of four males ($n = 37$ calls; Table 6), and the only vouchered recording corresponds to calls of the holotype. See Appendix II for locality and recording information. Descriptive statistics (mean and standard deviation) are given in Table 6. Calls are given at irregular intervals. The call consists of single, nonpulsed notes with rise time at 59–82% of their length (Fig. 13D). Although defined as nonpulsed, this species has weak/irregular amplitude modulations along the

note, in contrast to the smooth envelope of nominal *Leptodactylus latrans*. Note length ranges from 129–241 ms. Frequency range is mostly distributed across the first three harmonics, in that the second harmonic often has more energy at the very onset, when the fundamental frequency can still be barely detected, but almost all sound energy is contained in the fundamental harmonic throughout the note. The dominant frequency always coincides with the fundamental harmonic, ranging from 323–366 Hz. Notes have subtle frequency modulation, either negative (in most cases) or positive, ranging from –141 to 47 Hz.

Comparisons with other species (characteristics from other species are given within parentheses).—*Leptodactylus paranaru* differs from *L. silvanimbus*, the three species of the *L. bolivianus* complex (*L. bolivianus*, *L. guianensis*, and *L. insularum*) and *L. viridis* by exhibiting well-developed and complete dorsal longitudinal folds F1–F2 extending from behind the eye to the pelvic region (absent in *L. silvanimbus*, *L. bolivianus*, *L. guianensis*, and *L. insularum*, Heyer and de Sá 2011; Fig. 7A; and barely discernible or absent in *L. viridis*, Jim and Spirandeli-Cruz 1979; Fig. 7B). The single-lobed vocal sac differs male of *L. paranaru* from those of *L. macrosternum* (bilobed vocal sac; Gallardo 1964). The presence of two thumb spines differentiates males of *L. paranaru* from those of *L. bolivianus*, *L. guianensis*, and *L. viridis* (one thumb spine; Jim and Spirandeli-Cruz 1979; Heyer and de Sá 2011). *Leptodactylus paranaru* lacks the auxiliary dorsal fold (or if present is short and restricted to the body's anterior third) distinguishing it from *L. macrosternum* (long auxiliary fold extending from behind eye to mid-length of the body). The presence of a single longitudinal row of spicules on the posterior surface of tibia differentiates *L. paranaru* from *L. viridis* (three longitudinal rows of spicules; Jim and Spirandeli-Cruz 1979). By its larger body size (SVL = 78.9–126.3 mm, $\bar{X}$ = 96.0 mm), *L. paranaru* differs from *L. macrosternum* (SVL = 48.7–98.9 mm, $\bar{X}$ = 74.3 mm), *L. silvanimbus* (SVL = 35.8–55.0 mm, $\bar{X}$ = 47.8 mm SVL; de Sá et al. 2014), and *L. viridis* (SVL range = 63.0–70.9 mm; de Sá et al. 2014; Supplementary Material S3). The larger body size (maximum SVL = 126.3 mm) also differentiates *L. paranaru* from *L. payaya* (maximum SVL = 96.9 mm). The relatively shorter tympanum diameter distinguishes *L. paranaru* from *L. macrosternum* (Table 4). Additionally, *L. paranaru* differs from *L. viridis* by the overall brownish body coloration in life (body coloration predominantly green; Fig. 7B; Jim and Spirandeli-Cruz 1979; de Sá et al. 2014). In life, coloration of groin is generally not distinct to that of the body lateral region in *L. paranaru* (groin is distinctly green in *L. payaya* and *L. macrosternum*, or yellowish in *L. luctator*). In life, thigh posterior surface coloration varies from blue to gray shades in *L. paranaru* (generally green in *L. payaya* and *L. macrosternum*, or yellowish in *L. luctator*). The presence of black pigmentation on belly and on the posterior and underside surfaces of thigh also distinguishes *L. paranaru* from *L. macrosternum* (absent). Moreover, *L. paranaru* lacks black maculated patches on the underside surface of thigh, distinguishing it from *L. luctator* (present). *Leptodactylus paranaru* only exhibits a smooth pattern or faded brown ocellated blotches (without an outline) on dorsum differing from *L. macrosternum* (smooth pattern absent and outlined ocellated blotches present), *L. luctator* (outlined ocellated blotches present), and *L. payaya* (smooth pattern absent).

Leptodactylus paranaru is further distinguished from congeners in the *L. latrans* group based on acoustic traits. From the closest related species (i.e., *L. latrans* complex clade), *L. paranaru* differs from *L. payaya* (pulsed notes) and *L. latrans* (nonpulsed notes with smooth envelope) in having nonpulsed notes with weak/irregular amplitude modulations. From *L. luctator* (43–281 Hz), *L. paranaru* differs in generally having negative frequency modulation (–141 to 47 Hz). By having a single-note call, *L. paranaru* differs from the extended vocal repertoire of *L. macrosternum* made up of three distinct note types (referred as *L. chaquensis* in Heyer and Giaretta 2009; Camurugi et al. 2017). The three species of the *L. bolivianus* complex (*L. bolivianus*, *L. guianensis*, and *L. insularum*) have well-marked frequency upsweep in their calls, in contrast to the negative frequency modulation in *L. paranaru* (Table 6). Also, calls in the *L. bolivianus* complex always have higher dominant frequencies (combined range = 600–1130 Hz; Heyer and de Sá 2011) than the call of *L. paranaru* (range = 323–366 Hz). *Leptodactylus silvanimbus* has a broadband call without frequency sweeps (Fig. 14E; Heyer et al. 1996a), differing in both features from the call of *L. paranaru*, which is relatively more well tuned and usually with a negative frequency modulation. *Leptodactylus viridis* has a very short-length call (16–31 ms; Fig. 14F; Rocha et al. 2016) in comparison with that of *L. paranaru* (129–241 ms).

Leptodactylus paranaru exhibited from 32–112 base-pair (from 507) differences in the COI mitochondrial gene (or approximately 8–27% of genetic distance) in comparison to all other species in the *L. latrans* group. This clade is supported as a distinct evolutionary entity with significant support in all phylogenetic (posterior probability = 1.0/bootstrap score = 100) and delimitation (bGMYC; ABGD) analyses.

Geographic distribution.—This species is endemic to a narrow zone within the southeastern coastal Atlantic Forest region from Santos municipality in São Paulo state to northeastern Rio Grande do Sul state through low-elevation areas (but reaching up 500 m) located east of the Serra do Mar mountain range (Figs. 2 and 18).

Remarks.—Silva et al. (2000) reported on a particular C-banding pattern in chromosomes for specimens of *L. latrans* complex from Guaratuba municipality, Paraná state (now *L. paranaru*), indicating that they do not belong to the same species as that of individuals from the plateau areas (now *L. luctator*).

Discussion

General Patterns of Cryptic Diversity

During the past two decades, the use of DNA sequence data has revealed an impressive number of morphologically cryptic anuran taxa that are potentially new species to science (e.g., Fouquet et al. 2007; Vieites et al. 2009; Funk et al. 2012), especially those distributed in tropical regions. Despite such discoveries, advances in taxonomy do not follow the pace at which researchers have uncovered cryptic diversity (Fiser et al. 2018). For instance, because most complexes of morphologically cryptic species revealed by molecular data lack categorical diagnostic characters in-

formed by morphological data sets, formal descriptions of new taxa are predominantly absent in such research papers (e.g., Gehara et al. 2013; Fouquet et al. 2014), even in cases where there is evidence of strong geographic structure and deep genetic divergences (e.g., Lanna et al. 2018; Oliveira et al. 2018; Sabbag et al. 2018). Accordingly, the *Leptodactylus latrans* species complex, which includes conspicuous large-sized frogs, exhibits a strong pattern of geographic structure and high interspecific genetic distances compared to the average distances found for several currently recognized South American amphibian species (Fouquet et al. 2007; Lyra et al. 2017). Nevertheless, their highly conserved morphology coupled with chromatic polymorphism (most of which are shared among all species) hamper morphological-based species diagnoses (see below), as previously published for species in the *L. bolivianus* complex (Heyer and de Sá 2011).

On the other hand, advertisement calls have been increasingly employed as one of the most reliable diagnostic features for species discrimination in some anuran groups, notably in leptodactylid frogs of the genus *Leptodactylus* (e.g., Heyer et al. 1996b; Carvalho et al. 2013; Silva et al. 2020) and other genera across this frog family (e.g., Carvalho 2012; Carvalho et al. 2019; Santos et al. 2019; Leal et al. 2020). We found that most species in the *L. latrans* group can be diagnosed based on acoustic features, including *L. latrans*, *L. luctator*, and *L. paranaru*, for which differences are subtle and restricted to amplitude modulation patterns. Additionally, previous studies showed that species in the *L. latrans* group (lacking diagnostic morphological characters) can be distinguished by chromosomal arrangement (Silva et al. 2000) and biochemical, physiological, and serological features of their skins (e.g., Cei and Bertini 1961; Cei and Cohen 1965; Maxson and Heyer 1988), highlighting an interesting field to be explored in the future. Interestingly, members of the *L. latrans* group are strictly associated with aquatic environments during reproductive periods (e.g., males call with the body partially submerged in water during calling/breeding activity; Prado et al. 2000; Heyer and Giareta 2009; Camurugi et al. 2017). This indicates that aquatic biochemical communication may play an important role for species-specific recognition in this species group, thereby relaxing selection pressure towards distinct morphotypes (as proposed by Maxson and Heyer 1988). Although evidence supporting the existence of aquatic sex pheromones and chemical signaling among leptodactylid species is scarce (King et al. 2005), it is known that this could be an alternative channel for intraspecific communication in anurans (Belanger and Corkum 2009).

Recent studies have shown, mainly based on molecular data, that the geographic range of anuran species is generally narrower than previously reported in traditional taxonomic studies (Gehara et al. 2013) or show deep genetic divergences with strong geographic structure (Fouquet et al. 2014; Oliveira et al. 2018), as shown in the present study for species in the *Leptodactylus latrans* complex. For instance, *L. fuscus*, *Dendropsophus minutus*, and *Physalaemus cuvieri*, three anuran species with broad geographic distribution in South America, have deep genetic structure across their distributions (Camargo et al. 2006; Gehara et al. 2014; Miranda et al. 2019). In contrast to this prediction, we found no evidence for strong regional genetic structure in *L. macrosternum* as intraspecific genetic divergence did not exceed 4% in the mitochondrial COI gene (as previously reported; Lyra et al. 2017). This is the first reported case of a South American anuran species lacking strong regional structure or deep genetic divergences across a broad geographic range. It is very likely that the generalist habit, high tolerance to distinct environmental conditions, high vagility, and unique physiological adaptations explain why *L. macrosternum* populations are continuously distributed without noticeable genetic divergence throughout highly variable environmental gradients in South America.

Morphological Diagnostic Features

The series of taxonomic reviews by Cei (1950, 1962, 1970) and Gallardo (1964) on *Leptodactylus latrans* and allied species have ranked mainly the larger SVL, differences in leg features (e.g., toe length, foot, or the entire member) and head shape to diagnose species in this group by morphometric data. However, by measuring a large set of individuals with comprehensive geographic representativeness for all species, we found that differences in morphometric traits always overlapped to a certain degree. This hampers their approximation to discrete characters, as ratios or raw values will only distinguish species unequivocally when they are within narrow ranges of the spectrum of values possible for each species (e.g., SVL, and relative tympanum diameter and foot length; Table 4). Overall, our morphometric data set had a low discriminatory effect, and was most effective in separating *L. macrosternum* and *L. payaya* from remaining species in the *L. latrans* complex based on body-size differences. Accordingly, maximum SVL values of *L. latrans*, *L. luctator*, and *L. paranaru* males (reaching up to 121.6–126 mm; Table 4) are larger if compared to those of *L. macrosternum*, which reaches, as far as we know, a maximum size of 98.9 mm. Therefore, SVL larger than 100 mm may be used as a proxy to discriminate species of the *L. latrans* complex sympatric with *L. macrosternum*, and also the allopatric *L. paranaru* (Fig. 2). As mentioned throughout this work, interspecific SVL raw values considerably overlap, but certainly represent the most important source of morphometric variation to statistically discriminate species in the *L. latrans* group (Fig. 12B).

This scenario was also observed for several features we evaluated in the trait-by-trait analysis (mentioned in Morphology section of Results; Table 4). For instance, the color patterns of the posterior thigh surface provide a visual clue to identify in the field individuals of *Leptodactylus luctator* (the only species exhibiting yellow shades), *L. macrosternum*, and *L. payaya* (sharing green shades). Additionally, *L. luctator* is the only species exhibiting well-marked black maculated patches on the underside surface of thigh. Although not evaluated by us at a large geographic scale, the enlarged black triangular-shaped mark posterior to the tympanum may also provide a visual clue to distinguish sympatric individuals of *L. luctator* from *L. macrosternum* in Argentina, Uruguay, and southernmost Brazil (Cei 1950, 1980; Langone 1995; Teixeira et al. 2017; referred therein as *L. latrans/L. ocellatus* and *L. chaquensis*, respectively). Therefore, some of the morphological traits ranked by us provide relevant information for species discrimination, especially in regions where *L. macrosternum* and species of the *L. latrans* complex are found in sympatry. However,

because these features are not homogeneously found across all populations of the species range, none could be assigned as diagnostic and all (especially those mentioned in Table 4) should be used with caution. Given the broad geographic distribution and that we could not fully assess all morphological variation contained in the *L. latrans* group, we highly recommend the combined use of distinct lines of evidence, including the arrangement of dermal longitudinal folds, calls, and genetic data for accurate species assignments, and more importantly, accounting for geography, because species in the *L. latrans* group exhibit a clear pattern of nonoverlapping distribution (Figs. 2 and 18).

Acoustics of the *Leptodactylus latrans* Species Group

Sound recordings for members of the *Leptodactylus latrans* group are among the rarest across the genus. This is because species may be explosive breeders (e.g., populations of *L. macrosternum*) or simply because vocal activity is scarcely observed in nature. In addition, these calls are often emitted at relatively lower amplitudes, whereas many other frog species with louder sounds are also in calling activity at higher densities, such that obtaining good-quality recordings is a real challenge in the field. Members of the *L. latrans* group call from within the water, usually amid dense vegetation, and are extremely wary: they perceive movements at the water surface and often stop calling and dive when approached (Heyer and Giareta 2009; Camurugi et al. 2017). It is interesting that their calls are so low-pitched to the point that low-pass filters could be applied to recordings in order to remove calls of many other anuran species in the background. At the same time, these low-pitched calls are in many instances severely impacted by the background noise at lower frequencies caused by wind or rain. Hence, studies describing in detail vocal repertoires of species in the *L. latrans* group are still scanty in comparison with the volume of acoustic data already available for the other three *Leptodactylus* clades.

Nevertheless, a few call descriptions for species in the *Leptodactylus latrans* complex have been published, on which we comment next (calls of other species in the *L. latrans* group were described elsewhere; see Fouquette 1960; Heyer et al. 1996a; Heyer and de Sá 2011; Tárano 2010; Rocha et al. 2016). To our knowledge, Barrio (1966), Straughan and Heyer (1976), Straneck et al. (1993), and Nunes and Juncá (2006) are the only contributions (at least a brief quantitative description and/or sound figure provided) to the acoustics of the *L. latrans* complex, reported as *L. ocellatus* in all the cases. Barrio (1966) presented only frequency call traits, which essentially agree with calls of the *L. latrans* complex. Straneck et al. (1993) provided spectrograms without associated quantitative data, which can also be associated with the *L. latrans* complex based on the low frequency range and frequency modulation. Based on the region (Santa Fe/Entre Ríos, Argentina), it is only possible to associate both above-mentioned descriptions to *L. luctator*. Straughan and Heyer (1976) described calls from eastern Brazilian Amazonia (Belém municipality, Pará state), far beyond the geographic range of the *L. latrans* complex (Fig. 2). These authors did not provide spectrograms for the Amazonian calls, but we are aware that only *L. macrosternum* and species of the *L. bolivianus* complex are distributed in Amazonia. Based on dominant frequency (0.6–1.0 kHz), call duration (0.27 s on average), envelope (partially pulsed), and downward frequency modulation, it is clear that those calls are not from species of the *L. latrans* complex. Nunes and Juncá (2006) described multipulsed calls from Bahia, in northeastern Brazil. Based on the unique call envelope, we are certain that their description corresponds to the call of *L. payaya*. Moreover, we have genetic vouchers assigned to this species from the same locality where those authors recorded the calls (Serra de São João, Feira de Santana municipality, Bahia state).

The *Leptodactylus latrans* Species Group

The species number in the *Leptodactylus latrans* group rose to 10, considering that we synonymized *L. chaquensis* with *L. macrosternum* and revalidated *L. luctator,* and described two new species (*L. payaya* and *L. paranaru*). Still, the *L. viridis* population from Minas Gerais showed a strong genetic structure in comparison with the nominal species from Bahia and was inferred as a putative new species in our delimitation analyses, indicating that there might be an additional unnamed lineage in the *L. latrans* group. However, the limited data currently available for *L. viridis* and related populations prevent us from addressing the taxonomic status of the Minas Gerais population. The *Leptodactylus latrans* group is the least speciose clade among the four *Leptodactylus* groups proposed by Heyer (1969) and supported as monophyletic by de Sá et al. (2014). Historically, the *L. latrans* group is one of the less studied, mainly because the former *L. ocellatus* did not have an associated name-bearing type or an exact type locality (Lavilla et al. 2010). For instance, publications regarding the taxonomy and species limits within this group are scanty or restricted to species descriptions (e.g., Jim and Spirandeli-Cruz 1979; McCranie et al. 1980), except the reviews by Cei (1950, 1962) and Gallardo (1964) using morphological and physiological data. We elucidated species limits and hidden diversity in the widespread *L. latrans* group by means of integrating distinct lines of evidence with comprehensive geographic/taxa sampling. Taken together, our results reinforce the view that species in the *L. latrans* group are morphologically cryptic (Cei 1962; Gallardo 1964; Heyer and de Sá 2011). Accordingly, high levels of cryptic morphology can still be more common than expected in *Leptodactylus* (e.g., Heyer 1978, 1994, 2005) and should be carefully evaluated using integrative frameworks in the other three species groups of *Leptodactylus*.

Acknowledgments.—This work would never have been possible without the help and collaboration of several individuals. We would like to register our feelings and again thank P. Burella for her companionship and essential contribution in gathering data on the *L. latrans* group from Argentina. We thank H. Batalha-Filho, P.I. Simões, H.F.P. Araújo, and D. Baêta for suggestions and comments on the manuscript. FMM thanks the staff of Herpetology Laboratory and Zoology Museums from LGE (UNaM), UFBA, UFMS, UFPB, UNB, and UNESP-Rio Claro for their kind assistance and for all logistic support. We thank M. Jansen (Senckenberg Research Institute); D.O. Mesquita and G.H.C. Vieira from UFPB; L.P. Costa from UFES, P.C.A. Garcia from UFMG; N. Maciel from UFG; T. Motti from UFAL; F.A Juncá from MZFS; and C. Ribas, F. Werneck, and A.P. Lima from INPA institute for allowing the loan of genetic samples under their care. FMM and TRC are indebted to B.F.V. Teixeira, E.F. Oliveira, E.M. Fonseca, D.L. Bang, F.M. Lanna, F.S. de Andrade, L.B. Martins, R.M. Hoffmann, V.A. São-Pedro, and W. Pessoa for their support during field work. D. Barrasso collected the specimen designated as *Leptodactylus luctator* Neotype. T. Grant and the Museu de Zoologia, Universidade de São Paulo shared and authorized the use of *L. macro-*

sternum holotype images. C. Marinho, F. Camurugi, H. Palo, Jr., L.A. Silva, L.J.C. Moraes, M. Struett, R.O Abreu, P. Peloso, and R. Marques made available pictures of living specimens and/or tissue samples. We kindly thank L.R. Mariotto, A. Kwet, W.R. Heyer, Z. Tárano, P.C. Rocha, A. Wynn, J. Pointdexter (USNM recordings; Smithsonian institution) and L.F. Toledo and S. Dena (FNJV recordings; Fonoteca Neotropical Jacques Vielliard) for granting us access to sound recordings. FMM thanks Conselho Nacional de Desenvolvimento Científico e Tecnológico (CNPq; 140649/2015-8) for his doctoral fellowship and Instituto Chico Mendes de Conservação da Biodiversidade (ICMBio, 53175-1) for scientific collection permits. TRC was funded through São Paulo Research Foundation with a doctoral fellowship (FAPESP, 2012/15763-7) and is currently supported by the same funding agency with a postdoctoral fellowship (2017/08489-0). AAG thanks CNPq and FAPEMIG for financial support. CFBH thanks FAPESP (2013/50741-7), FAPESP/Fundação Grupo Boticário de Proteção à Natureza (2014/50342-8), and CNPq (306623/2018-8) for financial support. DJS thanks CNPq for his research fellowship (311492/2017-7). FB thanks Programa Nacional de Incentivo a Investigadores from the Consejo Nacional de Ciencia y Tecnología (PRONII, CONACYT, Paraguay). GRC thanks Coordenação de Apoio à Formação de Pessoal de Nível Superior (CAPES), CNPq, Fundação de Apoio à Pesquisa do Distrito Federal (FAPDF), and USAID's PEER program under cooperative agreement AID-OAA-A-11-00012 for financial support. MFN thanks the Fundação de Amparo à Pesquisa do Estado da Bahia (FAPESB) for financial support (TO PAM 5/2014 and TO PTX 3/2016), and CNPq for productivity grants (305849/2015-8 and 310490/2018-9) and financial support (440565/2015-4). MLL thanks FAPESP for a postdoctoral fellowship (2017/26162-8). This research was supported by resources supplied by the Cyberinfrastructure for Phylogenetic Research (CIPRES).

SUPPLEMENTAL MATERIAL

Supplemental material associated with this article can be found online at https://doi.org/10.1655/HERPMONOGRAPHS-D-19-00012.S1, https://doi.org/10.1655/HERPMONOGRAPHS-D-19-00012.S2, https://doi.org/10.1655/HERPMONOGRAPHS-D-19-00012.S3

LITERATURE CITED

Barbour, T. 1906. Vertebrata from the savanna of Panama: Reptilia and Amphibia. Bulletin of the Museum of Comparative Zoology 46:224–230.

Barley, A.J., J. White, A.C. Diesmos, and R.M. Brown. 2013. The challenge of species delimitation at the extremes: Diversification without morphological change in Philippine sun skinks. Evolution 67:3556–3572. DOI: https://doi.org/10.1111/evo.12219

Barrio, A. 1966. Divergencia acústica entre el canto nupcial de *Leptodactylus ocellatus* (Linne) y *L. chaquensis* Cei (Anura, Leptodactylidae). Physis 26:275–277.

Barrio-Amorós, C.L. 2004. Amphibians of Venezuela: Systematic list, distribution and references; an update. Revista de Ecología Latino Americana 9:1–48.

Belanger, R.M., and L.D. Corkum. 2009. Review of aquatic sex pheromones and chemical communication in anurans. Journal of Herpetology 43:184–191. DOI: https://doi.org/10.1670/08-054R1.1

Bertoluci, J., R.A. Brassaloti, J.W.R. Júnior, V.M.F.N. Vilela, and H.O. Sawakuchi. 2007. Species composition and similarities among anuran assemblages of forest sites in southeastern Brazil. Scientia Agricola 64:364–374. DOI: https://doi.org/10.1590/S0103-90162007000400007

Bokermann, W.C.A. 1965. Nota sobre los anfibios brasileños citados y descriptos por Raddi. Neotropica. La Plata 11:9–12.

Bokermann, W.C.A. 1966. Lista anotada das localidades tipo de anfíbios brasileiros. São Paulo, Serviço de Documentação, Reitoria da Universidade de São Paulo:1–183.

Boudin, M.H. 1978. Dicionário de Tupí Moderno (Dialeto Tembé-ténêtéhar do Alto Gurupi). Conselho Estadual de Artes e Ciências Humanas, Brazil.

Boulenger, G.A. 1882. Catalogue of the Batrachia Salientia s. Ecaudata in the Collection of the British Museum, 2nd ed. Taylor and Francis, UK. DOI: https://doi.org/10.5962/bhl.title.54882

Boulenger, G.A. 1898. A list of the reptiles and batrachians collected by the late Prof. L. Balzan in Bolivia. Annali del Museo Civico di Storia Naturale di Genova 19:128–133.

Breiman, L. 2001. Random forests. Machine learning 45:5–32. DOI: https://doi.org/10.1023/A:1010933404324

Breiman, L., and P. Spector. 1992. Submodel selection and evaluation in regression: The X-random case. International Statistical Review 60:291–319. DOI: https://doi.org/10.2307/1403680

Bruford, M.W., O. Hanotte, J.F.Y. Brookfield, and T. Burke. 1992. Single and multilocus DNA fingerprinting. Pp. 225–269 in Molecular Genetic Analysis of Populations: A Practical Approach (A.R. Hoelzel, ed.). I.R.L. Press, UK.

Burmeister, H. 1861. Reise durch die La Plata-Staaten mit Besonderer Rücksicht auf die Physische Beschaffenheit und den Culturzustand der Argentinische Republik: Ausgefuhrt in den Jahren 1857, 1858, 1859 un 1860, Volume 2. H.W. Schmidt, Germany.

Burnaby, T.P. 1966. Growth-invariant discriminant functions and generalized distances. Biometrics 22:96–110. DOI: https://doi.org/10.2307/2528217

Camargo, A., R.O. de Sá, and W.R. Heyer. 2006. Phylogenetic analyses of mtDNA sequences reveal three cryptic lineages in the widespread Neotropical frog *Leptodactylus fuscus* (Schneider, 1799) (Anura, Leptodactylidae). Biological Journal of the Linnean Society 87:325–341. DOI: https://doi.org/10.1111/j.1095-8312.2006.00581.x

Camurugi, F., F.M. Magalhães, M.H.C. Queiroz, T.C.S.O. Pereira, L. Tavares-Bastos, E.S. Lopes-Marinho, J.M.M. Neves, and A.A. Garda. 2017. Reproduction, sexual dimorphism, and diet of *Leptodactylus chaquensis* (Anura, Leptodactylidae) in northeastern Brazil. Herpetological Conservation and Biology 12:498–508.

Carvalho, T.R. 2012. A new species of *Pseudopaludicola* Miranda-Ribeiro (Leiuperinae: Leptodactylidae: Anura) from the Cerrado of southeastern Brazil with a distinctive advertisement call pattern. Zootaxa 3328:47–54. DOI: https://doi.org/10.11646/zootaxa.3328.1.4

Carvalho, T.R., F.S.F. Leite, and T.L. Pezzuti. 2013. A new species of *Leptodactylus* Fitzinger (Anura, Leptodactylidae, Leptodactylinae) from montane rock fields of the Chapada Diamantina, northeastern Brazil. Zootaxa 3701:349–364. DOI: https://doi.org/10.11646/zootaxa.3701.3.5

Carvalho, T.R., A.A. Giaretta, A. Angulo, C.F.B. Haddad, and P.L.V. Peloso. 2019. A new Amazonian species of *Adenomera* (Anura: Leptodactylidae) from the Brazilian state of Pará: A tody-tyrant voice in a frog. American Museum Novitates 3919:1–21. DOI: https://doi.org/10.1206/3919.1

Cei, J.M. 1948. El ritmo estacional en los fenómenos cíclicos endocrino sexuales de la rana criolla (*Leptodactylus ocellatus*) del norte Argentino. Acta Zoologica Lilloana 6:283–331.

Cei, J.M. 1949. La regulacion hormonal del ciclo sexual en *Leptodactylus ocellatus* (L.) de la Argentina. Acta Zoologica Lilloana 7:113–134.

Cei, J.M. 1950. *Leptodactylus chaquensis* n. sp. y el valor sistematico real de la especie Linneana *Leptodactylus ocellatus* en la Argentina. Acta Zoologica Lilloana 9:395–423.

Cei, J.M. 1962. Mapa preliminar de la distribución continental de las "sibling species" del grupo *ocellatus* (género *Leptodactylus*). Revista de la Sociedad Argentina de Biologia 38:258–265.

Cei, J.M. 1970. Relaciones serologicas entre los *Leptodactylus* del grupo *ocellatus-chaquensis* de la cuenca chaco-paranense y la forma *macrosternum*. Acta Zoologica Lilloana 27:299–306.

Cei, J.M. 1980. Amphibians of Argentina. Monitore Zoologico Italiano N.S. Monografia 2:1–609.

Cei, J.M., and F. Bertini. 1961. Serum proteins in allopatric and sympatric populations of *Leptodactylus ocellatus* and *L. chaquensis*. Copeia 1961:336–340. DOI: https://doi.org/10.2307/1439810

Cei, J.M., and R. Cohen. 1965. Serological relationships in the *Leptodactylus pachypus* species group (Amphibia, Salientia). Copeia 1965:155–158. DOI: https://doi.org/10.2307/1440717

Cei, J.M., V. Erspamer, and M. Roseghini. 1967. Taxonomic and evolutionary significance of biogenic amines and polypeptides occurring in amphibian skin. I. Neotropical leptodactylid frogs. Systematic Zoology 16:328–342. DOI: https://doi.org/10.2307/2412152.

Cochran, D.M. 1961. Type specimens of reptiles and amphibians in the U.S. National Museum. Bulletin of the United States National Museum 220:1–291. DOI: https://doi.org/10.5962/bhl.part.26967

Cole, C.J., C.R. Townsend, R.P. Reynolds, R.D. MacCulloch, and A. Lathrop. 2013. Amphibians and reptiles of Guyana, South America: Illustrated keys, annotated species accounts, and a biogeographic synopsis. Proceedings of the Biological Society of Washington 125:317–578. DOI: https://doi.org/10.2988/0006-324x-125.4.317

De la Riva, I., and M. Maldonado. 1999. First record of *Leptodactylus ocellatus* (Linnaeus, 1758) (Amphibia, Anura, Leptodactylidae) in Bolivia and comments on related species. Graellsia 55:193–197. DOI: https://doi.org/10.3989/graellsia.1999.v55.i0.328

De la Riva, I., J. Köhler, S. Lötters, and S. Reichle. 2000. Ten years of

research on Bolivian amphibians: Updated checklist, distribution, taxonomic problems, literature and iconography. Revista Española de Herpetología 14:19–164.

de Sá, R.O., T. Grant, A. Camargo, W.R. Heyer, M.L. Ponssa, and E. Stanley. 2014. Systematics of the Neotropical genus *Leptodactylus* Fitzinger, 1826 (Anura: Leptodactylidae): Phylogeny, the relevance of non-molecular evidence, and species accounts. South American Journal of Herpetology 9:S1–S128. DOI: https://doi.org/10.2994/sajh-d-13-00022.1

Deng, H. 2013. Guided random forest in the RRF package. arXiv 1306.0237v1:1–2.

Dixon, J.R., and M.A. Staton. 1976. Some aspects of the biology of *Leptodactylus macrosternum* Miranda-Ribeiro (Anura: Leptodactylidae) of the Venezuelan Llanos. Journal of Herpetology 32:227–232. DOI: https://doi.org/10.2307/3891743

Duméril, A.M.C., and G. Bibron. 1841. Erpétologie Générale ou Histoire Naturelle Complète des Reptiles, Volume 8. Librarie Enclyclopedique de Roret, France. DOI: https://doi.org/10.5962/bhl.title.45973

Felsenstein, J. 1981. Evolutionary trees from DNA sequences: A maximum likelihood approach. Journal of Molecular Evolution 17:368–376. DOI: https://doi.org/10.1007/BF01734359

Felsenstein, J., and H. Kishino. 1993. Is there something wrong with the bootstrap on phylogenies? A reply to Hillis and Bull. Systematic Biology 42:193–200. DOI: https://doi.org/10.1093/sysbio/42.2.193

Fiser, C., C.T. Robinson, and F. Malard. 2018. Cryptic species as a window into the paradigm shift of the species concept. Molecular Ecology 27:613–635. DOI: https://doi.org/10.1111/mec.14486

Flower, S.S. 1928. Reptilia and Batrachia (1927). Zoological Record 64:1–28.

Fouquet, A., A. Gilles, M. Vences, C. Marty, M. Blanc, and N. Gemmell. 2007. Underestimation of species richness in Neotropical frogs revealed by mtDNA analyses. PLOS One 2:e1109. DOI: https://doi.org/10.1371/journal.pone.0001109

Fouquet, A., B.P. Noonan, M.T. Rodrigues, N. Pech, A. Gilles, and N.J. Gemmell. 2012. Multiple Quaternary refugia in the eastern Guiana Shield revealed by comparative phylogeography of 12 frog species. Systematic Biology 61:461–489. DOI: https://doi.org/10.1093/sysbio/syr130

Fouquet, A., C. Cassini, C.F.B. Haddad, N. Pech, and M.T. Rodrigues. 2014. Species delimitation, patterns of diversification and historical biogeography of a Neotropical frog genus *Adenomera* (Anura, Leptodactylidae). Journal of Biogeography 41:855–870. DOI: https://doi.org/10.1111/jbi.12250

Fouquette, M.J., Jr. 1960. Call structure in frogs of the family Leptodactylidae. The Texas Journal of Science 12:201–215.

Freitas, A.A. 1936. Vocabulario Nheengatú (Vernaculizado pelo Portuguez Falado em São Paulo): Língua Tupi-Guarani. Edição Nacional, Brazil.

Frost, D.R. 2020. Amphibian species of the world: An online reference, Version 6.1. Available at http://research.amnh.org/herpetology/amphibia/index.html. Accessed on 21 May 2020. American Museum of Natural History, USA. DOI: https://doi.org/10.5531/db.vz.0001

Funk, W.C., M. Caminer, and S.R. Ron. 2012. High levels of cryptic species diversity uncovered in Amazonian frogs. Proceedings of the Royal Society B: Biological Sciences 279:1806–1814. DOI: https://doi.org/10.1098/rspb.2011.1653

Gallardo, J.M. 1964. Consideraciones sobre *Leptodactylus ocellatus* (L.) (Amphibia, Anura) y species aliadas. Physis 24:373–384.

Gehara, M.C., C. Canedo, C.F.B. Haddad, and M. Vences. 2013. From widespread to microendemic: Molecular and acoustic analyses show that *Ischnocnema guentheri* (Amphibia: Brachycephalidae) is endemic to Rio de Janeiro, Brazil. Conservation Genetics 2013:1–10.

Gehara, M., A.J. Crawford, V.G. Orrico . . . J. Kohler. 2014. High levels of diversity uncovered in a widespread nominal taxon: Continental phylogeography of the Neotropical tree frog *Dendropsophus minutus*. PLOS One 9:e103958. DOI: https://doi.org/10.1371/journal.pone.0103958

Girard, C. 1853. Descriptions of new species of reptiles, collected by the U.S. Exploring Expedition, under the command of Capt. Charles Wilkes, U.S.N. Second part—including the species of batrachians, exotic to North America. Proceedings of the Academy of Natural Sciences of Philadelphia 6:420–424. DOI: https://doi.org/10.5962/bhl.part.9360.

Girard, C. 1858. United States Exploring Expedition During the Years 1838, 1839, 1840, 1841, 1842, under the command of Charles Wilkes, U.S.N. Volume 20 (Herpetology). C. Sherman, USA. Available at https://biodiversitylibrary.org/page/40418548.

Glaw, F., and M. Franzen. 2006. Type catalogue of amphibians in the Zoologische Staatsammlung München. Spixiana 29:153–192. Available at http://www.biodiversitylibrary.org/page/28195131.

Gorham, S.W. 1966. Liste der rezenten Amphibien und Reptilien. Ascaphidae, Leiopelmatidae, Pipidae, Discoglossidae, Pelobatidae, Leptodactylidae, Rhinophrynidae. Das Tierreich 85:1–222.

Gorzula, S., and J.C. Señaris. 1998. Contribution to the herpetofauna of the Venezuelan Guayana I. A data base. Scientia Guaianae 8:1–268.

Gridi-Papp, M. 2007. SoundRuler: Acoustic analysis for research and teaching. Available at http://soundruler.sourceforge.net. Accessed on 10 November 2019. Free Software Foundation, Inc., USA.

Günther, A.C.L.G. 1858. Catalogue of the Batrachia salientia in the collection of the British Museum. Taylor and Francis, UK. DOI: https://doi.org/10.5962/bhl.title.12077

Hayward, K.J. 1963. Lista de los tipos de vertebrados conservados en el Instituto Miguel Lillo. Acta Zoologica Lilloana 19:507–510.

Hebert, P.D.N., A. Cywinska, S.L. Ball, and J.R. deWaard. 2003. Biological identifications through DNA barcodes. Proceedings of the Royal Society B: Biological Sciences 270:313–321. DOI: https://doi.org/10.1098/rspb.2002.2218

Heyer, W.R. 1969. The adaptive ecology of the species groups of the frog genus *Leptodactylus* (Amphibia, Leptodactylidae). Evolution 23:421–428. DOI: https://doi.org/10.2307/2406697

Heyer, W.R. 1973. Systematics of the *marmoratus* group of the frog genus *Leptodactylus* (Amphibia, Leptodactylidae). Contributions in Science. Natural History Museum of Los Angeles County 251:1–50.

Heyer, W.R. 1978. Systematics of the *fuscus* group of the frog genus *Leptodactylus* (Amphibia, Leptodactylidae). Science Bulletin. Natural History Museum of Los Angeles County 29:1–85.

Heyer, W.R. 1994. Variation within the *Leptodactylus podicipinus-wagneri* complex of frogs (Amphibia: Leptodactylidae). Smithsonian Contributions to Zoology 546:1–124. DOI: https://doi.org/10.5479/si.00810282.546.i

Heyer, W.R. 2005. Variation and taxonomic clarification of the large species of the *Leptodactylus pentadactylus* species group (Amphibia, Leptodactylidae) from Middle America, Northern South America, and Amazonia. Museu de Zoologia da Universidade de São Paulo 37:269–348.

Heyer, W.R. 2014. Morphological analyses of frogs of the *Leptodactylus latrans* complex (Amphibia, Leptodactylidae) from selected localities in South America. Proceedings of the Biological Society of Washington 126:369–378. DOI: https://doi.org/10.2988/0006-324X-126.4.369

Heyer, W.R., and R.O. de Sá. 2011. Variation, systematics, and relationships of the *Leptodactylus bolivianus* complex (Amphibia: Anura: Leptodactylidae). Smithsonian Contributions to Zoology 635:1–58. DOI: https://doi.org/10.5479/si.00810282.635.1

Heyer, W.R., and A.A. Giaretta. 2009. Advertisement calls, notes on natural history, and distribution of *Leptodactylus chaquensis* (Amphibia: Anura: Leptodactylidae) in Brasil. Proceedings of the Biological Society of Washington 122:292–305. DOI: https://doi.org/10.2988/08-42.1

Heyer, W.R., R.O. de Sá, J.R. McCranie, and L.D. Wilson. 1996a. *Leptodactylus silvanimbus* (Amphibia: Anura: Leptodactylidae): Natural history notes, advertisement call, and relationships. Herpetological Natural History 4:169–174.

Heyer, W.R., J.M. García-Lopez, and A.J. Cardoso. 1996b. Advertisement call variation in the *Leptodactylus mystaceus* complex (Amphibia: Leptodactylidae) with a description of a new sibling species. Amphibia-Reptilia 17:7–31. DOI: https://doi.org/10.1163/156853896X00252

Hillis, D.M., and J.J. Bull. 1993. An empirical test of bootstrapping as a method for assessing confidence in phylogenetic analysis. Systematic Biology 42:182–192. DOI: https://doi.org/10.1093/sysbio/42.2.182

Hoogmoed, M.S., and U. Gruber. 1983. Spix and Wagler type specimens of reptiles and amphibians in the Natural History Musea in Munich (Germany) and Leiden (the Netherlands). Spixiana 9:319–415.

Hudson, W.H. 1892. The Naturalist in La Plata. Chapman and Hall, Ltd., UK. DOI: https://doi.org/10.5962/bhl.title.13554

ICZN (International Commission on Zoological Nomenclature). 1999. International Code of Zoological Nomenclature, 4th edition. International Trust for Zoological Nomenclature, Singapore.

ITZN (International Trust for Zoological Nomenclature). 2003. *Leptodactylus chaquensis* Cei, 1950 (Amphibia, Anura): Specific name conserved. The Bulletin of Zoological Nomenclature 60:173.

Jim, J., and E.F. Spirandeli-Cruz. 1979. Uma nova espécie de *Leptodactylus* do estado da Bahia, Brasil (Amphibia, Anura). Revista Brasileira de Biologia 39:707–710.

Jiménez de la Espada, M. 1875. Vertebrados del viaje al Pacífico verificado de 1862 a 1865 por una comisión de naturalistas enviada por el gobierno

Español. Batracios. A. Miguel Ginesta, Spain. DOI: https://doi.org/10.5962/bhl.title.5769

Jolicoeur, P. 1963. The multivariate generalization of the allometry equation. Biometrics 19:497–499. DOI: https://doi.org/10.2307/2527939

Juncá, F.A. 2005. Anfíbios e Répteis. Pp. 337–356 in Biodiversidade e Conservação da Chapada Diamantina (F.A. Juncá, L. Funch, and W. Rocha, eds.). Ministério do Meio Ambiente (MMA), Brasil.

Katoh, K., K. Misawa, K. Kuma, and T. Miyata. 2002. MAFFT: A novel method for rapid multiple sequence alignment based on fast Fourier transform. Nucleic Acids Research 30:3059–3066. DOI: https://doi.org/10.1093/nar/gkf436

Kearse, M., R. Moir, A. Wilson … A. Drummond. 2012. Geneious basic: An integrated and extendable desktop software platform for the organization and analysis of sequence data. Bioinformatics 28:1647–1649. DOI: https://doi.org/10.1093/bioinformatics/bts199

Kimura, M. 1981. Estimation of evolutionary distances between homologous nucleotide sequences. Proceedings of the National Academy of Sciences of the USA 78:454–458. DOI: https://doi.org/10.1073/pnas.78.1.454

King, J.D., L.A. Rollins-Smith, P.F. Nielsen, A. John, and J.M. Conlon. 2005. Characterization of a peptide from skin secretions of male specimens of the frog *Leptodactylus fallax* that stimulates aggression in male frogs. Peptides 26:597–601. DOI: https://doi.org/10.1016/j.peptides.2004.11.004

Klappenbach, M.A. 1968. Notas herpetológicas, III. Identificación de las especies uruguayas descriptas por Philippi en el "Suplemento a los Batraquios chilenos". Investigaciones Zoológicas Chilenas 23:147–151.

Lanfear, R., P.B. Frandsen, A.M. Wright, T. Senfeld, and B. Calcott. 2016. PartitionFinder 2: New methods for selecting partitioned models of evolution for molecular and morphological phylogenetic analyses. Molecular Biology and Evolution 34:772–773. DOI: https://doi.org/10.1093/molbev/msw260

Langone, J.A. 1995. Ranas y sapos del Uruguay (reconocimiento y aspectos biológicos). Museo Dámaso Antonio Larrañaga. Intendencia Municipal de Montevideo. Serie Divulgación 5:1–127.

Lanna, F.M., F.P. Werneck, M. Gehara, E.M. Fonseca, G.R. Colli, J.W. Sites, Jr., M.T. Rodrigues, and A.A. Garda. 2018. The evolutionary history of *Lygodactylus* lizards in the South American open diagonal. Molecular Phylogenetics and Evolution 127:638–645. DOI: https://doi.org/10.1016/j.ympev.2018.06.010

Lavilla, E.O. 1992. Tipos portadores de nombres y localidades tipo de anfibios de Argentina. Acta Zoologica Lilloana 42:61–100.

Lavilla, E.O., J.A. Langone, U. Caramaschi, W.R. Heyer, and R.O. de Sá. 2010. The identification of *Rana ocellata* Linnaeus, 1758. Nomenclatural impact on the species currently known as *Leptodactylus ocellatus* (Leptodactylidae) and *Osteopilus brunneus* (Gosse, 1851) (Hylidae). Zootaxa 2346:1–16. DOI: https://doi.org/10.5281/zenodo.275558

Leal, F., F.S.F. Leite, W.P. Costa, L.B. Nascimento, L.B. Lourenço, and P.C.A. Garcia. 2020. Amphibians from Serra do Cipó, Minas Gerais, Brasil. VI: A new species of the *Physalaemus deimaticus* group (Anura, Leptodactylidae). Zootaxa 4766:306–330. DOI: https://doi.org/10.11646/zootaxa.4766.2.3

Leite, F.S.F., F.A. Juncá, and P.C. Eterovick. 2008. Status do conhecimento, endemismo e conservação de anfíbios anuros da Cadeia do Espinhaço, Brasil. Megadiversidade 4:158–176.

Liaw, A., and M. Wiener. 2002. Classification and regression by randomForest. R News 2:18–22.

Ligges, U., S. Krey, O. Mersmann, and S. Schnackenberg. 2017. tuneR: Analysis of Music and Speech, Version 1.3.2. Available at https://CRAN.R-project.org/package=tuneR. R Foundation for Statistical Computing, Austria.

Littlejohn, M.J. 2001. Patterns of differentiation in temporal properties of acoustic signals of anurans. Pp. 102–120 in Anuran Acoustic Communication (M.J. Ryan, ed.). Smithsonian Institution Press, USA.

Lutz, A. 1930. Segunda memoria sobre espécies brasileiras do gênero *Leptodactylus*, incluindo outras alliadas. Memorias Do Instituto Oswaldo Cruz 23:1–20. DOI: https://doi.org/10.1590/S0074-02761930000100001

Lyra, M.L., C.F.B. Haddad, and A.M.L. Azeredo-Espin. 2017. Meeting the challenge of DNA barcoding Neotropical amphibians: Polymerase chain reaction optimization and new COI primers. Molecular Ecology Resources 17:966–980. DOI: https://doi.org/10.1111/1755-0998.12648

Machado, I.F., R.G. Becker, and A.S. Mesquita. 2014. Geographic distribution: *Leptodactylus chaquensis*. Herpetological Review 45:277.

Magalhães, F.M., D.O. Laranjeiras, T.B. Costa, F.A. Juncá, D.O. Mesquita, D.L. Rohr, W.P. Silva, G.H.C. Vieira, and A.A. Garda. 2015. Herpetofauna of protected areas in the Caatinga IV: Chapada Diamantina National Park, Bahia, Brazil. Herpetology Notes 8:243–261.

Maniatis, T., E.F. Fritsch, and J. Sambrook. 1982. Molecular Cloning: A Laboratory Manual. Cold Spring Harbor Laboratory, USA.

Maxson, L.R., and W.R. Heyer. 1988. Molecular systematics of the frog genus *Leptodactylus* (Amphibia: Leptodactylidae). Fieldiana: Zoology 41:1–13. DOI: https://doi.org/10.5962/bhl.title.3187

Mayer, A.F.J.C. 1835. Analecten für Vergleichende Anatomie. Eduard Weber, Germany.

McCranie, J.R., L.D. Wilson, and L. Porras. 1980. A new species of *Leptodactylus* from the cloud forests of Honduras. Journal of Herpetology 14:361–367. DOI: https://doi.org/10.2307/1563691

Meyer, C. 2003. Molecular systematics of cowries (Gastropoda: Cypraeidae) and diversification patterns in the tropics. Biological Journal of Linnean Society 79:401–459. DOI: https://doi.org/10.1046/j.1095-8312.2003.00197.x

Mingers, J. 1989. An empirical comparison of selection measures for decision-tree induction. Machine Learning 3:319–342. DOI: https://doi.org/10.1007/BF00116837

Miranda, N.E.O., N.M. Maciel, M.S. Lima-Ribeiro, G.R. Colli, C.F.B. Haddad, and R.G. Collevatti. 2019. Diversification of the widespread Neotropical frog *Physalaemus cuvieri* in response to Neogene-Quaternary geological events and climate dynamics. Molecular Phylogenetics and Evolution 132:67–80. DOI: https://doi.org/10.1016/j.ympev.2018.11.003

Miranda-Ribeiro, A. 1926. Notas para servirem ao estudo dos Gymnobatrachios (Anura) brasileiros. Arquivos do Museu Nacional 27:1–227.

Miranda-Ribeiro, A. 1927. Os Leptodactylidae do Museu Paulista. Revista do Museu Paulista 15:113–134.

Murphy, J.C. 1997. Amphibians and Reptiles of Trinidad and Tobago. Krieger Publishing Company, USA.

Narvaes, P., J. Bertoluci, and M.T. Rodrigues. 2009. Composição, uso de hábitat e estações reprodutivas das espécies de anuros da floresta de restinga da Estação Ecológica Juréia-Itatins, sudeste do Brasil. Biota Neotropica 9:117–123. DOI: https://doi.org/10.1590/S1676-06032009000200011

Nieden, F. 1923. Anura I. Subordo Aglossa und Phaneroglossa. Sectio I Arcifera. Das Tierreich 46. De Gruyter, Germany.

Nunes, I., and F.A. Juncá. 2006. Advertisement calls of three leptodactylid frogs in the state of Bahia, northeastern Brazil (Amphibia, Anura, Leptodactylidae), with considerations on their taxonomic status. Arquivos do Museu Nacional 64:151–157.

Oda, F.H., D.L. Santos, P.G. Gambale, V.A. Campos, V.G. Batista, I.P. Affonso, and C. Strüssmann. 2014. New Brazilian records of *Leptodactylus chaquensis* Cei, 1950, at the species' southern range limit. Herpetozoa 26:195–200.

Oliveira, E.F., M. Gehara, V.A. São-Pedro, G.C. Costa, F.T. Burbrink, G.R. Colli, M.T. Rodrigues, and A.A. Garda. 2018. Phylogeography of Muller's termite frog suggests the vicariant role of the Central Brazilian Plateau. Journal of Biogeography 45:2508–2519. DOI: https://doi.org/10.1111/jbi.13427

Palumbi, S.R., A. Martin, S. Romano, W.O. McMillan, L. Stice, and G. Grabowski. 1991. The Simple Fool's Guide to PCR, Version 2.0. Department of Zoology, Kewalo Marine Laboratory, University of Hawaii, USA.

Pedrosa, I.M.M.C., T.B. Costa, R.G. Faria … A.A. Garda. 2014. Herpetofauna of protected areas in the Caatinga III: The Catimbau National Park, Pernambuco, Brazil. Biota Neotropica 14:1–12. DOI: https://doi.org/10.1590/1676-06032014004614

Peters, W.C.H. 1872. Über die von Spix in Brasilien gesammelten Batrachier des Königl. Naturalienkabinet zu München. Monatsberichte der Königlichen Preussische Akademie des Wissenschaften zu Berlin 1872:196–227.

Philippi, R.A. 1902. Suplemento a los Batraquios Chilenos Descritos en la Historia Física y Politica de Chile de Don Claudio Gay. E. Blanchard–Chessi, Chile.

Pons, J., T.G. Barraclough, J. Gomez-Zurita, A. Cardoso, D.P. Duran, S. Hazell, S. Kamoun, W.D. Sumlin, and A.P. Vogler. 2006. Sequence-based species delimitation for the DNA taxonomy of undescribed insects. Systematic Biology 55:595–609. DOI: https://doi.org/10.1080/10635150600852011

Posso-Terranova, A., and J. Andrés. 2018. Multivariate species boundaries and conservation of harlequin poison frogs. Molecular Ecology 27:3432–3451. DOI: https://doi.org/10.1111/mec.14803

Prado, C.P.A., M. Uetanabaro, and F.S. Lopes. 2000. Reproductive

strategies of *Leptodactylus chaquensis* and *L. podicipinus* in the Pantanal, Brazil. Journal of Herpetology 34:135–139.

Puillandre, N., A. Lambert, S. Brouillet, and G. Achaz. 2012. ABGD, automatic barcode gap discovery for primary species delimitation. Molecular Ecology 21:1864–1877. DOI: https://doi.org/10.1111/j.1365-294X.2011.05239.x

Puntoni, P. 2002. A Guerra dos Bárbaros: Povos Indígenas e a Colonização do Sertão Nordeste do Brasil, 1650–1720. Hucitec/Edusp, Brazil.

R Core Team. 2018. R: A Language and Environment for Statistical Computing, Version 3.0.2. Available at http://www.R-project.org. R Foundation for Statistical Computing, Austria.

Raddi, G. 1823. Continuazione della descrizione dei rettili Brasiliani. Memorie della Societa Italiana delle Scienze 19:58–73.

Rambaut, A. 2014. FigTree: A Graphical Viewer of Phylogenetic Trees, Version 1.4.2. Available at http://tree.bio.ed.ac.uk/software/figtree/. Institute of Evolutionary Biology, University of Edinburgh, UK.

Rambaut, A., A.J. Drummond, D. Xie, G. Baele, and M.A. Suchard. 2018. Posterior summarisation in Bayesian phylogenetics using Tracer 1.7. Systematic Biology 67:901–904. DOI: https://doi.org/10.1093/sysbio/syy032

Reid, N., and B. Carstens. 2012. Phylogenetic estimation error can decrease the accuracy of species delimitation: A Bayesian implementation of the general mixed Yule-coalescent model. BMC Evolutionary Biology 12:196. DOI: https://doi.org/10.1186/1471-2148-12-196

Roberto, I.J., C.R. Oliveira, J.A. Araújo-Filho, H.F. Oliveira, and R.W. Ávila. 2017. The herpetofauna of the Serra do Urubu mountain range: A key biodiversity area for conservation in the Brazilian Atlantic Forest. Papéis Avulsos de Zoologia 57:347–373. DOI: https://doi.org/10.11606/0031-1049.2017.57.27

Rocha, P.C., T.L. Pezzuti, and P.C.A. Garcia. 2016. Advertisement call of *Leptodactylus viridis* (Anura: Leptodactylidae) from Minas Gerais, Brazil. Salamandra 52:342–344.

Rodrigues, A.D. 1953. Morfologia do verbo Tupi. Letras 1:121–152.

Rohlf, F.J., and F.L. Bookstein. 1987. A comment on shearing as a method for "size correction." Systematic Zoology 36:356–367. DOI: https://doi.org/10.2307/2413400

Sabaj, M.H. 2016. Standard Symbolic Codes for Institutional Resource Collections in Herpetology and Ichthyology: An Online Reference, Version 6.5. Available at http://www.asih.org/. Accessed on 16 August 2016. American Society of Ichthyologists and Herpetologists, USA.

Sabbag, A.F., L.M. Lyra, K.R. Zamudio, C.F.B. Haddad, R.N. Feio, F.S.F. Leite, J.L. Gasparini, and C.A. Brasileiro. 2018. Molecular phylogeny of Neotropical rock frogs reveals a long history of vicariant diversification in the Atlantic forest. Molecular Phylogenetics and Evolution 2018:142–156. DOI: https://doi.org/10.1016/j.ympev.2018.01.017

Santos, M.T.T., S.H. Oliveira, T.R. Carvalho, B.F. Zaidan, N.R. Silva, B.V.M. Berneck, and P.C.A. Garcia. 2019. A new species of *Paratelmatobius* (Anura: Leptodactylidae: Paratelmatobiinae) from the Atlantic Forest of southern Brazil. Zootaxa 4648:473–493. DOI: https://doi.org/10.11646/zootaxa.4648.3.4

Santos, T.G., and S.Z. Cechin. 2008. Amphibia, Anura, Leptodactylidae, *Leptodactylus chaquensis*: Distribution extension in the state of Rio Grande do Sul, Brazil. Check List 4:142–144. DOI: https://doi.org/10.15560/4.2.142

Schneider, J.G. 1799. Historia Amphibiorum Naturalis et Literarariae. Fasciculus Primus. Continens Ranas, Calamitas, Bufones, Salamandras et Hydros in Genera et Species Descriptos Notisque suis Distinctos. Friederici Frommanni, Germany.

Serié, P. 1935. Observaciones de Hudson sobre algunos saurios y batrachios. Physis 11:493–494.

Silva, A.P., C.F.B. Haddad, and S. Kasahara. 2000. Chromosomal studies on five species of the genus *Leptodactylus* Fitzinger, 1826 (Amphibia, Anura) using differential staining. Cytobios 103:25–38.

Silva, L.A., F.M. Magalhães, H. Thomassen, F.S.F. Leite, A.A. Garda, R.A. Brandão, C.F.B. Haddad, A.A. Giaretta, and T.R. Carvalho. 2020. Unraveling the species diversity and relationships in the *Leptodactylus mystaceus* complex (Anura, Leptodactylidae), with the description of three new Brazilian species. Zootaxa 4779:151–189. DOI: https://doi.org/10.11646/zootaxa.4779.2.1

Somers, K.M. 1986. Multivariate allometry and removal of size with principal component analysis. Systematic Zoology 35:359–368. DOI: https://doi.org/10.1093/sysbio/35.3.359

Spix, J.B. 1824. Animalia nova sive Species novae Testudinum et Ranarum quas in itinere per Brasiliam annis MDCCCXVII–MDCCCXX jussu et auspiciis Maximiliani Josephi I. Bavariae Regis. Typis Franc. Seraph. Hübschmanni, Monachii. DOI: https://doi.org/10.5962/bhl.title.3665

Stamatakis, A. 2014. RAxML version 8: A tool for phylogenetic analysis and post-analysis of large phylogenies. Bioinformatics 30:1312–1313. DOI: https://doi.org/10.1093/bioinformatics/btu033

Steffen, G.A. 1815. De Ranis Nonnullis Observationes Anatomicae quas Consensu Gratiosae Facultatis Medicae. Joannis Friderici Starckii, Germany.

Stekhoven, D.J. 2011. Using the missForest Package, R package 1–11. Available at https://cran.r-project.org/. R Foundation for Statistical Computing, Austria.

Straneck, R., E.V. Olmedo, and G.R. Carrizo. 1993. Catálogo de Voces de Anfíbios Argentinos, Tomo I. Ediciones LOLA, Argentina.

Straughan, I.R., and W.R. Heyer. 1976. A functional analysis of the mating calls of the Neotropical frog genera of the *Leptodactylus* complex (Amphibia, Leptodactylidae). Papéis Avulsos de Zoologia 29:221–245.

Suchard, M.A., P. Lemey, G. Baele, D.L. Ayres, A.J. Drummond, and A. Rambaut. 2018. Bayesian phylogenetic and phylodynamic data integration using BEAST 1.10. Virus Evolution 4:vey016. DOI: https://doi.org/10.1093/ve/vey016

Sueur, J., T. Aubin, and C. Simonis. 2008. Seewave: A free modular tool for sound analysis and synthesis. Bioacoustics 18:213–226. DOI: https://doi.org/10.1080/09524622.2008.9753600

Tamura, K., and M. Nei. 1993. Estimation of the number of nucleotide substitutions in the control region of mitochondrial DNA in humans and chimpanzees. Molecular Biology and Evolution 10:512–526. DOI: https://doi.org/10.1093/oxfordjournals.molbev.a040023

Tamura, K., G. Stecher, D. Peterson, A. Filipski, and S. Kumar. 2013. MEGA6: Molecular Evolutionary Genetics Analysis version 6.0. Molecular Biology and Evolution 30:2725–2729. DOI: https://doi.org/10.1093/molbev/mst197

Tárano, Z. 2010. Advertisement calls and calling habitats of frogs from a flooded savanna of Venezuela. South American Journal of Herpetology 5:221–240. DOI: https://doi.org/10.2994/057.005.0308

Teixeira, V.H.S., F.M. Quintela, and D. Loebmann. 2017. *Leptodactylus chaquensis* Cei, 1950 (Leptodactylidae, Leptodactylinae): Extension of the distribution in state of Rio Grande do Sul, southern Brazil. Brazilian Journal of Biology 77:893–894. DOI: https://doi.org/10.1590/1519-6984.04316

Tschudi, J.J. 1838. Classification der Batrachier mit Berücksichtigung der Fossilen Thiere dieser Abtheilung der Reptilien. Petitpierre, Switzerland.

Vanzolini, P.E. 1968. Geography of the South American Gekkonidae (Sauria). Arquivos de Zoologia 17:85–112. DOI: https://doi.org/10.11606/issn.2176-7793.v17i2p85-112

Vanzolini, P.E. 1981. Introduction: The scientific and political contexts of the Bavarian expedition to Brazil. Pp. 9–29 in Herpetology of Brazil by Johan Baptist von Spix and Johann Georg Wagler (K.A. Adler, ed.). Society for the Study of Amphibians and Reptiles, USA.

Vanzolini, P.E., and C.W. Myers. 2015. The herpetological collection of Maximilian, Prince of Wied (1782–1867), with special reference to Brazilian materials. Bulletin of the American Museum of Natural History 395:1–155. DOI: https://doi.org/10.5531/sd.sp.9

Vieites, D.R., M.-S. Min, and D.B. Wake. 2007. Rapid diversification and dispersal during periods of global warming by plethodontid salamanders. Proceedings of the National Academy of Sciences of the USA 104:19903–19907. DOI: https://doi.org/10.1073/pnas.0705056104

Vieites, D.R., K.C. Wollenberg, F. Andreone, J. Kohler, F. Glaw, and M. Vences. 2009. Vast underestimation of Madagascar's biodiversity evidenced by an integrative amphibian inventory. Proceedings of the National Academy of Sciences of the USA 106:8267–8272. DOI: https://doi.org/10.1073/pnas.0810821106

Wachlevski, M., and C.F.D. Rocha. 2010. Amphibia, Anura, restinga of Baixada do Maciambu, municipality of Palhoça, state of Santa Catarina, southern Brazil. Check List 6:602–604.

Werle, E., C. Schneider, M. Renner, M. Völker, and W. Fiehn. 1994. Convenient single-step, one tube purification of PCR products for direct sequencing. Nucleic Acids Research 22:4354–4355.

Werneck, F.P. 2011. The diversification of eastern South American open vegetation biomes: Historical biogeography and perspectives. Quarterly Science Reviews 30:1630–1648. DOI: https://doi.org/10.1016/j.quascirev.2011.03.0

Wied-Neuwied, M.A.P. 1824. Verzeichniss der Amphibien, welche im zweiten Bande der Naturgeschichte Brasiliens vom Prinz Max. Von Neuwied beschrieben werden. Isis von Oken 14:661–673.

Wied-Neuwied, M.A.P. 1825. Beitrage zur Naturgeschichte von Brasilien.

Vol. 1. Verzeichniss de Amphibien. Gr. H.S. priv. Landes–Industrie–Comptoir, Germany.

Zina, J., C.P.A. Prado, C.A. Brasileiro, and C.F.B. Haddad. 2012. Anurans of the sandy coastal plains of the Lagamar Paulista, state of São Paulo, Brazil. Biota Neotropica 12:251–260. DOI: https://doi.org/10.1590/S1676-06032012000100020

Accepted on 13 June 2020
ZooBank.org registration LSID: 8A418DF6-7CCB-4403-BDA7-26844E3E1C85
Published on 11 December 2020

Appendix I

Specimens Examined

Leptodactylus latrans.—BRAZIL: Bahia: Aurelino Leal: 14.31°S, 39.33°W (CFBH18730); Camacan: 15.401°S, 39.512°W (CHUFPB28115–16); Camamu: 13.944°S, 39.124°W (CFBH29492–94, 29496–97, 29499–500); Gandu: 13.744°S, 39.485°W (CFBH27965–66); Ibirapitanga: 13.9°S, 39.454°W (UFBA03927); Ilhéus: 14.806°S, 39.053°W (AAGUFU0251, CFBH29514–15, UFBA10836, 10839–40); Itamaraju: 17.028°S, 39.55°W (CFBH32137); Itapebi: 15.889°S, 39.532°W (UFBA14648, 14650; Ituberá: 13.723°S, 39.151°W (UFBA03146); Mata de São João: 12.567°S, 38.039°W (UFBA03894); Porto Seguro: 16.396°S, 39.049°W (CFBH32117); Porto Seguro: Caraíva: 16.801°S, 39.152°W (CFBH13379); Salvador: 12.946°S, 38.398°W (CFBH32167, UFBA04107, 12074, 15099, 15101, 15104–05); Saubara: 12.752°S, 38.771°W (UFBA11730); Terra Nova: 12.453°S, 38.678°W (MZFS5137–39); Una: 15.187°S, 39.321°W (CFBH29517); Uruçuca: 14.59°S, 39.296°W (CFBH21060, 32362, 32388–89, 34023, 37945); Varzedo: 12.965°S, 39.438°W (CHUFPB28147–48). Espírito Santo: Alegre: 20.777°S, 41.533°W (CFBH25122); Anchieta: 20.716°S, 40.774°W (CFBH13377); Conceição da Barra: 18.355°S, 39.844°W (CFBH02435–40, 33324, 35399, 41604–05); Linhares: 19.399°S, 40.074°W (CFBH11328, 26266–27); Marataízes: 21.038°S, 40.845°W (CFBH18470); Mimoso do Sul: 21.074°S, 41.369°W (CFBH11322, 25484, 25490–91, 25493–94); São Mateus: 18.708°S, 39.843°W (CFBH01690–91); Vargem Alta: 20.669°S, 41.016°W (CFBH25080); Vitória: 20.331°S, 40.309°W (CFBH01994–95, 33277–78). Minas Gerais: Cataguases: 21.377°S, 42.716°W (CHUFPB28110–12); Chiador: 22.006°S, 43.052°W (AAGUFU0667); Divino: 20.605°S, 42.156°W (MAP0331, ZUFMSAMP6455–56); Juiz de Fora: 21.733°S, 43.37°W (CFBH42737–38); Muriaé: 21.155°S, 42.387°W (MAP1264–67, 1272); Ponte Nova: 20.285°S, 42.956°W (CFBH42697, 42699–703, 42731–33); Viçosa: 20.775°S, 42.876°W (CHUFPB28117). Rio de Janeiro: Duas Barras: 22.058°S, 42.517°W (AAGUFU0501); Itatiaia: 22.479°S, 44.57°W (CFBH42774–77); Macaé: 22.38°S, 41.816°W (AAGUFU0527); Rio de Janeiro: 22.962°S, 43.289°W (CFBH11320, UFBA00572); Teresópolis: 22.32°S, 42.82°W (CFBH42763–69, 42772). São Paulo: Ilha Bela: 23.828°S, 45.383°W (CFBH40853); São Sebastião: 23.748°S, 45.413°W (CFBH09764–65); Ubatuba: 23.445°S, 45.089°W (AAGUFU2147, 4406–14, CFBH01070, 01072, 01324, 01692); Ubatuba: Núcleo Picinguaba: 23.369°S, 44.826°W (CFBH11941, 30033, 42979–80, 42994–96, 42998–99, 43074).

Leptodactylus payaya.—BRAZIL: Bahia: Andaraí: 12.841°S, 41.316°W (MZFSPDB140); Brejinho das Ametistas: 14.266°S, 42.522°W (CFBH37913, 37918); Brotas de Macaúbas: 12.004°S, 42.624°W (UFBA11022–24); Caetité: 14.041°S, 42.283°W (UFBA08971, 08974); Campo Formoso: 10.509°S, 40.326°W (CHUFPB28196–99); Cocos: 14.176°S, 44.526°W (CHUNB38811); Dário Meira: 14.437°S, 39.907°W (CHUNB53236, 53238–39); Feira de Santana: 12.115°S, 39.043°W (CFBH13387; MZFS4957); Jacobina: 11.161°S, 40.535°W (CHUFPB28184, 28186–93, UFBA00149, 00153, 00160, 00162, 00166, 00168–69); Jaguarari: 10.267°S, 40.199°W (CHUFPB28200–02); Jequié: 13.928°S, 40.077°W (CFBH21065, 29510); Lençóis: 12.553°S, 41.383°W (UFBA14591); Maracás: 13.432°S, 40.405°W (CFBH18807, UFBA14300–02); Morro do Chapéu: 11.614°S, 41.155°W (CHUFPB28195, CHUNB57258); Morro do Chapéu: Santa Úrsula: 11.666°S, 41.131°W (MZFSPDB066, 068); Palmeiras: 12.572°S, 41.492°W (CHUFPB28143); Santa Terezinha: 12.783°S, 39.513°W (MZFS4360, 4720); Senhor do Bonfim: 10.466°S, 40.219°W (MZFS2282–83, 2286, 2801).

Leptodactylus luctator.—ARGENTINA: Buenos Aires: La Plata: 34.977°S, 57.87°W (LGE22146); Chaco: San Fernando: 27.439°S, 58.854°W (LGE14928); Córdoba: Juárez Celman: 33.511°S, 63.289°W (LGE13299); Punilla: 31.383°S, 64.605°W (LGE14945); Tulumba: San Pedro Norte: 30.083°S, 64.15°W (LGE14942). Corrientes: Corrientes: 27.433°S, 58.75°W (LGE11278); Ituzaingó: 27.744°S, 56.475°W (LGE07658, 07667); Ituzaingó: Santo Domingo: 27.671°S, 56.14°W (LGE03574, 03618); Ituzaingó: Yacryetá: 27.563°S, 56.659°W (LGE14931); Santo Tomé: Garruchos: 28.088°S, 55.747°W (LGE09025, 09027–29); Santo Tomé: Gobernador Virasoro: 28.046°S, 56.0°W (LGE06340, 14887–88). Entre Rios: Federal: 30.954°S, 58.771°W (LGE18856). Misiones: 25 de Mayo: 27.566°S, 54.838°W (LGE04262); 25 de Mayo: Arroyo Melo: 27.421°S, 54.701°W (LGE03444); 25 de Mayo: Puerto Londero: 27.37°S, 54.409°W (LGE14946); Candelaria: Barrio UPCN: 27.482°S, 55.745°W (LGE14878, 20110); Candelaria: El Puma: 27.461°S, 55.799°W (LGE03361); Candelaria: Isla: 27.496°S, 55.775°W (LGE20150); Candelaria: Reserva EBY: 27.495°S, 55.795°W (LGE20229); Capital: Fachinal: 27.648°S, 55.816°W (LGE06182, 14900); Concepción: 27.982°S, 55.531°W (LGE13169–73); Concepción: La Corita: 27.896°S, 55.359°W (LGE19995); Eldorado: 26.217°S, 54.601°W (LGE14904); Eldorado: Colonia Delicia: 26.164°S, 54.251°W (LGE13297); Garupá: 27.494°S, 55.821°W (LGE09546, 09553–54, 09570–71); Garupá: Santa Helena: 27.465°S, 55.888°W (LGE03720, 03725, 04909); General Manuel Belgrano: 26.116°S, 53.81°W (LGE07486); General Manuel Belgrano: Macaca: 26.395°S, 53.723°W (LGE03418); General Manuel Belgrano: Ruta Nacional N14: 26.116°S, 53.81°W (LGE03974, 07487, 07524, 07629); General Manuel Belgrano: San Sebastián: 25.858°S, 53.975°W (LGE14909–10); General Manuel Belgrano: Tajamar: 26.116°S, 53.81°W (LGE02277–79); Guaraní: El Soberbio: 27.283°S, 54.2°W (LGE14881); Iguazú: 25.972°S, 54.176°W (LGE05860); Ituzaingó: 27.533°S, 56.6°W (LGE03459); Leandro N. Alem: 27.56°S, 55.519°W (LGE05045); Posadas: 27.463°S, 55.963°W (LGE02630); Posadas: Campus: 27.437°S, 55.894°W (LGE14917); Posadas: Ruta Nacional N12: 27.453°S, 56.022°W (LGE22147–49); San Ignacio: Gobernador Roca: 27.183°S, 55.45°W (LGE13296); San Ignacio: Santo Pipó: 27.127°S, 55.471°W (LGE14919); San Javier: Arroyo Toribio: 27.841°S, 55.147°W (LGE07305); San Pedro: 26.789°S, 53.907°W (LGE08889); San Pedro: El Piñalito: 26.43°S, 53.852°W (LGE16551, 18223–24, 20454); San Pedro: Ruta Provincial N20: 26.561°S, 54.066°W (LGE00239, 21893). Santa Fe: General Obligado: 28.485°S, 59.722°W (LGE14947); General Obligado: Florencia: 28.031°S, 59.308°W (LGE18681); Rosario: 32.991°S, 60.907°W (LGE18741–42); Vera: 29.467°S, 60.233°W (LGE14912, 14915–16); Vera: Ruta Provincial N30: 28.105°S, 60.167°W (LGE20630); Vera: Ruta Provincial N40, Fortín Olmos: 29.096°S, 60.623°W (LGE20669–70). BRAZIL: Bahia: Côcos: 14.176°S, 44.526°W (CHUNB38812); Guiné: 12.827°S, 41.518°W (CHUFPB28146); Jaborandi: 13.629°S, 44.464°W (CFBH20512); Piatã: 13.153°S, 41.787°W (AAGUFU1680, CHUFPB28149–51, MZFS4438–40, UFBA/AAGARDA10080–81). Mato Grosso: Alto Araguaia: 17.32°S, 53.243°W (CHUNB67030). Mato Grosso do Sul: Corumbá: Base de Estudos do Pantanal: 19.577°S, 57.019°W (MAP1530–31, ZUFMSAMP2081, ZUFMSAMP2085–86, 2091–92, 2099–2100). Minas Gerais: Araguari: 18.624°S, 48.22°W (AAGUFU4918); Fama: 21.402°S, 45.838°W (CFBH01763); Itapagibe: 19.913°S, 49.217°W (MAP0823); Marmelópolis: 22.501°S, 45.151°W (CFBH43028, 43033, 43045); Poços de Caldas: 21.836°S, 46.531°W (AAGUFU1173, 4801, CFBH35883); Sacramento: 19.861°S, 47.46°W (CFBH36507); Santana do Riacho: 19.257°S, 43.533°W (CFBH30905, 39825, 40109); Tapira: 19.919°S, 46.818°W (AAGUFU0612); Uberlândia: 18.986°S, 48.298°W (AAGUFU2146, 4478–79). Paraná: Jaguariaiva: 24.238°S, 49.712°W (CFBH21025, CFBH24729–30); Piraquara: 25.466°S, 49.053°W (CFBH11046); Quatro Barras: 25.378°S, 49.085°W (CFBH18134); Tijucas do Sul: 25.925°S, 49.174°W (CFBH08446). Rio Grande do Sul: São Sepé: 30.37°S, 53.664°W (CFBH12044); Sapiranga: 29.552°S, 51.016°W (CFBH12415). Santa Catarina: Bom Jardim da Serra: 28.352°S, 49.599°W (CFBH11015–16, 11029, CHUFPB28113); Mafra: 26.114°S, 49.757°W (CFBH08597). São Paulo: Apiaí: 24.562°S, 48.67°W (CFBH25614–15); Bauru: 22.346°S, 49.007°W (CFBH19761); Buri: 23.612°S, 48.533°W (CFBH42813–14); Campinas: 22.883°S, 46.935°W (CFBH00938, 35545); Corumbataí: 22.216°S, 47.618°W (CFBH04186); Cunha: 23.223°S, 44.962°W (CFBH43007, 43019); Guará: 20.492°S, 47.859°W (CFBH39955); Itirapina: 22.248°S, 47.826°W (CFBH06022, 06441); Lindóia: 22.523°S, 46.643°W (CFBH42662–63); Luís Antônio: 21.573°S, 47.738°W (CFBH31870–71); Mairiporã: 23.322°S, 46.562°W (CFBH13877); Mogi das Cruzes: 23.719°S, 46.168°W (CFBH41881); Parelheiros: 23.987°S, 46.743°W (CFBH38481, 38484); Pedregulho: 20.254°S, 47.455°W (CFBH13991); Pilar do Sul: 23.832°S, 47.713°W (CFBH08352); Piquete: 22.596°S, 45.23°W (CFBH43029–32, 43044, 43064–65); Ribeirão Branco: 24.217°S, 48.754°W (CFBH02323–25, 04463, 06897, 06899–900, 41603); Rio Claro: 22.317°S, 47.697°W (CFBH08022); São José do Barreiro: 22.722°S, 44.617°W (CFBH43068); São Luís do Paraitinga: 23.335°S, 45.147°W (CFBH10773, 38731, 38760); São Miguel Arcanjo: 23.986°S, 47.921°W (UFBA07977–78); São Paulo: 23.675°S,

46.732°W (CFBH31074); Teodoro Sampaio: 22.537°S, 52.125°W (CFBH18395). URUGUAY: Montevideo: Montevideo: 34.861°S, 56.249°W (LGE22129–32).

Leptodactylus paranaru.—BRAZIL: Paraná: Antonina: 25.419°S, 48.733°W (CFBH11064); Morretes: 25.458°S, 48.818°W (UFBA09112). Rio Grande do Sul: Torres: 29.348°S, 49.748°W (CFBH41677). Santa Catarina: Angelina: 27.566°S, 48.99°W (CFBH08481); Corupá: 26.435°S, 49.245°W (CFBH12432); Lauro Muller: 28.399°S, 49.504°W (CFBH30351); São Francisco do Sul: 26.249°S, 48.635°W (CFBH39301); Treviso: 28.519°S, 49.464°W (CFBH08500, 12391). São Paulo: Apiaí: 24.562°S, 48.67°W (CFBH38695); Cubatão: 23.886°S, 46.453°W (CFBH10546, 11376); Eldorado: 24.532°S, 48.122°W (CFBH30993); Iguape: 24.379°S, 47.075°W (CFBH09752); Peruíbe: 24.379°S, 47.075°W (CFBH12455, 24121, 38572, 42804–05, 42807); Praia Grande: 24.005°S, 46.485°W (AAGUFU4900–01); Santos: 23.9°S, 46.26°W (CFBH23925); São Vicente: 23.964°S, 46.366°W (CFBH38034); Sete Barras: 24.384°S, 47.933°W (CFBH36494, 36505, 36555).

Leptodactylus macrosternum.—ARGENTINA: Chaco: Chacabuco: Charata: 27.26°S, 61.198°W (LGE05221); Chacabuco: Mesón de Fierro: 27.403°S, 60.932°W (LGE05260, 05278); Fray Justo Santa María de Oro : Santa Sylvina: 27.803°S, 61.088°W (LGE05373); General Güemes: 25.078°S, 61.627°W (LGE14712); General Güemes: Comandancia Frias: 24.491°S, 62.119°W (LGE14709–11); General Güemes: El Pintado: 24.654°S, 61.472°W (LGE14827); General Güemes: El Sauzalito: 24.439°S, 61.683°W (LGE14722, 14724, 14733, 14842, 14857, 18722); General Güemes: Fuerte Esperanza: 25.085°S, 61.644°W (LGE14714–15, 14717); General Güemes: Misión Nueva Pompeya: 24.78°S, 61.694°W (LGE12209, 14704, 14753, 14762, 14766, 17012, 20698); General Güemes: Paraje Zanjas: 24.519°S, 61.811°W (LGE14773–74); General Güemes: Rio Bermejito: 24.769°S, 61.808°W (LGE14752, 14755); General Güemes: Wichi: 24.692°S, 61.431°W (LGE14852); Maipú: Tres Isletas: 26.212°S, 60.329°W (LGE10092, 10094, 10096). Corrientes: Corrientes: Capital: 27.433°S, 58.75°W (LGE11272–73, 14765); Curuzú Cuatiá: El Oscuro: 29.168°S, 58.517°W (LGE14780, 14784); Ituzaingó: Santo Domingo: 27.671°S, 56.14°W (LGE04815). Entre Rios: Federal: 30.954°S, 58.771°W (LGE18857–59). Formosa: Pilcomayo: Palma Sola: 25.251°S, 57.999°W (LGE14837–39, 14864); Pirané: Campo Villafañe: 26.158°S, 59.03°W (LGE09409); Pirané: Ruta Provincial N8: 25.678°S, 59.081°W (LGE14791). Misiones: Candelaria: Estancia San Juan: 27.429°S, 55.622°W (LGE14825). Salta: General José de San Martín: Embarcación: 23.182°S, 64.076°W (LGE14813); Iruya: Isla de Cañas: 22.918°S, 64.646°W (LGE14840); Orán: Hipólito Irigoyen: 23.255°S, 64.273°W (LGE21647). Santa Fe: Nueve de Julio: Villa Minetti: 28.613°S, 61.677°W (LGE20717); General Obligado: Florencia: 28.028°S, 59.348°W (LGE18675–76); General Obligado: Villa Ana S: 28.573°S, 59.641°W (LGE14819); Rosario: Zavala: 32.991°S, 60.907°W (LGE18740); San Javier: 30.551°S, 59.999°W (LGE18703); Sauce Viejo: 31.766°S, 60.836°W (LGE14848–49); Vera: Los Amores: 28.107°S, 59.989°W (LGE20623, 20631); Vera: Ruta Provincial N40, Fortín Olmos: 29.096°S, 60.623°W (LGE20641–42, 20648). Santiago del Estero: General Taboada: Anatuya, Ruta Provincial N7: 28.416°S, 62.603°W (LGE20794–95); General Taboada: Colonia Dora: 28.516°S, 62.888°W (LGE05499–501, 14801, 14803, 14809); General Taboada: Los Juries: 28.508°S, 62.134°W (LGE05454, 05458, 05504–05, 05507–08); Juan Felipe Ibarra: El Sobrante: 27.643°S, 63.481°W (LGE08345); Juan Felipe Ibarra: Suncho Corral: 27.822°S, 63.472°W (LGE08348); Moreno: Tintina: 27.141°S, 63.056°W (LGE08276, 08282); Río Hondo: 27.509°S, 64.838°W (LGE00323, 20927, 20938–39); Robles: Fernández: 27.974°S, 63.8°W (LGE14831). Tucumán: Lules: 26.863°S, 65.299°W (LGE14841, 14869). BRAZIL: Acre: Cruzeiro do Sul: 7.602°S; 72.658°W (CFBH00039–40). Alagoas: Passo de Camaragibe: 9.262°S; 35.457°W (CFBH07325). Amapá: Macapá: 0.007°S, 51.107°W (AAGUFU6008). Bahia: Amargosa: 13.085°S, 39.649°W (UFBA06440); Barra: 11.083°S, 43.142°W (CHUNB57262); Barreiras: 12.111°S, 44.967°W (UFBA12903, 12907–08, 12918, 13109–10, 13120–21); Belmonte: 15.849°S, 38.878°W (UFBA14331); Bom Jesus da Lapa: 13.267°S, 43.420°W (UFBA07692); Brotas de Macaúbas: 12.004, 42.623 (UFBA13119); Caetité: 14.041°S, 42.282°W (UFBA08547); Camacan: 15.400°S, 39.512°W (CHUFPB28183); Camaçari: 12.762°S, 38.170°W (UFBA00633–35, 01049–54, 07809–10, 07815–16, 11824, 11827–28, 13103, 13106–07, 13104, 14285, 14287); Conde: 11.853°S, 37.578°W (UFBA11829, 11831–32, 14060); Condeúba: 14.907°S, 41.963°W (CHUFPB28153–55); Curaçá: 9.009°S, 39.918°W (UFBA11359–60); Dário Meira: 14.437°S, 39.907°W (CFBH29511–12); Dom Basílio: 13.752°S, 41.768°W (CFBH21088); Entre Rios: 12.365°S, 37.882°W (UFBA05902, 05957, 06065, 06076, 06109); Ibiraba: 10.792°S, 42.824°W (UFBA02096, 02098, 02100–01); Itapebi: 15.889°S, 39.532°W (UFBA14649); Jacobina: 11.160°S, 40.534°W (CHUFPB28185); Jacobina: 11.189°S, 40.555°W (CHUNB57253, 57261); Jacobina: 11.323°S, 40.469°W (UFBA00142, 00154, 00157–58, 00161, 00163); Jaguarari: 10.266°S, 40.198°W (CHUFPB28203); Jandaíra: 11.663°S, 37.482°W (UFBA15093–95); Jequié: 13.928°S, 40.077°W (CFBH29507–09); Macaúbas: 13.026°S, 42.687°W (UFBA13116, 13118); Mata de São João: 12.551°S, 38.0°W (UFBA02377, 08158); Mucugê: 13.013°S, 41.369°W (UFBA07402–03, 07763); Palmeiras: 12.572°S, 41.491°W (CHUFPB28141–42, 28144–45); Paratinga: 12.689°S, 43.190°W (CHUFPB28194); Paulo Afonso: 9.683°S, 38.630°W (CHUFPB28134–38, UFBA07632, 07634–36 9.242, 38.125); Pilão Arcado: 10.043°S, 42.416°W (MZFS2500, 2584, 2586, 2588, UFBA07264–65, 07267–71); Salvador: 12.919°S, 38.325°W (UFBA11131); Santa Rita de Cássia: 11.016°S, 44.505°W (UFBA08735, 08737–42, 09478–79); São Desidério: 12.784°S, 45.943°W (CFBH20514, UFBA12911–12); Senhor do Bonfim: 10.466°S, 40.219°W (MZFS2284–85); Serra do Ramalho: 13.550°S, 43.585°W (CFBH27663–64); Terra Nova: 12.452°S, 38.678°W (MZFS5140–41). Ceará: Quixadá: 4.958°S, 38.968°W (CHUFPB28167, CHUFPB28168–82 4.958, 38.968); Ubajara: 3.841°S, 40.905°W (CFBH16121). Goiás: Alvorada do Norte: 14.599°S, 46.631°W (CHUNB33867–69, 33878, 33884, 33886); Palmeiras de Goiás: 16.933°S, 50.002°W (CFBH26141–42); Porangatu: 13.411°S, 49.108°W (CFBH27048); Quirinópolis: 18.402°S, 50.455°W (CFBH04597, 26009); São Domingos: 13.396°S, 46.311°W (CHUNB33876–77, 43865). Maranhão: Alcântara: 2.406°S, 44.411°W (CFBH19229); Humberto de Campos: 2.402°S, 43.51°W (CFBH24313); Porto Franco: 6.337°S, 47.407°W (CFBH08197, 08203); Riachão: 7.362, 46.629 (ZUFMSAMP/SIL37, 66–68, 82–83). Mato Grosso: Cuiabá: 15.574°S, 56.128°W (AAGUFU2131); Nova Xavantina: 14.522°S, 52.181°W (CHUNB63992); Novo Santo Antônio: 12.29°S, 50.967°W (CHUNB57800–02, 57893, 57902, 57904); Poconé: 16.283°S, 56.641°W (CHUNB35950); Ribeirão Cascalheira: 12.931°S, 51.814°W (CHUNB22772, 22774, 67794–95, 67798, 67807, 67815, 67841). Mato Grosso do Sul: Aquidauana: 20.450°S, 55.621°W (AAGUFU4099); Bela Vista: 22.101°S, 56.545°W (AAGUFU0156–57); Bonito: 20.982°S, 56.51°W (CFBH14243, CHUNB49276, ZUFMSAMP5609); Camapuã: 19.013°S, 53.858°W (ZUFMSAMP/MAP1094, ZUFMSAMP5565, 5567); Campo Grande: 20.538°S, 54.751°W (ZUFMSAMP/MAP0205, 0259, 0524–25, ZUFMSAMP/STAFE01); Corguinho: 19.790°S, 54.931°W (ZUFMSAMP/MAP2426, ZUFMSAMP5605–06); Corumbá: Base de Estudos do Pantanal: 19.576°S, 57.018°W (ZUFMSAMP/MAP1731, ZUFMSAMP5583, 5585, 5587, 5594, 5600); Corumbá: Nhumirim: 18.988°S, 56.619°W (ZUFMSAMP/MAP0860); Porto Murtinho: 21.668°S, 57.713°W (CFBH30534); Porto Murtinho: 20.999°S, 57.281°W (ZUFMSAMP/MAP2432); Selviria: 20.384°S, 51.383°W (ZUFMSAMP/MAP0653). Minas Gerais: Almenara: 16.166°S, 40.671°W (UFBA14444, 14455, 14457); Araguari: 18.623°S, 48.220°W (AAGUFU4096); Bambuí: 19.986°S, 45.964°W (AAGUFU0297); Jacinto: 16.194°S, 40.341°W (UFBA14209, 14557–59); Lagoa Grande: 17.809°S, 46.496°W (ZUFMSAMP/MAP2366, 2369–71, 2376); Sacramento: 19.861°S, 47.460°W (AAGUFU0886). Pará: Monte Alegre: 1.933°S, 54.032°W (CHUNB31189); Paraíba: Areia: 6.965°S, 35.718°W (CHUFPB28118–33); Puxinanã: 7.148°S, 35.955°W (CHUFPB28114). Pernambuco: Igarassu: 7.823°S, 34.869°W (CFBH02488). Piauí: Brejo do Piauí: 8.195°S, 42.835°W (CFBH14023); Caracol: 9.279°S, 43.338°W (CHUFPB28157–66); Guadalupe: 6.762°S, 43.617°W (ZUFMSAMP/MAP0536); PARNA Serra das Confusões: 9.219°S, 43.49°W (CHUFPB28156). Rio Grande do Norte: Angicos: 5.67°S, 36.642°W (CHUFPB28152); Canguaretama: 6.386°S, 35.136°W (CHUFPB28108–09); Macaíba: Escola Agrícola de Jundiaí: 5.885°S, 35.368°W (AAGUFU3573–74, CHUFPB28102–07); Extremoz: 5.684°S, 35.241°W (CHUFPB28139); João Câmara: 5.364°S, 35.884°W (CHUFPB28140); Rafael Godeiro: 6.081°S, 37.716°W (CHUFPB28098–101). Rondônia: Costa Marques: 12.454°S, 64.198°W (AAGUFU5272–76, 5281–84, CHUNB28978). Roraima: Cantá: 2.61°N, 60.597°W (AAGUFU5558). São Paulo: Gália: 22.397°S, 49.681°W (CFBH38950); Guararapes: 21.213°S, 50.631°W (AAGUFU2019); Teodoro Sampaio: 22.537°S, 52.125°W (CFBH10086, 18294). Tocantins: Brejinho do Nazaré: 11.026°S, 48.589°W (AAGUFU0916); Caseara: 9.372°S, 49.843°W (CHUNB45653, 45658, 45660, 45662, 58158); Colinas do Tocantins: 8.069°S, 48.487°W (CFBH19894, 28429); Combinado: 12.806°S, 46.547°W (CHUNB62725); Figueirópolis: 12.166°S, 48.988°W (CFBH28335); Mateiros: 10.702°S, 46.413°W (CHUNB28843); Pium: 9.946°S, 49.792°W (CHUNB73955, 73957); Porto Nacional: 10.986°S, 48.561°W (CFBH28290, 28893); Ribeirão Cascalheira: 12.931°S, 51.815°W (CHUNB73967); Wanderlândia: 6.903°S, 47.923°W (CFBH28475).

Leptodactylus viridis.—BRAZIL: Bahia: Dário Meira: 14.437°S, 39.907°W (CFBH29505–06, 29513).

APPENDIX II.—Sound Recordings and Associated Information.

Sound file	Species	Voucher	Locality (state)	Air/Water
ASUFRN664	*L. latrans*	CFBH42763	Teresópolis (RJ)	21/–°C
ASUFRN666	*L. latrans*	Unvouchered	Teresópolis (RJ)	21/–°C
ASUFRN668	*L. latrans*	CFBH42772	Teresópolis (RJ)	22/–°C
AAG1a	*L. latrans*	Unvouchered	Ubatuba (SP)	23/23°C
AAG2b	*L. latrans*	Unvouchered	Ubatuba (SP)	23/23°C
AAG3b	*L. latrans*	Unvouchered	Ubatuba (SP)	25/24°C
AAG5d	*L. latrans*	Unvouchered	Ubatuba (SP)	24/29°C
AAG6e	*L. latrans*	Unvouchered	Ubatuba (SP)	25/–°C
TRC1a	*L. latrans*	AAG-UFU6148	Santa Teresa (ES)	22/–°C
AAG1b	*L. luctator*	AAG-UFU1680	Piatã (BA)	24/25°C
AAG2a	*L. luctator*	Unvouchered	Piatã (BA)	24/25°C
AAG1b	*L. luctator*	Unvouchered	Araguari (MG)	24/26°C
AAG5c	*L. luctator*	Unvouchered	Uberlândia (MG)	23/23°C
AAG6a	*L. luctator*	Unvouchered	Uberlândia (MG)	23/23°C
AAG7a	*L. luctator*	Unvouchered	Uberlândia (MG)	24/27°C
AAG8a	*L. luctator*	Unvouchered	Uberlândia (MG)	23/24°C
AAG10a	*L. luctator*	Unvouchered	Uberlândia (MG)	22/23°C
AAG2b	*L. macrosternum*	AAG-UFU4108	Araguari (MG)	25/31°C
TRC1c	*L. macrosternum*	AAG-UFU3573	Macaíba (RN)	28/–°C
ASUFRN670	*L. paranaru*	Unvouchered	Peruíbe (SP)	23/–°C
ASUFRN671	*L. paranaru*	CFBH42804	Peruíbe (SP)	23/–°C
BNU25_95.01	*L. paranaru*	Unvouchered	Blumenau (SC)	–/–
BNU25_95.02	*L. paranaru*	Unvouchered	Blumenau (SC)	–/–
ASUFRN672	*L. payaya*	Unvouchered	Jacobina (BA)	26/–°C
ASUFRN673	*L. payaya*	CHUFPB28187	Jacobina (BA)	26/–°C
ASUFRN676.1	*L. payaya*	CHUFPB28189	Jacobina (BA)	27/–°C
ASUFRN676.2	*L. payaya*	CHUFPB28189	Jacobina (BA)	27/–°C